Doctoral Dissertation

Investigation of tetrodotoxin in pufferfish and screening of bioactive compounds in marine invertebrates from the Solomon Islands

（ソロモン諸島のフグのテトロドトキシンの調査と海洋無脊椎動物からの生理活性物質の探索）

Clyde Gorapava Puilingi

Laboratory of Bioorganic Chemistry of Natural Products

Division of Bioscience and Biotechnology for Future Industries

Graduate School of Agricultural Science

Tohoku University

Academic Supervisor

Professor Mari Yotsu-Yamashita Ph.D.

Acknowledgements

I would like to express my deepest gratitude to my principal academic advisor Professor Mari Yotsu-Yamashita for your immense support, guidance, kindness and patience throughout this doctoral program. Your constant advice, passion and intellectual view towards research has been one of the source of motivation during my study and will always be in years to come. Thank you very much.

I wish to acknowledge the contribution of my other academic advisor and good friend, Associate Professor Keiichi Konoki for your support and advice towards my work. Your encouragement both in research and in general living in Japan has been very valuable.

To other thesis reviewers, Professor Kiyotaka Nakagawa and Associate Professor Masaru Enomoto, thanks a lot for your time in reviewing my work.

To Assistant Professor Yuko Cho, your help in my study and guidance in analytical instruments (LCMS) has been highly appreciated. Thanks to my colleagues, Dr. Yuta Kudo and Mr. Shigeki Tsuchiya (D3) for being very reliable when I needed research help or general guidance. To the other laboratory students, your presence brought so much fun and exciting memories. I wish you all the best in your future careers.

I would like to acknowledge the academic advice and support from Professor Emeritus Minoru Sato, Associate Professor Toshiyasu Yamaguchi and Assistant Professor Toshiki Nakano during my master program at the laboratory of Marine Biochemistry. You've helped me with research and provided a good study environment. Thanks, a lot.

I also owe this success to my family. Special thanks to my wife Tina and son Lachlan for your moral support, sacrifice and encouragement throughout my research. To my parents, other family members and friends, you all have always been an inspiration to many aspects of my life. Tagio tumas (Thank you very much).

I wish to acknowledge the Japanese Government for awarding me the MEXT scholarship to study in Japan. I'm honoured to have been awarded this scholarship giving me this opportunity to do this research.

Above all, I would like to thank the Lord for all that He has bestowed upon us.

Contents

Appendices

List of Tables

List of Schemes

List of Figures

Chapter 1.0 Introduction to Marine Toxins and Toxicology

Marine natural toxins are commonly classified as natural chemicals or substances produced by specific marine organisms that may cause deterring or harmful effects on other organisms. Whether toxin productions are triggered by natural cycle, environmental changes or produced by organisms primarily for the ecological counter balance of predator-prey relationships, humans in many ways have become the unfortunate victims in this cycle. Throughout the years, intoxication from marine toxins occur globally with higher prevalence usually occurring in regions of low monitoring regulations and surveillances. A wider pre-empted knowledge of the likely occurrence of certain intoxications either stem from past experiences or as awareness by authorities have proven to be an effective risk-reduction approach.

The marine environment with its harsh conditions predominantly harbours some of the most life-threatening toxins known to mankind. Toxins produced by tiny marine organisms such as bacteria, dinoflagellates and micro algae are amongst the prevailing causes of seafood poisoning. To date, there are an estimate of 60-80 toxic marine microalgae that exist globally, and dinoflagellate accounts for 75% of all marine toxins related poisoning[1)]. Marine toxins are usually classified according to their specific producers, vector-borne producers, chemical-based categories or clinical syndromes etc. Some common marine toxins are ciguatera fish poisoning, scombroid poisoning, pufferfish poisoning, shellfish poisoning which include diarhetic shellfish poisoning (DSP), paralytic shellfish poisoning (PSP), neurotoxic shellfish poisoning (NSP), amnesic shellfish poisoning (ASP) and azaspiracid shellfish poisoning (AZP), and the much rarer but potent poisoning such as seaweed poisoning and turtle poisoning.

As one of the frequent intoxicating agent in the Pacific, ciguatera poisoning is a neurotoxic form of ichthyosarcotoxism that can result from consuming flesh of certain species of barracuda, grouper, snapper, mackerel, moray[2,3)] etc. The principle neurotoxic agent, ciguatoxins (CTX), are a group of lipophilic, polycyclic polyether toxins consisting of 13 or 14 rings fused into rigid ladder-like structures.[4)] (Figure 1.1). Over the years, many analogues have been isolated or modified.[5,6,7)] Different geographical locations accounts for different CTX forms, however, the Pacific

ciguatoxin-1 (P-CTXs) and the Caribbean ciguatoxin-1 (C-CTXs) seems to be the common CTXs and are known to possess considerable potency, though neurological activities vary among analogue types.[8)] These sodium channel activators are produced by dinoflagellate of genus *Gambierdiscus* which are bioaccumulated in the tissues of higher hierarchical organisms via the marine food chain.[5,9,10)]

On the onset, victims of ciguatera poisoning often suffer from nausea, vomiting, abdominal pain and neurologic symptoms such as tingling fingers or toes. Victims may also experience pathognomonic conditions of cold allodynia caused by ciguatoxins' specific target on cold pain pathways in the primary sensory neurons.[11)] Ciguatera has no cure. Symptoms usually go away in days or weeks however; severe cases can last for few years. Since the producer ecologically strives in warmer regions, ciguatera outbreaks often occur in tropical and subtropical countries most of which rely on seafood and especially fresh fish as their source of daily protein. Ciguatera is amongst the most common non-bacterial food poisoning with an estimated global case of 50,000-500,000 annually.[12)]

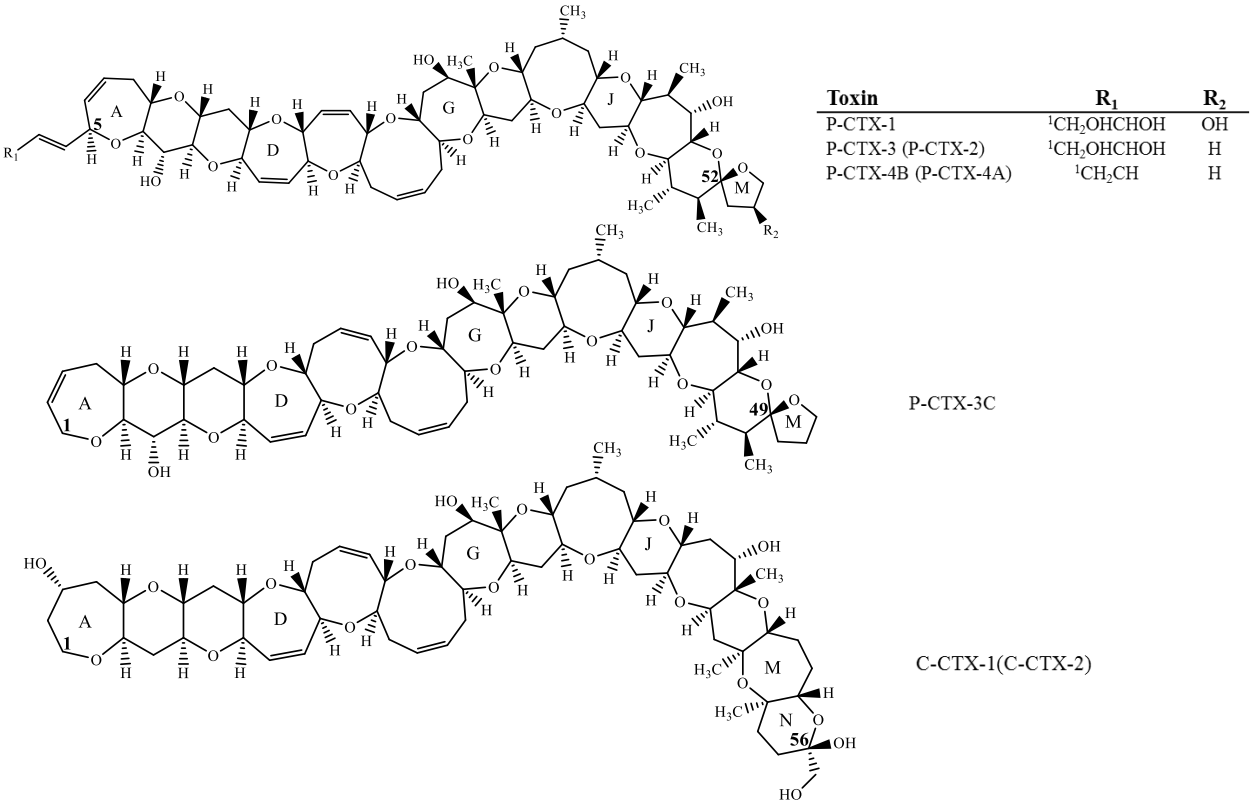

Toxin	R_1	R_2
P-CTX-1	$^1CH_2OHCHOH$	OH
P-CTX-3 (P-CTX-2)	$^1CH_2OHCHOH$	H
P-CTX-4B (P-CTX-4A)	$^1CH_2CH$	H

P-CTX-3C

C-CTX-1(C-CTX-2)

Figure 1-1. Structures of ciguatoxins.

Scombroid poisoning or usually known as histamine food poisoning is caused by consumption of mishandled fish, particularly common in fish with high levels of free histidine in their muscle tissue. These may include the scombridae family like tunas (Thunini tribe), bonitos (Sardini tribe), mackerel (Scombrini tribe) and others such as mahi mahi (*Coryphaena* spp.), sardines (*Sardinella* spp.) herring (*Clupea* spp.).[13)] Poisoning is implicated when higher levels of naturally occurring free histidine (enzyme substrate) is converted to histamine by bacterial histidine decarboxylase at mid cooling temperature (Figure 1-2) Though endogenous histamine is important in normal physiological functions, an increase of histamine levels in the circulatory system from contaminated food may trigger histamine receptors to activate biological responses and produce various toxicological effects. Symptoms may include flushing, rash (urticaria), hypotension, headache, tachycardia, abdominal cramps, diarrhoea, vomiting, pain, itching, oral burning sensation, peppery taste, nausea, swelling of tongue.[14)]

Severe effects usually subside following antihistamine treatment therapy which include H1 antagonists (e.g. diphenhydramine) and H2 antagonists (e.g. cimetidine), however, for mild cases only maintenance support (eg. fluid replacements) is required.[15)]

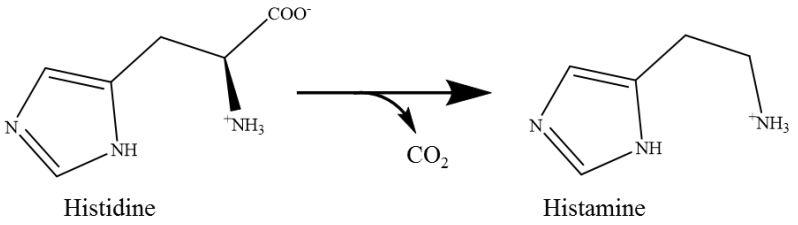

Figure 1-2. Formation of histamine by decarboxylation of histidine.

Shellfish poisoning (SFP) is a generic term used to describe the phytotoxic poisoning caused by the consumption of contaminated shellfish such as oyster, clams, scallops or mussels. SFP are categorised into five groups namely a) paralytic shellfish toxins causing PSP; b) diarrheic shellfish toxins causing DSP; c) amnesic shellfish toxins causing ASP; d) neurotoxic shellfish toxins causing NSP; and e) azaspiracid shellfish toxins causing AZP.[16,17] Each of the group is characterized by the chemicals or toxic compounds that are implicated in the contaminated shellfish. Besides their different mode of actions, chemical and structural properties of the principle toxins and their analogues also vary in their structures and biological potency.[18,19] Some classes display specific symptoms while others are non-specific and seem to show merging neurological and gastrointestinal symptoms.

As one of the common SFP, PSP is categorized as the ingestion of contaminated shellfish containing tetrahydropurines related toxins such as saxitoxin and its analogues (Figure 1-3) which are produced by the dinoflagellate genus *Alexandrium*. PSP toxins display pharmacological effects by inhibiting the voltage-gated sodium channel which involve slowing or abolishing the propagation of the action potential in plasma membrane of excitable cells. The very high selectivity and affinity mode of action between certain PSP toxins and the sodium ion channel protein makes PSP toxins few of the most potent marine biotoxins in shellfish poisoning. Symptoms of PSP range from parathesias sensation, loss of muscle coordination, speech defects, nausea, vomiting, respiratory paralysis and death.[4]

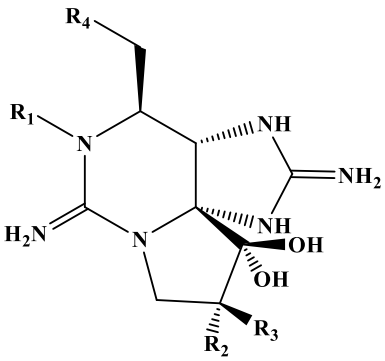

Toxin	R_1	R_2	R_3	R_4
Saxitoxin (STX)	H	H	H	$OCONH_2$
neoSTX	OH	H	H	$OCONH_2$
DecabarmoylSTX (dcSTX)	H	H	H	OH
Gonyautoxin 1 (GTX1)	OH	OSO_3^-	H	$OCONH_2$
Gonyautoxin 2 (GTX2)	H	OSO_3^-	H	$OCONH_2$
C1	H	OSO_3^-	H	$OCONHSO_3^-$
C2	H	H	OSO_3^-	$OCONHSO_3^-$

Figure 1-3. Structures of STX and its analogues.

Chapter 2-1.0 Introduction of Tetrodotoxin (TTX)

Tetrodotoxin (TTX) is a well-known natural toxin and the fatal agent in TTX poisoning. TTX and its analogues are distributed in both marine and terrestrial animals such as pufferfish,[20,21] marine nails,[22] blue-ringed octopus,[23] starfish,[24] crabs,[25] sea slugs,[26] clams,[27,28] mussels and oysters,[29] frogs,[30,31] and newts.[32,33] TTX blocks the voltage-gated sodium channels which results in the incapacitation of nerve conduction and muscle action potentials, causing progressive paralysis and death due to failure of the respiratory system.[34,35] Due to its neurological properties, TTX was also developed as a therapeutic agent to ease off severe pain in cancer patients.[36]

TTX, as the principal cause of pufferfish poisoning, are reported to have been originated from the TTX-producing bacteria such as in genus *Vibrio* spp. *Aeromonas* spp. and *Pseudomonas* spp. and is accumulated into the marine invertebrate and pufferfish via the food chain.[37,38] The role of TTX in animals has been an ongoing theme of study for many years. Among other reasons, the obvious roles of TTX are for protection, defense and helps in foraging. Newts for instance, use TTX as part of its defense strategy to void off predators[39] and TTX is used to capture mobile prey as demonstrated by flatworms in Guam.[40]

Apart for TTX, there are more than 30 analogues already been discovered. The major analogues (Figure 2-1), can be classified into (1) hemilactal type analogues, (2) 5-deoxy-10,7-lactone type analogues, (3) 4,9- and 4,4a-anhydro type analogues and (4) tetrodonic acid type analogue.[41,42]

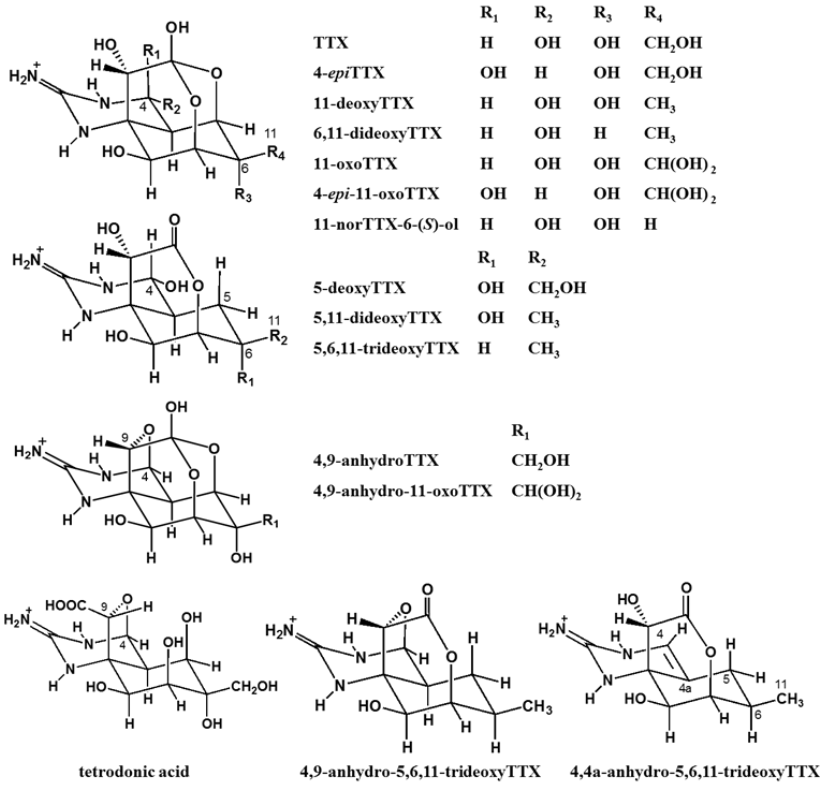

Figure 2-1. Structures of TTX and its analogues.

Based on the structures of these analogues, few researchers have also attempted to predict a stepwise oxidative pathway of TTX in marine animals.[42] This was made possible by the recently discovered C5–C10 directly bonded TTX analogues in newts, which suggested a monoterpene origin of TTX.[43]

Previous mouse bioassay toxicity experiments have established the LD_{50} (50% lethal dose, mice, i.p.) of TTX and few analogues. For instance, TTX being more potent than other analogues affects mice at LD_{50} of 10 μg/kg[34], while its analogues such as 11-deoxyTTX[44] and 6,11-dideoxyTTX[45] have LD_{50} of 70 μg/kg, and 420 μg/kg, respectively and 5,6,11-trideoxyTTX, a LD_{99} of 750 μg/kg.[46] The toxicity of 11-oxoTTX was initially reported at 120 μg/kg (minimum lethal dose, mice, i.p.),[47] however, experiments on rat skeletal muscle fibers revealed an ED_{50} (50% effective dose) of 0.7 nM compared to TTX 4.1 nM[48] and smaller K_d values of 11-oxoTTX (to rat brain membrane) compared to TTX[49] which suggested that 11-oxoTTX is much more potent than TTX. The potency of TTX and its analogue such as 11-oxoTTX highlighted the importance of proper regulations in seafood safety, especially in

pufferfish species. Pufferfish poisoning has been reported in Asian countries such as Hong Kong,[50] Thailand,[51] Bangladesh,[52] and Japan,[53] Eastern Mediterranean Sea,[54] Suez Canal region,[55] and also in the United States mainly from illegally imported pufferfish.[56,57] Due to the increase of global occurrences especially in regions not been recorded in the past, the need for proper regulation and scientific research is vital.

Unlike ciguatera and other seafood poisoning, the documentation of pufferfish was not well represented in the South Pacific, although few occurrences that fits its description were reported to have taken place in localized rural areas.[58] In the Solomon Islands, no clear records were established to date of the victims who may have suffered from pufferfish poisoning. Probably, the dangers of pufferfish consumption may have been widely known due to past intoxication, thereby reducing the cases of pufferfish poisoning. However, since most people eat seafood, especially fish as a protein source and along with the socioeconomic pressures that may affect food security and possibly alter food selectivity, the investigation of TTX in common Solomon Islands pufferfish is of great importance. Having a clear information based on scientific evidence will definitely help citizens refrain from consuming toxic pufferfish species, and thus reduce the potential risk of pufferfish poisoning. Like TTX, the paralytic shellfish toxins can also be accumulated by few pufferfish. Past occurrences of saxitoxin (STX) and decarbamoyl STX (dcSTX) in pufferfish were reported in South-eastern Asia, Japan[59-61] and the United States.[62]

In this research project, Solomon Islands pufferfish *Arothron hispidus* and *A. nigropunctatus* were investigated for TTX and its analogues, as well as STX and its analogues for the first time, using high resolution hydrophilic interaction chromatography (HR-HILIC) LC-MS. In a parallel experiment, the same species from Okinawa, Japan, were also investigated for comparison with those from the Solomon Islands. Moreover, since few organs of *Diodon. holocanthus* are officially allowed for consumption in Japan,[63] Solomon Islands' *D. holocanthus* species were also collected to examine the possible presence of TTXs and its analogues.

2-2.0 Procedure

2-2.1 Sampling and Test Materials

Field collection of the samples were carried out in May and July 2014, in the Tomba group of islets (latitude 8.427° S, longitude 157.929° W), situated along the coastal open waters on the other side of the enclosed Marovo Lagoon, Solomon Islands. The samples consisted of three specimens of *A. hispidus*, three specimens of *A. nigropunctatus* and two specimens of *D. holocanthus*. The gender, body length and body weight of each specimen are recorded in Tables 2-1 to 2-3 and 2-6. Soon after collection, each of the pufferfish specimen was dissected into various organs such as skin, liver, gonad, stomach, intestine, flesh and the whole organ or a part (where organ size is too large) soaked in separate disposable plastic tube (TPP, Trasadingen, Switzerland) containing approximately 15 mL of ethanol-water (7:3, *v/v*). Samples were then transported to Tohoku University, Sendai, Japan. Note that samples were transported at room temperature due to the lack of proper freezing equipment and longer (two weeks) transportation period which involved air-shipments and formal quarantine checkups by authorities from Solomon Islands and Japan. Upon arrival, samples were kept below −25 °C until use.

Table 2-1. Characterisation of *A. hispidus* specimens from Solomon Islands

***A. hispidus* specimens**	**Gender**	**Body Length**	**Body Weight**
A. hispidus No.1	Female	19 cm	130 g
A. hispidus No.2	Male	17 cm	118 g
A. hispidus No.3	Male	18 cm	120 g

Table 2-2. Characterisation of *A. nigropunctatus* specimens from Solomon Islands

***A. nigropunctatus* specimens**	**Gender**	**Body Length**	**Body Weight**
A. nigropunctatus No.1	Female	19 cm	163 g
A. nigropunctatus No.2	Male	37 cm	320 g
A. nigropunctatus No.3	Female	20 cm	180 g

Table 2-3. Characterisation of *D. holocanthus* specimens from Solomon Islands

***D. holocanthus* specimens**	**Gender**	**Body Length**	**Body Weight**
D. holocanthus No.1	Female	30 cm	310 g
D. holocanthus No.2	Male	35 cm	350 g

For comparison, four living specimens of *A. nigropunctatus* and three living specimens of *A. hispidus* were collected from April to June 2015 in Okinawa, Japan and were sent to Tohoku University. Upon arrival, each specimen was dissected into organs and kept frozen at −25 °C until use. The characterisation of pufferfish from Okinawa, Japan were recorded in Tables 2-4, 2-5 and 2-7.

Table 2.4. Characterisation of *A. hispidus* specimens from Okinawa, Japan

***A. hispidus* specimens**	**Gender**	**Body Length**	**Body Weight**
A. hispidus No.1	Male	17 cm	112 g
A. hispidus No.2	Female	17 cm	124 g
A. hispidus No.3	Male	10 cm	31 g

Table 2-5. Characterisation of *A. nigropunctatus* specimens from Okinawa, Japan

***A. nigropunctatus* specimens**	**Gender**	**Body Length**	**Body Weight**
A. nigropunctatus No.1	Male	15 cm	67 g
A. nigropunctatus No.2	Male	21 cm	375 g
A. nigropunctatus No.3	Male	14 cm	70 g
A. nigropunctatus No.4	Female	16 cm	130 g

Table 2-6. Solomon Islands *A. hispidus* No.1-3, *A. nigropunctatus* No.1-3 and *D. holocanthus* No.1-2 (weight in grams)

Specimens	**Skin**	**Liver**	**Gonad**	**Stomach**	**Intestine**	**Flesh**
A. hispidus No.1	24.9 g	8.0 g	82.5 g	2.8 g	0.8 g	
A. hispidus No.2	17.9 g	8.0 g	0.7 g	1.0 g		
A. hispidus No.3	13.7 g	4.6 g	0.5 g	2.3 g	0.4 g	7.9 g
A. nigropunctatus No.1	21.9 g	3.7 g	2.8 g	1.5 g	0.5 g	
A. nigropunctatus No.2	3.4 g	20.4 g	16.0 g			
A. nigropunctatus No.3	9.2 g	3.9 g	0.7 g	2.5 g		
D. holocanthus No.1	21.7 g	18.5 g	19.5 g	7.0 g		
D. holocanthus No.2	22.2 g	28.5 g	17.0 g	11.0 g	29.5 g	21.3 g

Table 2-7. Okinawan *A. hispidus* No. 1-3 and *A. nigropunctatus* No. 1-4 (weight in grams).

Specimens	**Skin**	**Liver**	**Gonad**	**Stomach**	**Intestine**	**Flesh**	**Spleen**
A. hispidus No.1	17.6 g	2.7 g	0.3 g	1.2 g	7.4 g	6.8 g	0.3 g
A. hispidus No.2	15.0 g	2.0 g	0.9 g	1.5 g	5.5 g	7.5 g	0.2 g
A. hispidus No.3	8.6 g	1.5 g	0.1 g	0.9 g	2.4 g	3.0 g	0.09 g
A. nigropunctatus No.1	37.7 g	0.4 g	0.8 g	3.2 g	0.5 g	26.2 g	0.3 g
A. nigropunctatus No.2	67.1 g	29.9 g	14.2 g	5.8 g	50.4 g	38.8 g	0.5 g
A. nigropunctatus No.3	20.2 g	1.3 g	0.5 g	0.8 g	4.5 g	8.8 g	0.4 g
A. nigropunctatus No.4	12.4 g	2.6 g	1.1 g	1.7 g	5.3 g	8.0 g	0.3 g

The pictures of few pufferfish specimens used in the study and a general procedure involved in sample preparations, toxin extraction and preliminary analysis of toxins are outlined in Scheme 2-1.

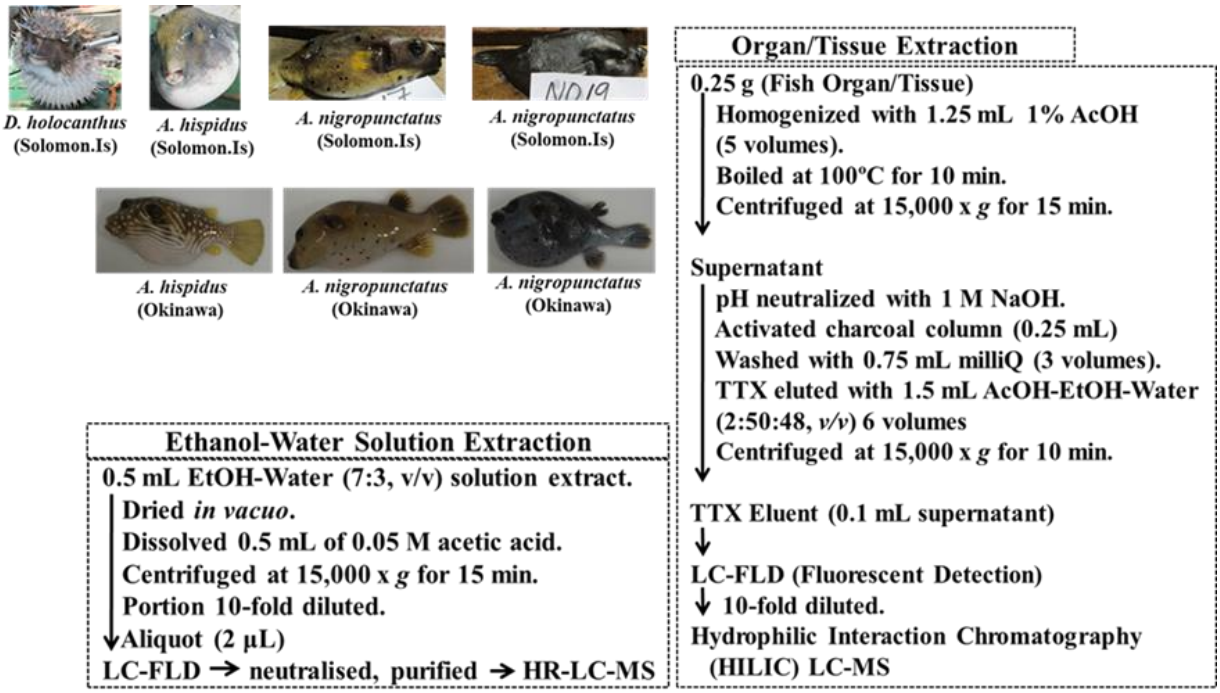

Scheme 2-1. General procedure used in the TTX analysis.

2-2.2 Standards and Reagents

The standard used in the analysis was a semi-purified TTXs mixture prepared from the ovary of *Takifugu poecilonolus* which was treated with charcoal column,[42,46] while the authentic 11-oxoTTX was obtained by a chemical oxidation of TTX.[49]

A highly purified TTX was used to create a calibration curve for HR-LC-MS analysis. Standard mixture of STX, dcSTX, and neoSTX were prepared (approved under AOAC guidelines) by Prof. Emeritus Dr. Yasukatsu Oshima.[64] Activated charcoal and all the solvents for LC and the reagents were purchased from Wako Pure Chemical Industries (Osaka, Japan), while the ammonium formate for LC-MS, heptafluorobutyrate acid, and acetonitrile for LC-FLD were purchased from Sigma-Aldrich (St. Louis, MO, USA).

2-2.3 Preliminary Liquid Chromatography-Fluorescent Detection (LC-FLD) Analysis of TTXs in the Skin of A. hispidus from the Solomon Islands

From the ethanol-water (7:3, *v/v*) solution used as a preserving solvent mixture for the skin of the Solomon Islands *A. hispidus*, an aliquot of 0.5 mL was acidified with acetic acid, dried *in vacuo*, and then dissolved in 0.5 mL of 0.05 M acetic acid. After centrifugation, a small volume of supernatant was diluted ten-fold with 0.05 M acetic acid. An aliquot (2 μL) of the diluted solution was then applied to the LC-FLD for TTXs measurement. Likewise, a part (0.25 g) of the actual skin specimen preserved in the tube of ethanol solution was extracted with 1.25 mL of 0.2 M acetic acid (*v/v*) in boiling water. The extract was centrifuged at 15,000 × *g* and an aliquot (2 μL) of the supernatant was applied to the LC-FLD.[65,66)]

2-2.4 Preparation of samples for HR-LC-MS Analysis

2-2.4.1 Ethanol-water (7:3, v/v) solution (preserving solvent mixture) from the organs of Solomon Islands Pufferfish

From the preserving solvent mixture (15 mL of ethanol-water (7:3, *v/v*) solution) of each of the pufferfish organs, an aliquot of 0.5 mL was separately mixed with 5 μL of acetic acid, and dried *in vacuo*. The dried residue was dissolved in 0.5 mL of 0.05 M acetic acid and neutralized with 1 M NaOH aqueous solution. The neutralized solution was then applied to the activated charcoal with a column volume of 250 μL packed in a glass pipette that was pre-equilibrated with water. After further washing the charcoal with 0.75 mL (3 volumes) of water, TTXs were eluted with 1.5 mL of acetic acid-ethanol-water (2:50:48, *v/v*) solution mixture. A part (50 μL) of this eluate was dried *in vacuo* and dissolved in 50 μL of 0.05 M acetic acid, and then filtered through Cosmospin Filter H (Nacalai Tesque, Inc., Kyoto, Japan). After the filtrate was diluted with 0.05 M acetic acid, a part of this solution was used for HR-LC-MS. From the LC-FLD quantitative analysis, the estimated recovery of TTXs in the organs from the activated charcoal was approximately 70%. This recovery ratio was also used in the calculation of the final TTXs concentrations in the organs from Solomon Islands pufferfish.

2-2.4.2 Organs of Pufferfish from both Solomon Islands and Okinawa, Japan

A part (0.25 g) of the organ from each specimen was weighed out and homogenized with 1.25 mL of acetic acid-water (1:99, *v/v*). The mixture was then boiled for 10 minutes in a 1.5 mL micro (Eppendorf) tube, and centrifuged at 15,000 × *g* for 15 minutes at 4 °C. Half (0.75 mL) of the supernatant was neutralized with 1 M NaOH, and then applied to the pre-equilibrated charcoal (column volume 250 μL). Further steps involved in sample treatment follows the same procedure outlined in Sections *2.2.3* and *2.2.4.1*.

2-2.5 LC-FLD for TTXs

Post-column LC-fluorescent detection (LC-FLD) for TTXs was performed as previously described[65,66] (Figure 2-2). Briefly, the LC conditions were as follow: Develosil C30 UG-5 (0.46 cm i.d. × 25 cm) (Nomura Chemical, Seto, Japan) with 30 mM ammonium heptafluorobutyrate buffer (pH 5.0) and 10 mM ammonium formate buffer (pH 5.0) containing 1% (*v/v*) acetonitrile at a flow rate of 0.4 mL/min; for the post column reaction 4 M NaOH at a flow rate of 0.7 mL/min to be heated at 105 °C in the stainless tube (0.46 mm i.d. × 3.5 m). The chromatography was performed at 20 °C. The derived fluorophores by post column reaction were detected by a Jasco FP2025 plus fluoromonitor (Jasco, Tokyo, Japan) with the excitation wavelength set at 365 nm and emission wavelength at 510 nm.

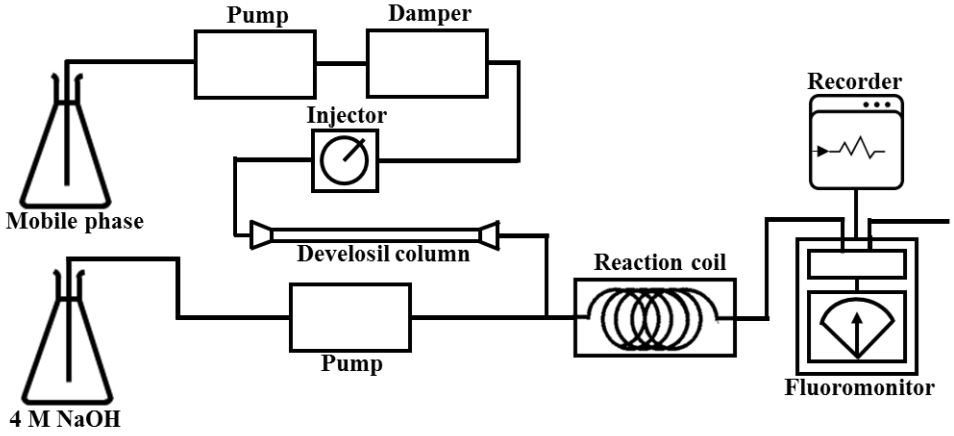

Diagram adapted from Yasumoto T and Michishita T. *Agric. Biol. Chem.* **1985** 49, 3077–3080.

Figure 2-2. A flow diagram of LC-FLD used in the TTX investigation.

2-2.6 High Resolution LC-MS and LC-MS/MS for TTXs

HILIC LC-MS and MS/MS methods were performed as reported by Yotsu -Yamashita M, *et al*.[42] The LC system for TTXs was a Shimadzu Nexera UHPLC System (Shimadzu, Kyoto, Japan) and consisted of LC-10AD pump (Shimadzu, Kyoto, Japan), autosampler (SIL-30AC, Shimadzu) and TSKgel Amide-80 column (150 × 2.0 mm i.d., particle size 5 μm, Tosoh, Tokyo, Japan). The mobile phase was 16 mM ammonium formate in water/acetonitrile/formic acid (30:70:0.002, *v/v*) with a flow rate of 0.2 mL/min at 28 °C in the isocratic mode with an injection volume of 2–3 μL and run time of 25 min.

The LC system connected to a Q-TOF MS spectrometer, MicrOTOFQII (Bruker Daltonics, Bremen, Germany) was equipped with an ESI source and consisted of the following MS spectrometer conditions: positive ionization mode, dry gas: nitrogen 7 L/min, dry temperature: 180 °C, nebulizer:1.6 Bar, capillary: −4500 V. All the preset ions (listed below) corresponding to the $[M + H]^+$ ions were analyzed in the extracted ion chromatograms (EIC). Ions were set at *m/z* 320.1088 (TTX, 4-*epi*TTX), 302.0983 (4,9-anhydroTTX), 304.1139 (11-deoxyTTX, 5-deoxyTTX), 288.1190 (6,11-trideoxyTTX, 5,11-dideoxyTTX), 272.1241 (5,6,11-trideoxyTTX, 4-*epi*-5,6,11-trideoxyTTX) and 254.1135 (4,9-anhydro-5,6,11-trideoxyTTX, 4,4a-anhydro-5,6,11-trideoxyTTX), 336.1038 (11-oxoTTX, 4-*epi*-11-oxoTTX) and 318.0932 (4,9-anhydro-11-oxoTTX). While all TTX analogues were quantified by HR-LC/MS based on the standard curve for TTX, the peak of 11-oxoTTX and 4-*epi*-11-oxoTTX in the samples from the Solomon Islands seemed to be suppressed by certain compounds eluting at the same retention time. Thus, 11-oxoTTX and 4-*epi*-11-oxoTTX were quantified using LC-FLD.

Besides 11-oxoTTX and 4-*epi*-11-oxoTTX, the limit of detection (LOD) for all TTX analogues were (*S/N* > 3, 0.01 μg/g) and their limit of quantitation (LOQ) were (*S/N* > 10, 0.03 μg/g), while the LOD and LOQ of 11-oxoTTX and 4-*epi*-11-oxoTTX were 0.04 μg/g and 0.14 μg/g, respectively. MS/MS was performed in AutoMS/MS mode setting $[M + H]^+$ as the precursor ions. The precursor ions and sweeping collision energy were 320.1088 ± 0.1, 36.9–55.4 eV for TTX, and 336.1038 ± 0.1, 38.1–57.1 eV for 11-oxoTTX.

2-2.7 High Resolution LC-MS for STXs

STX, dcSTX and neoSTX were analyzed using HR-LC-MS. The LC system for STXs was a Shimadzu Nexera UHPLC System (Shimadzu, Kyoto, Japan) and consisted of LC-10AD pump (Shimadzu, Kyoto, Japan), autosampler (SIL-30AC, Shimadzu) and TSKgel Amide-80 column (150 × 2.0 mm i.d., particle size 5 μm, Tosoh, Tokyo, Japan). The mobile phase used in STXs was 2 mM ammonium formate in water/acetonitrile/formic acid (30:62:0.0125, *v/v*) at a flow rate of 0.2 mL/min at 25 °C in the isocratic mode with an injection volume of 2.0 μL and run time of 30 min.[64)] The mass spectrometer and its condition were same as those of TTXs analysis described above (see section 2-2.6). STX, dcSTX and neoSTX were detected as $[M + H]^+$ ions at *m/z* 300.1415 ± 0.05, 257.1356 ± 0.05, and 316.1365 ± 0.05, respectively. LOD (*S/N* > 3) and LOQ (*S/N* > 10) for STX were 0.02 μg/g and 0.07 μg/g, neoSTX, 0.05 μg/g and 0.18 μg/g, and dcSTX, 0.07 μg/g and 0.25 μg/g, respectively.

2-3.0 Results

2-3.1 Evaluation of TTX and its analogues in pufferfish from the Solomon Islands

2-3.1.1 Results on preliminary LC-FLD analysis of TTXs in the skin of A. hispidus from the Solomon Islands

Due to longer transit time and the lack of proper freezing equipment during flight duration, the feasibility of the specimens for analysis were checked as soon as the samples arrived at Tohoku University. Practically, there are several stable solvents and condition that can give maximum amount of TTXs recovery which were unfortunately unavailable in our case. TTX powder is known to be stable in diluted citrate or acetate buffer solutions at 1 mg/mL while in aqueous form it is much stable in mild acidic solvents of pH 4-5 and is in excellent state when stored in frozen condition.[67] On the other hand, strong acidic and alkaline conditions can easily decompose the TTX and this was avoided during the specimen preservation. Ethanol-water (7:3 *v*/*v*) solution was used due to its preservative properties especially for marine samples, being polar in nature (approx. pH 7) which is fairly soluble for the TTXs and of its ease of accessibility.

However, although ethanol may be soluble for TTXs, its hydroxyl group may slightly shift the pH towards basic condition which can potentially decompose the TTXs. Therefore, a preliminary analysis of TTX was carried out to see if specimens were still in good conditions for TTXs analysis or that specimens have been badly decomposed during the two weeks of transportation and transit period. Under such conditions and during longer period, certain TTX and its analogues are more likely to be hydrolyzed or degraded into tetrodonic acid (Figure 2-3) type compounds or other quinazoline related compounds,[41,68] and this conversion can be detected using LC-FLD for TTXs [65,66] without specific pre-purification.

In this preliminary analysis, both the preserving ethanol solution of the skin of *A. hispidus* (three specimens) and the skin specimen that was soaked in this preserving ethanol solution were analyzed using LC-FLD.[69)] This procedure was repeated for each of the sample specimen from the Solomon Islands. An exemplary LC-FLD chromatogram obtained in the skin of the *A. hispidus* No.3 specimen is shown in Figure 2-3. Result showed that the peak area of tetrodonic acid type analogues (peak A) in both the ethanol solution (Figure 2-3b) and the extract of the skin (Figure 2-3c) was approximately 60% to that of TTX (peak C). Since the samples from the Solomon Islands may naturally contain a considerable amount of tetrodonic acid even before collection, the content of tetrodonic acid as revealed by the peak was assumed to be the combination of natural and the hydrolyzed forms of some TTXs compounds.

Other clearly observed peaks included 11-oxoTTX and 4-*epi*-11-oxoTTX (peak B composition), 4,9-anhydro-11-oxoTTX (peak D), 4-*epi*TTX (peak E) and 4,9-anhydroTTX (peak F). Despite the partial conversion of TTXs into tetrodonic acid type analogues, pufferfish samples transported from the Solomon Islands were still in good condition for TTXs analysis as confirmed by this LC-FLD data.[69)]

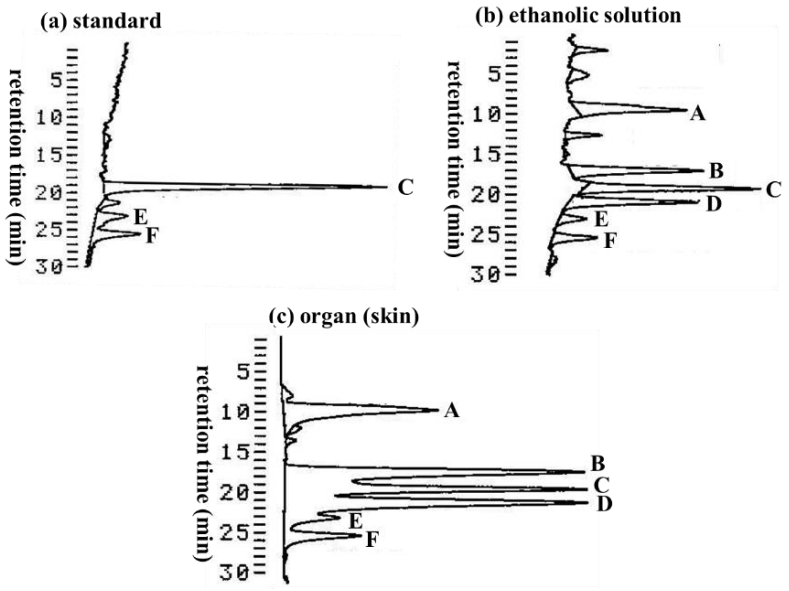

Figure 2-3. The LC-FLD chromatograms of the skin extracts of the *A. hispidus* No.3 specimen from the Solomon Islands. (**a**) The TTXs standard solution (5 μL) containing TTX 1.0 μg/mL, 4-*epi*TTX 0.18 μg/mL, and 4,9-anhydroTTX 0.24 μg/mL (attenuation 3), (**b**) Aliquot sample (6 μL) prepared from the ethanol-water (7:3, *v/v*) solution used to soak the skin of *A. hispidus* No.3 specimen (10.5 mL/g) (attenuation 6), (**c**) The sample solution (2 μL) prepared from 0.2 M acetic acid (*v/v*) extract of the skin of *A. hispidus* No.3 specimen soaked in ethanol solution (5.0 mL/g) (attenuation 6). A: tetrodonic acid types, B: 11-oxoTTX and 4-*epi*-11-oxoTTX, C: TTX, D: 4,9-anhydro-11-oxoTTX, E: 4-*epi*TTX, F: 4,9-anhydroTTX.

2-3.1.2 High Resolution-LC-MS characterization and quantitation of TTX and its analogues.

Organs soaked in the preserving solvent were separately extracted with 0.2 M acetic acid (*v/v*) and boiling water. After passing each extract through an activated charcoal column, each sample was analyzed using High Resolution (HR) HILIC-LC-MS (Q-TOF MS) with the conditions in section 2-2.6. [42,66-72] An example of the mass chromatograms with the tolerance width of the ions of TTX and its analogues in the skin of *A. hispidus* (No.3 specimen) are shown in Figure 2-4, while other examples are in the appendix p.92-93. TTX and all its analogues were quantified using HR-LC-MS based on the calibration curve drawn from the TTX standard.

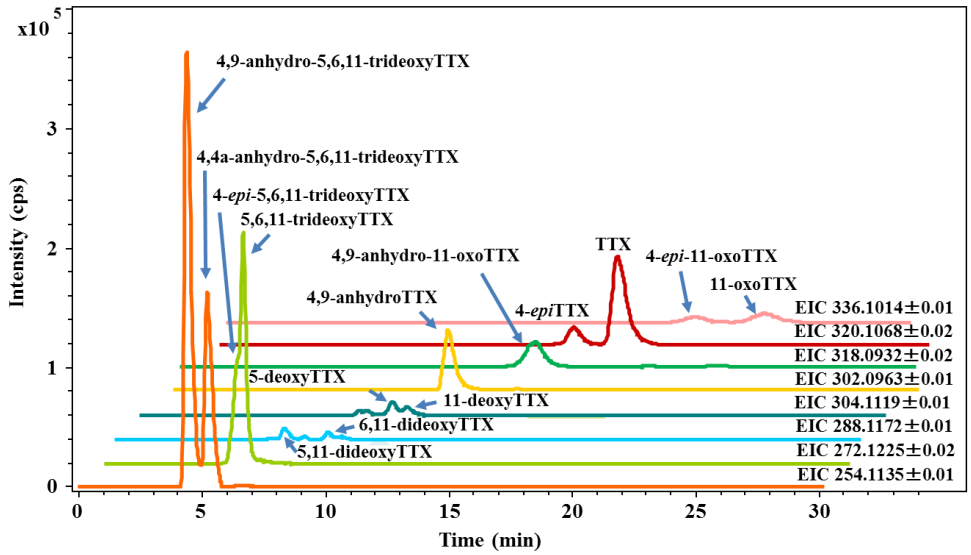

Figure 2-4. HR-LC-MS chromatograms (extracted ion chromatograms: EICs) of charcoal treated sample solution (2 µL) prepared from the skin of *A. hispidus* No.3 specimen (25 mL/g) from the Solomon Islands soaked in ethanol solution. The sample solution contained TTX 1.4 µg/mL, 4-*epi*TTX 0.30 µg/mL, 4,9-anhydroTTX 0.80 µg/mL, 5-deoxyTTX 0.13 µg/mL, 6,11-dideoxyTTX 0.03 µg/mL, 5,11-dideoxyTTX 0.09 µg/mL, 5,6,11-trideoxyTTX and 4-*epi*-5,6,11-trideoxyTTX (total of two analogues 1.8 µg/mL), 4,4a-anhydro-5,6,11-trideoxyTTX 2.7 µg/mL, 11-oxoTTX 0.50 µg/mL, 4-*epi*-11-oxoTTX 0.50 µg/mL, and 4,9-anhydro-11-oxoTTX 0.60 µg/mL.

However, based on the HR-LC-MS method, the Solomon Islands samples showed that the peak areas of 11-oxoTTX and 4-*epi*-11-oxoTTX on the extracted ion chromatograms (EIC) at *m/z* 336.1014 were much reduced than were initially predicted by the LC-FLD analysis. It was assumed that ionization may have been suppressed by certain compounds eluting at the same retention time, therefore quantification of 11-oxoTTX and 4-*epi*-11-oxoTTX were instead carried out using LC-FLD system. The limit of detection (LOD) for TTX and its analogues, excluding 11-oxoTTX and 4-*epi*-11-oxoTTX from the Solomon Islands samples, was (*S/N* > 3, 0.01 μg/g), while the limit of quantitation (LOQ) was (*S/N* > 10, 0.03 μg/g). Since 11-oxoTTX and 4-*epi*-11-oxoTTX from the Solomon Islands samples were quantified by LC-FLD system, their LOD and LOQ were adjusted accordingly and at 0.04 μg/g and 0.14 μg/g, respectively.

Results showed that the major constituents in almost all the skin samples were TTX, 4,9-anhydroTTX, 5,6,11-trideoxyTTX (with its 4-*epi* form), 4,4a-anhydro-5,6,11-trideoxyTTX, and 4,9-anhydro-5,6,11-trideoxyTTX.[69] Interestingly, 11-oxoTTX, a rare but more potent analogue[44,45] with its 4-*epi* and 4,9-anhydro forms were also observed in almost all the *A. hispidus* and *A. nigropunctatus* from both Solomon Islands and Okinawa, Japan.[69] Due to its potent pharmacological effect as revealed by previous studies, the detection and quantification of 11-oxoTTX concentration (with more accuracy) in toxic pufferfish is much more of an important finding in this study.

The HR-ESIMS/MS spectrum of 11-oxoTTX and TTX showed a similar fragmentation pattern with characteristic fragment ions detected at *m/z* 162.0660 ($C_8H_8N_3O$) and 178.0614 ($C_8H_8N_3O_2$) which corresponded to the two major fragment ions believed to be 2-aminohydroquinazoline and 2-aminodihydroquinazone, respectively[42] (Figure 2-5). Besides the major analogues, few minor analogues such as the monodeoxyTTX (11-deoxyTTX and 5-deoxyTTX) and dideoxyTTX (5,11-dideoxyTTX and 6,11-dideoxyTTX) types were also detected. Additional small peaks observed in most of the toxic pufferfish from both regions may potentially correspond to other unconfirmed minor analogues such as 4,9-anhydro-5,11-dideoxyTTX (*m/z* 270 eluting at 5 min), frequent peak with *m/z* 270 (eluting at 6.2 min), 4,9-anhydro-5-deoxyTTX (*m/z* 286 eluting at 7.7 min) and 4-*epi*-6,11-dideoxyTTX (*m/z* 288 eluting at 8.6 min).

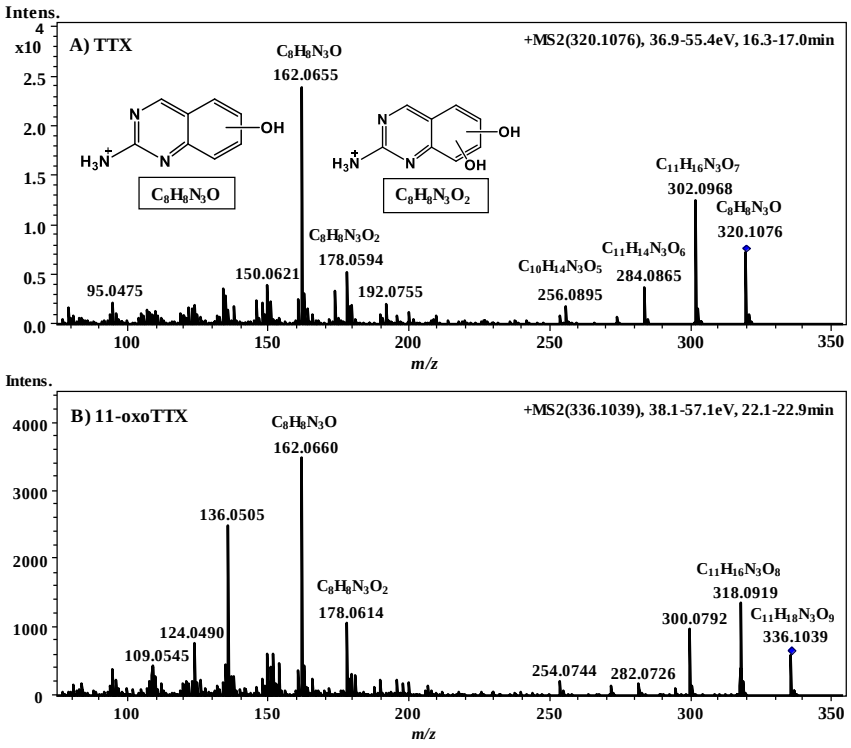

Figure 2-5. HR-LC-MS/MS spectra of TTX (a) and 11-oxoTTX (b) in the skin of *A. hispidus* No.3 specimen from the Solomon Islands. The sample solution (2 μL) was same as shown in Figure 2-4. The predicted structures of the major fragment ions were superimposed in the spectra.

2-3.1.3 The concentrations of TTX and its analogues in organs of A. hispidus, A. nigropunctatus, and D. holocanthus from the Solomon Islands

All of the Solomon Islands specimens were analyzed for the presence of TTX and its analogues. This included specimens *A. hispidus* No.1-3 (Tables 2-8 to 2-11), *A. nigropunctatus* No.1-3 (Tables 2-12 to 2-15), and *D. holocanthus* No.1-2 (All < LOD, and a representative chromatogram can be seen in appendix p.93). TTX and its analogues both in the ethanol preserving solutions and in soaked organs were separately quantified using HR-LC-MS just after the prepurification procedure. To calculate for the overall concentration of TTX and its analogues in each organ, individual concentration from the organ was added to the TTX concentration obtained from the ethanol preserving solvent which is initially calculated based on the corresponding organ weight soaked in each tube. Also of importance in this calculation is the inclusion of the 70% recovery rate obtained in charcoal column eluent measured in HR-LC-MS and that in the LC-FLD.

The results of individual toxic specimen in Tables 2-8 to 2-10 and 2-12 to 2-14 showed that the amount of TTX concentrations vary in both the ethanol preserving solutions and the actual organs. For TTX, more content seems to have remained in the organs compared to those (TTX) that were naturally extracted and released into the ethanol solutions during the storage period. On the contrary, in analogues like 5,6,11-trideoxyTTX and 4,9-anhydro-5,6,11-trideoxyTTX, their levels seemed to be higher in the ethanol preserving solutions than in the actual organs of some specimens (See appendix p.92). Probably organ texture in relation to the compounds' structures may contribute to the rate of toxin release during the storage condition.

Based on the result in the TTXs concentration tables, it is evident that TTX, 5,6,11-trideoxyTTX, 4,4a-anhydro-5,6,11-trideoxyTTX, and 4,9-anhydro-5,6,11-trideoxyTTX were the most abundant analogues in all organs of the toxic Solomon Islands pufferfish species.[69] Other minor analogues were also present but in a relatively lower content. Besides TTX, of much importance to risks of food poisoning in the Solomon Islands is the confirmed presence of potent analogue[48,49], 11-oxoTTX which was detected in the skin of almost all Solomon Islands toxic specimens.

A general toxin profile also showed that TTX concentrations in the skin were higher in all specimens, compared to the relatively lower concentrations in the liver, ovary, testis, stomach, and intestine. As seen from the tables of collective data, Tables 2-11 and 2-15, the highest TTX concentrations in the skin of *A. hispidus* and *A. nigropunctatus* were 51.0 and 28.7 μg/g, respectively. Moreover, the study also confirmed that TTXs in skin, liver, gonad, stomach, intestine, and flesh of the two specimens (a male and a female) of *D. holocanthus* from the Solomon Islands were less than the limit of detection: LOD; $S/N > 3$, 0.01 μg/g. (See appendix p.93).

Table 2-8. TTX and its analogues (μg/g) in the organs of *A. hispidus* No.1 from the Solomon Islands.

Organ	Skin	Skin-EtOH	Total	Liver	Liver-EtOH	Total	Ovary	Ovary-EtOH	Total	Stomach	Stomach-EtOH	Total	Intestine	Intestine-EtOH	Total
TTX	36.10	14.86	51.0	2.14	0.56	2.70	1.73	0.15	1.89	2.34	0.23	2.57	1.90	0.06	1.95
4-*epi*TTX	9.70	5.07	14.8	0.30	0.13	0.43	0.18	0.04	0.23	0.10	0.03	0.12	0.25	0.02	0.27
4,9-anhydroTTX	19.32	6.65	26.0	0.95	<LOD	0.95	<LOD	<LOD	<LOD	0.94	<LOD	0.94	0.02	<LOD	0.02
11-deoxyTTX	1.73	0.91	2.6	0.11	<LOD	0.11	<LOD	<LOD	<LOD	0.09	<LOD	0.09	0.06	<LOD	0.06
5-deoxyTTX	1.10	0.54	1.6	0.21	<LOD	0.21	<LOD	<LOD	<LOD	0.16	<LOD	0.16	0.10	<LOD	0.10
6,11-dideoxyTTX	0.49	0.32	0.8	0.08	<LOD	0.08	<LOD	<LOD	<LOD	<LOD	<LOD	<LOD	<LOD	<LOD	<LOD
5,11-dideoxyTTX	0.68	0.35	1.0	0.14	<LOD	0.14	<LOD	<LOD	<LOD	0.12	<LOD	0.12	<LOD	<LOD	<LOD
5,6,11-trideoxyTTX	14.49	15.03	29.5	4.91	3.72	8.64	3.73	3.38	7.11	<LOD	<LOD	<LOD	2.96	0.87	3.83
4,4a-anhydro-5,6,11-trideoxyTTX	12.51	12.31	24.8	8.15	2.29	10.44	5.51	1.23	6.74	6.35	1.57	7.92	4.99	0.36	5.36
4,9-anhydro-5,6,11-trideoxyTTX	24.79	45.63	70.4	9.19	2.96	12.15	6.16	1.78	7.94	5.84	1.87	7.71	4.60	0.43	5.04
11-norTTX-6(*S*)-ol	1.67	0.56	2.2	<LOD	<LOD	<LOD	0.04	<LOD	0.04	0.06	<LOD	0.06	0.07	<LOD	0.07
11-oxoTTX	2.07	0.84	2.9	0.30	<LOD	0.30	0.01	<LOD	0.01	0.02	<LOD	0.02	0.05	<LOD	0.05
4-*epi*-11-oxoTTX	2.82	0.39	3.2	0.03	<LOD	0.03	<LOD	<LOD	<LOD	<LOD	<LOD	<LOD	0.04	<LOD	0.04
4,9-anhydro-11-oxoTTX	7.40	1.78	9.2	0.16	0.01	0.18	0.22	<LOD	0.22	0.29	<LOD	0.29	0.21	<LOD	0.21

Table 2-9. TTX and its analogues (μg/g) in the organs of *A. hispidus* No.2 from the Solomon Islands.

Organ	Skin	Skin-EtOH	Total	Liver	Liver-EtOH	Total	Testis	Testis-EtOH	Total	Stomach	Stomach-EtOH	Total
TTX	5.64	1.59	7.22	7.02	0.97	7.99	11.59	0.14	11.72	9.29	0.16	9.45
4-*epi*TTX	1.46	0.37	1.82	1.13	0.16	1.29	1.91	0.02	1.93	1.50	0.03	1.52
4,9-anhydroTTX	3.04	0.61	3.65	3.60	0.40	4.00	6.57	0.06	6.63	4.86	0.07	4.93
11-deoxyTTX	<LOD	0.10	0.10	0.61	0.06	0.67	1.16	0.01	1.17	0.65	0.01	0.66
5-deoxyTTX	<LOD	<LOD	<LOD	0.13	<LOD	0.13	0.35	<LOD	0.35	<LOD	<LOD	<LOD
6,11-dideoxyTTX	<LOD	<LOD	<LOD	0.08	<LOD	0.08	<LOD	<LOD	<LOD	<LOD	<LOD	<LOD
5,11-dideoxyTTX	<LOD	<LOD	<LOD	<LOD	<LOD	<LOD	<LOD	<LOD	<LOD	<LOD	<LOD	<LOD
5,6,11-trideoxyTTX	1.04	0.13	1.17	6.26	1.08	7.33	9.88	0.14	10.02	10.62	0.22	10.84
4,4a-anhydro-5,6,11-trideoxyTTX	1.12	0.24	1.36	5.00	0.99	5.99	8.84	0.15	8.99	7.70	0.19	7.89
4,9-anhydro-5,6,11-trideoxyTTX	1.78	0.28	2.06	6.60	1.90	8.49	8.93	0.22	9.15	8.56	0.30	8.86
11-norTTX-6(*S*)-ol	<LOD	<LOD	<LOD	0.49	0.03	0.51	1.01	0.01	1.02	0.73	0.01	0.74
11-oxoTTX	0.21	0.11	0.32	0.32	0.03	0.35	0.41	<LOD	0.41	0.31	<LOD	0.31
4-*epi*-11-oxoTTX	0.03	0.03	0.06	0.06	<LOD	0.06	0.09	<LOD	0.09	0.13	<LOD	0.13
4,9-anhydro-11-oxoTTX	<LOD	<LOD	<LOD	0.35	0.02	0.37	0.58	<LOD	0.58	0.40	<LOD	0.41

Table 2-10. TTX and its analogues (μg/g) in the organs of *A. hispidus* No.3 from the Solomon Islands.

Organ	Skin	Skin-EtOH	Skin-Total	Liver	Liver-EtOH	Liver-Total	Testis	Testis-EtOH	Testis-Total	Stomach	Stomach-EtOH	Stomach-Total	Intestine	Intestine-EtOH	Intestine-Total	Flesh	Flesh-EtOH	Flesh-Total
TTX	28.09	19.53	47.62	0.03	<LOD	0.03	<LOD	<LOD	<LOD	0.30	0.27	0.58	0.15	5.30	5.45	0.02	0.05	0.07
4-*epi*TTX	5.24	3.46	8.70	<LOD	<LOD	<LOD	<LOD	<LOD	<LOD	<LOD	<LOD	<LOD	<LOD	<LOD	<LOD	<LOD	<LOD	<LOD
4,9-anhydroTTX	15.19	7.39	22.57	<LOD	<LOD	<LOD	<LOD	<LOD	<LOD	<LOD	<LOD	<LOD	<LOD	<LOD	<LOD	<LOD	<LOD	<LOD
11-deoxyTTX	2.65	1.67	4.32	<LOD	<LOD	<LOD	<LOD	<LOD	<LOD	<LOD	<LOD	<LOD	<LOD	<LOD	<LOD	<LOD	<LOD	<LOD
5-deoxyTTX	2.91	2.60	5.51	<LOD	<LOD	<LOD	<LOD	<LOD	<LOD	<LOD	0.15	0.15	0.10	<LOD	0.10	<LOD	<LOD	<LOD
6,11-dideoxyTTX	0.66	0.81	1.47	<LOD	<LOD	<LOD	<LOD	<LOD	<LOD	0.06	<LOD	0.06	<LOD	<LOD	<LOD	<LOD	<LOD	<LOD
5,11-dideoxyTTX	1.70	1.53	3.23	<LOD	<LOD	<LOD	<LOD	<LOD	<LOD	0.28	0.29	0.56	0.16	<LOD	0.16	<LOD	<LOD	<LOD
5,6,11-trideoxyTTX	46.52	37.76	84.28	<LOD	<LOD	<LOD	<LOD	<LOD	<LOD	7.21	12.33	19.54	5.54	<LOD	5.54	<LOD	<LOD	<LOD
4,4a-anhydro-5,6,11-trideoxyTTX	37.71	32.37	70.08	0.08	0.118	0.19	<LOD	<LOD	<LOD	3.15	4.19	7.34	2.93	2.00	4.93	0.03	0.08	0.11
4,9-anhydro-5,6,11-trideoxyTTX	66.03	67.19	133.21	0.13	0.210	0.34	<LOD	<LOD	<LOD	5.32	16.24	21.56	4.92	5.74	10.66	0.05	0.06	0.11
11-norTTX-6(*S*)-ol	<LOD	<LOD	<LOD	<LOD	<LOD	<LOD	<LOD	<LOD	<LOD	<LOD	<LOD	<LOD	<LOD	<LOD	<LOD	<LOD	<LOD	<LOD
11-oxoTTX	4.23	2.84	7.07	<LOD	<LOD	<LOD	<LOD	<LOD	<LOD	0.01	<LOD	0.01	<LOD	1.68	1.68	0.02	0.01	0.04
4-*epi*-11-oxoTTX	2.37	1.16	3.53	<LOD	<LOD	<LOD	<LOD	<LOD	<LOD	0.01	<LOD	0.01	<LOD	0.26	0.26	0.01	<LOD	0.01
4,9-anhydro-11-oxoTTX	9.74	3.99	13.73	<LOD	<LOD	<LOD	<LOD	<LOD	<LOD	0.08	<LOD	0.08	0.26	1.47	1.72	<LOD	0.01	0.01

Table 2-11. Collective data of TTX and its analogues (μg/g) in the organs of *A. hispidus* from the Solomon Islands.

Organ	Skin *(n=3)*	Liver *(n=3)*	Ovary *(n=1)*	Testis *(n=2)*	Stomach *(n=3)*	Intestine *(n=2)*	Flesh *(n=1)*
TTX	7.20–51.0	0.03–7.99	1.89	< LOD, 11.7	0.58–9.45	1.95, 5.45	0.07
4-*epi*TTX	1.80–14.8	< LOD-1.29	0.23	< LOD, 1.93	< LOD-1.52	< LOD, 0.27	< LOD
4,9-anhydroTTX	3.60–26.0	< LOD-4.00	< LOD	< LOD, 6.63	< LOD-4.93	< LOD, < LOQ (0.02)	< LOD
11-deoxyTTX	0.10–4.32	< LOD-0.67	< LOD	< LOD, 1.17	< LOD-0.66	< LOD, 0.06	< LOD
5-deoxyTTX	< LOD-5.51	< LOD-0.21	< LOD	< LOD, 0.35	< LOD-0.16	0.10, 0.10	< LOD
6,11-dideoxyTTX	< LOD-1.47	< LOD-0.08	< LOD	< LOD	< LOD-0.06	< LOD	< LOD
5,11-dideoxyTTX	< LOD-3.23	< LOD-0.14	< LOD	< LOD	< LOD-0.56	< LOD, 0.16	< LOD
5,6,11-trideoxyTTX	1.47–84.3	< LOD-16.4	10.1	< LOD, 14.6	< LOD-19.5	5.54, 7.20	0.05
4,4a-anhydro-5,6,11-trideoxyTTX	1.36–70.1	< LOD-10.4	6.74	< LOD, 8.99	7.34–7.92	4.93, 5.36	0.11
4,9-anhydro-5,6,11-trideoxyTTX	2.06–133.2	0.34–12.2	7.94	< LOD, 9.15	7.71–21.6	5.04, 10.7	0.11
11-norTTX-6(*S*)-ol	< LOD-2.23	< LOD-0.51	0.04	< LOD, 1.02	< LOD-0.74	< LOD, 0.07	< LOD
11-oxoTTX	0.32–7.07	< LOD-0.35	< LOD	< LOD, 0.41	< LOD-0.31	< LOQ(0.05), 1.68	< LOD
4-*epi*-11-oxoTTX	< LOQ(0.06)-3.53	< LOD- < LOQ(0.06)	< LOD	< LOD, < LOQ(0.09)	< LOD- < LOQ(0.13)	< LOD, 0.26	< LOD
4,9-anhydro-11 oxoTTX	< LOD-13.7	< LOD-0.18	0.22	< LOD, 0.58	< LOQ(0.08)-0.41	0.21, 1.72	< LOD

Table 2-12. TTX and its analogues (μg/g) in the organs of *A. nigropanctatus* No.1 from the Solomon Islands.

Organ	Skin	Skin-EtOH	Total	Liver	Liver-EtOH	Total	Ovary	Ovary-EtOH	Total	Stomach	Stomach-EtOH	Total	Intestine	Intestine-EtOH	Total
TTX	18.93	1.22	20.15	0.97	1.20	2.17	0.56	0.58	1.14	1.01	0.55	1.57	0.46	0.09	0.55
4-*epi*TTX	4.53	0.54	5.07	0.15	0.32	0.47	0.05	0.22	0.28	0.13	0.28	0.41	0.04	0.03	0.08
4,9-anhydroTTX	10.01	0.78	10.79	0.46	0.00	0.46	0.23	0.68	0.91	<LOD	<LOD	<LOD	0.17	0.10	0.27
11-deoxyTTX	<LOD	<LOD	<LOD	<LOD	<LOD	<LOD	<LOD	<LOD	<LOD	<LOD	<LOD	<LOD	<LOD	<LOD	<LOD
5-deoxyTTX	<LOD	<LOD	<LOD	<LOD	<LOD	<LOD	<LOD	<LOD	<LOD	<LOD	<LOD	<LOD	<LOD	<LOD	<LOD
6,11-dideoxyTTX	0.01	<LOD	0.01	<LOD	<LOD	<LOD	<LOD	<LOD	<LOD	<LOD	<LOD	<LOD	<LOD	<LOD	<LOD
5,11-dideoxyTTX	<LOD	<LOD	<LOD	0.01	<LOD	0.01	<LOD	<LOD	<LOD	<LOD	<LOD	<LOD	<LOD	<LOD	<LOD
5,6,11-trideoxyTTX	3.59	0.40	3.99	1.26	3.01	4.26	0.92	0.33	1.25	1.25	<LOD	1.25	0.71	0.07	0.78
4,4a-anhydro-5,6,11-trideoxyTTX	2.06	0.33	2.39	1.17	1.50	2.67	0.75	0.17	0.92	1.18	0.14	1.32	0.50	0.02	0.52
4,9-anhydro-5,6,11-trideoxyTTX	3.11	0.79	3.91	1.08	2.08	3.17	0.66	0.41	1.07	0.98	0.33	1.31	0.48	0.06	0.54
11-norTTX-6(*S*)-ol	0.10	<LOD	0.10	0.01	<LOD	0.01	<LOD	<LOD	<LOD	0.01	<LOD	0.01	<LOD	<LOD	<LOD
11-oxoTTX	0.47	0.04	0.51	0.02	<LOD	0.02	<LOD	<LOD	<LOD	0.01	0.04	0.05	<LOD	<LOD	<LOD
4-*epi*-11-oxoTTX	0.48	<LOD	0.40	<LOD	<LOD	<LOD	<LOD	<LOD	<LOD	0.01	<LOD	0.01	<LOD	<LOD	<LOD
4,9-anhydro-11-oxoTTX	1.12	0.04	1.16	0.17	<LOD	0.17	0.11	0.02	0.13	0.18	0.02	0.19	0.07	<LOD	0.07

Table 2-13. TTX and its analogues (μg/g) in the organs of *A. nigropanctatus* No.2 from the Solomon Islands.

Organ	Skin	Skin-EtOH	Total	Liver	Liver-EtOH	Total	Testis	Testis-EtOH	Total
TTX	8.51	<LOD	8.51	<LOD	<LOD	<LOD	<LOD	<LOD	<LOD
4-*epi*TTX	1.61	<LOD	1.61	<LOD	<LOD	<LOD	<LOD	<LOD	<LOD
4,9-anhydroTTX	5.15	<LOD	5.15	<LOD	<LOD	<LOD	<LOD	<LOD	<LOD
11-deoxyTTX	0.83	<LOD	0.83	<LOD	<LOD	<LOD	<LOD	<LOD	<LOD
5-deoxyTTX	0.14	<LOD	0.14	<LOD	<LOD	<LOD	<LOD	<LOD	<LOD
6,11-dideoxyTTX	0.08	<LOD	0.08	<LOD	<LOD	<LOD	<LOD	<LOD	<LOD
5,11-dideoxyTTX	0.00	<LOD	0.00	<LOD	<LOD	<LOD	<LOD	<LOD	<LOD
5,6,11-trideoxyTTX	8.97	<LOD	8.97	<LOD	<LOD	<LOD	<LOD	<LOD	<LOD
4,4a-anhydro-5,6,11-trideoxyTTX	6.05	<LOD	6.05	0.010	<LOD	0.01	<LOD	<LOD	<LOD
4,9-anhydro-5,6,11-trideoxyTTX	7.20	<LOD	7.20	<LOD	<LOD	<LOD	<LOD	<LOD	<LOD
11-norTTX-6(*S*)-ol	0.74	<LOD	0.74	<LOD	<LOD	<LOD	<LOD	<LOD	<LOD
11-oxoTTX	0.16	<LOD	0.16	<LOD	<LOD	<LOD	<LOD	<LOD	<LOD
4-*epi*-11-oxoTTX	0.09	<LOD	0.09	<LOD	<LOD	<LOD	<LOD	<LOD	<LOD
4,9-anhydro-11-oxoTTX	0.33	<LOD	0.33	<LOD	<LOD	<LOD	<LOD	<LOD	<LOD

Table 2-14. TTX and its analogues (μg/g) in the organs of *A. nigropanctatus* No.3 from the Solomon Islands.

Organ	Skin	Skin-EtOH	Total	Liver	Liver-EtOH	Total	Testis	Testis-EtOH	Total	Stomach	Stomach-EtOH	Total
TTX	23.24	5.43	28.67	18.39	1.35	19.74	19.49	0.25	19.73	20.88	0.97	21.85
4-*epi*TTX	5.56	1.12	6.68	2.89	0.23	3.11	3.12	0.04	3.16	2.89	0.14	3.04
4,9-anhydroTTX	13.97	1.97	15.94	10.24	0.51	10.76	8.53	0.07	8.60	10.67	0.34	11.01
11-deoxyTTX	0.83	<LOD	0.83	<LOD	<LOD	<LOD	<LOD	<LOD	<LOD	<LOD	<LOD	<LOD
5-deoxyTTX	0.14	<LOD	0.14	<LOD	<LOD	<LOD	<LOD	<LOD	<LOD	<LOD	<LOD	<LOD
6,11-dideoxyTTX	0.08	<LOD	0.08	<LOD	<LOD	<LOD	<LOD	<LOD	<LOD	<LOD	<LOD	<LOD
5,11-dideoxyTTX	<LOD	<LOD	<LOD	<LOD	<LOD	<LOD	<LOD	<LOD	<LOD	<LOD	<LOD	<LOD
5,6,11-trideoxyTTX	9.91	3.09	13.00	9.50	1.18	10.68	6.00	0.13	6.13	8.50	0.67	9.17
4,4a-anhydro-5,6,11-trideoxyTTX	5.23	3.21	8.44	8.86	1.21	10.07	5.75	0.14	5.89	7.94	0.69	8.63
4,9-anhydro-5,6,11-trideoxyTTX	8.08	3.02	11.10	9.46	1.51	10.96	6.55	0.18	6.73	8.12	0.82	8.94
11-norTTX-6(*S*)-ol	0.84	<LOD	0.84	<LOD	<LOD	<LOD	<LOD	<LOD	<LOD	<LOD	<LOD	<LOD
11-oxoTTX	0.50	0.16	0.67	0.70	0.07	0.77	0.55	0.01	0.56	0.75	0.05	0.80
4-*epi*-11-oxoTTX	0.40	0.09	0.49	0.25	0.02	0.27	0.22	<LOD	0.22	0.24	0.01	0.26
4,9-anhydro-11-oxoTTX	1.32	0.16	1.49	1.05	0.06	1.11	0.65	0.01	0.66	0.89	0.03	0.93

Table 2-15. Collective data of TTX and its analogues (μg/g) in the organs of *A. nigropunctatus* from the Solomon Islands.

Organ	Skin *(n=3)*	Liver *(n=3)*	Ovary *(n=2)*	Testis *(n=1)*	Stomach *(n=2)*	Intestine *(n=1)*
TTX	8.51–28.7	< LOD-19.7	1.14, 19.7	< LOD	1.57, 21.9	0.38
4-*epi*TTX	1.61–6.68	< LOD-3.11	0.28, 3.16	< LOD	0.41, 3.04	0.05
4,9-anhydroTTX	5.15–15.9	< LOD-10.8	0.91, 8.60	< LOD	< LOD, 11.0	0.19
11-deoxyTTX	< LOD-0.83	< LOD	< LOD	< LOD	< LOD	< LOD
5-deoxyTTX	< LOD-0.14	< LOD	< LOD	< LOD	< LOD	< LOD
6,11-dideoxyTTX	< LOD-0.10	< LOD	< LOD	< LOD	< LOD	< LOD
5,11-dideoxyTTX	< LOD	< LOD	< LOD	< LOD	< LOD	< LOD
5,6,11-trideoxyTTX	3.99–13.0	< LOD-10.7	1.12, 6.14	< LOD	1.25, 9.17	0.55
4,4a-anhydro-5,6,11-trideoxyTTX	2.39–8.44	0.02–10.1	0.92, 5.89	< LOD	1.32, 8.63	0.53
4,9-anhydro-5,6,11-trideoxyTTX	3.90–11.1	< LOD-11.0	1.07, 6.73	< LOD	1.31, 8.94	0.54
11-norTTX-6(*S*)-ol	0.10–0.84	< LOD	< LOD	< LOD	< LOD	< LOD
11-oxoTTX	0.16–0.67	< LOD-0.77	< LOD, 0.56	< LOD	< LOQ(0.05), 0.80	< LOD
4-*epi*-11-oxoTTX	< LOQ(0.09)-0.50	< LOD-0.27	< LOD, 0.22	< LOD	< LOD, 0.26	< LOD
4,9-anhydro-11-oxoTTX	0.33–1.49	< LOD-1.11	< LOD, 0.66	< LOD	0.19, 0.93	< LOQ(0.07)

For 11-oxoTTX and 4-*epi*-11-oxoTTX: LOD = 0.04 μg/g (*S/N* > 3), LOQ = 0.14 μg/g (*S/N* > 10), for other analogues: LOD = 0.01 μg/g (*S/N* > 3), LOQ = 0.03 μg/g (*S/N* > 10). 5,6,11-TrideoxyTTX was measured as the mixture with its 4-*epi* form

2-3.2 The concentrations of TTX and its analogues in organs of A. hispidus and A. nigropunctatus from Okinawa, Japan

To compare the same pufferfish species from both the Solomon Islands waters and Okinawa, Japan, similar organs from three specimens of *A. hispidus* and four specimens of *A. nigropunctatus* were extracted, pre-purified with activated charcoal, and analyzed using HR-LC-MS. Results are shown in Tables 2-16 through to 2-24. As a general comparison, almost all toxins analysed in these *Arothron* species displayed distribution profile similar to those from the Solomon Islands. Just like the Solomon Islands toxic specimens, skin also contained higher levels of TTX although concentrations varied markedly. For instance, *A. nigropunctatus* No.2 from Okinawa showed a significantly higher level (highest in all tested specimens) of TTX and 11-oxoTTX in the skin at 255 and 42.4 μg/g, respectively compared to the lowest TTX concentration, *A. hispidus* No. 1 (TTX - 4.26 μg/g) and *A. hispidus* No.3 (11-oxoTTX - 0.07 μg/g) all from the same region. Similarly, other organs such as stomach also showed higher level of TTX concentration (25.5 μg/g) compared to other organs such as liver or gonads which were known to accumulate TTX in other pufferfish species.[45)] 11-OxoTTX with its *epi* and anhydro forms were also detected in the skin of most Okinawan specimens.[69)]

Table 2-16. TTX and its analogues (μg/g) in the organs of *A. hispidus* No.1 from Okinawa, Japan.

Organ	Skin	Liver	Testis	Stomach	Intestine	Flesh	Spleen
TTX	4.26	0.17	1.08	<LOD	1.61	0.31	0.15
4-*epi*TTX	0.40	<LOD	0.07	<LOD	0.10	<LOD	<LOD
4,9-anhydroTTX	2.22	0.02	0.46	0.12	0.59	0.06	<LOD
11-deoxyTTX	1.34	<LOD	0.18	<LOD	0.32	<LOD	<LOD
5-deoxyTTX	1.19	<LOD	0.16	<LOD	0.22	<LOD	<LOD
6,11-dideoxyTTX	0.13	<LOD	0.05	<LOD	<LOD	<LOD	<LOD
5,11-dideoxyTTX	0.11	<LOD	0.03	<LOD	<LOD	<LOD	<LOD
5,6,11-trideoxyTTX	1.09	<LOD	0.56	0.11	0.36	0.23	<LOD
4,4a-anhydro-5,6,11-trideoxyTTX	1.91	0.43	0.67	0.20	0.65	0.31	0.05
4,9-anhydro-5,6,11-trideoxyTTX	7.36	0.44	3.79	0.46	1.77	0.45	0.15
11-norTTX-6(*S*)-ol	0.51	<LOD	0.06	0.04	0.12	0.02	<LOD
11-oxoTTX	0.20	<LOD	0.12	0.03	0.04	<LOD	<LOD
4-*epi*-11-oxoTTX	0.03	<LOD	<LOD	0.01	0.04	<LOD	<LOD
4,9-anhydro-11-oxoTTX	0.14	<LOD	0.07	0.08	0.03	<LOD	<LOD

Table 2-17. TTX and its analogues (μg/g) in the organs of *A. hispidus* No.2 from Okinawa, Japan.

Organ	Skin	Liver	Ovary	Stomach	Intestine	Flesh	Spleen
TTX	12.69	0.55	0.37	2.44	1.67	0.61	2.09
4-*epi*TTX	2.75	0.03	0.04	0.52	0.30	0.04	0.25
4,9-anhydroTTX	8.84	0.26	0.17	1.74	1.36	0.18	0.74
11-deoxyTTX	1.45	<LOD	<LOD	0.21	<LOD	<LOD	0.11
5-deoxyTTX	0.73	<LOD	<LOD	<LOD	<LOD	<LOD	<LOD
6,11-dideoxyTTX	0.12	<LOD	<LOD	<LOD	<LOD	<LOD	<LOD
5,11-dideoxyTTX	0.30	<LOD	<LOD	<LOD	<LOD	<LOD	<LOD
5,6,11-trideoxyTTX	6.02	0.06	0.18	0.19	0.21	0.03	0.10
4,4a-anhydro-5,6,11-trideoxyTTX	18.57	0.31	0.33	0.80	0.73	0.14	0.55
4,9-anhydro-5,6,11-trideoxyTTX	46.71	1.66	1.11	2.23	1.93	0.33	1.10
11-norTTX-6(*S*)-ol	0.92	<LOD	<LOD	0.18	0.11	0.05	0.12
11-oxoTTX	0.11	<LOD	<LOD	<LOD	<LOD	<LOD	<LOD
4-*epi*-11-oxoTTX	<LOD	<LOD	<LOD	<LOD	<LOD	<LOD	<LOD
4,9-anhydro-11-oxoTTX	0.15	<LOD	<LOD	<LOD	<LOD	<LOD	<LOD

Table 2-18. TTX and its analogues (μg/g) in the organs of *A. hispidus* No.3 from Okinawa, Japan.

Organ	Skin	Liver	Testis	Stomach	Intestine	Flesh	Spleen
TTX	4.72	0.29	1.11	0.52	2.05	0.23	0.51
4-*epi*TTX	1.27	<LOD	0.17	0.05	0.36	0.02	0.02
4,9-anhydroTTX	4.72	<LOD	0.52	0.19	1.10	0.04	0.09
11-deoxyTTX	2.12	<LOD	0.04	<LOD	0.12	<LOD	<LOD
5-deoxyTTX	0.99	<LOD	0.11	0.05	0.31	<LOD	0.01
6,11-dideoxyTTX	0.31	<LOD	<LOD	<LOD	0.02	<LOD	<LOD
5,11-dideoxyTTX	0.52	<LOD	<LOD	<LOD	0.02	<LOD	<LOD
5,6,11-trideoxyTTX	4.31	<LOD	0.20	0.10	0.35	<LOD	0.07
4,4a-anhydro-5,6,11-trideoxyTTX	5.73	0.46	0.24	0.14	0.42	0.07	0.03
4,9-anhydro-5,6,11-trideoxyTTX	26.96	0.54	1.70	0.83	2.80	0.21	0.29
11-norTTX-6(*S*)-ol	0.27	<LOD	0.04	0.01	0.08	<LOD	0.02
11-oxoTTX	0.07	<LOD	0.02	<LOD	0.05	<LOD	<LOD
4-*epi*-11-oxoTTX	0.02	<LOD	0.01	<LOD	0.02	<LOD	<LOD
4,9-anhydro-11-oxoTTX	0.12	<LOD	0.03	0.01	0.09	<LOD	<LOD

Table 2-19. Collective data of TTX and its analogues (μg/g) in the organs of *A. hispidus* No.1 from Okinawa, Japan.

Organ	Skin *(n=3)*	Liver *(n=3)*	Ovary *(n=1)*	Testis *(n=2)*	Stomach *(n=3)*	Intestine *(n=3)*	Flesh *(n=3)*	Spleen *(n=3)*
TTX	4.26–12.7	0.17–0.55	0.37	1.08, 1.11	< LOD-2.44	1.61-2.05	0.23–0.61	0.15–2.09
4-*epi*TTX	0.40-2.75	< LOD-0.03	0.04	0.07, 0.17	< LOD-0.52	0.10-0.36	< LOD-0.04	< LOD-0.25
4,9-anhydroTTX	2.22–8.84	< LOD-0.26	0.17	0.46, 0.52	< LOD-1.74	0.59–1.36	0.04–0.18	< LOD-0.74
11-deoxyTTX	1.34–2.12	< LOD	< LOD	0.04, 0.18	< LOD-0.21	< LOD-0.32	< LOD	< LOD-0.11
5-deoxyTTX	0.73–1.19	< LOD	< LOD	0.11, 0.16	< LOD-0.05	< LOD-0.31	< LOD	< LOD
6,11-dideoxyTTX	0.12–0.31	< LOD	< LOD	< LOD, 0.05	< LOD	< LOD-< LOQ(0.02)	< LOD	< LOD
5,11-dideoxyTTX	0.11–0.52	< LOD	< LOD	< LOD, 0.03	< LOD	< LOD-< LOQ(0.02)	< LOD	< LOD
5,6,11-trideoxyTTX	1.09–6.02	< 0.06	0.18	< 0.20, 0.56	< 0.10-0.19	0.21–0.36	0.03–0.23	< LOD-0.10
4,4a-anhydro-5,6,11-trideoxyTTX	1.91–18.6	0.31–0.46	0.33	0.24, 0.67	< 0.14–0.80	0.42–0.73	0.07–0.31	0.03–0.55
4,9-anhydro-5,6,11-trideoxyTTX	7.36–46.7	0.44–1.66	1.11	1.70, 3.79	< 0.46–2.23	1.77–2.80	0.21–0.45	0.15–1.10
11-norTTX-6(*S*)-ol	0.27–0.92	< LOD	< LOD	0.04, 0.06	< LOD-0.18	0.08–0.12	< LOD-0.05	< LOD-0.12
11-oxoTTX	< LOQ(0.07)-0.20	< LOD	< LOD	< LOD, < LOQ(0.12)	< LOD	< LOD-< LOQ(0.05)	< LOD	< LOD
4-*epi*-11-oxoTTX	< LOD	< LOD	< LOD	< LOD	< LOD	< LOD	< LOD	< LOD
4,9-anhydro-11 oxoTTX	< LOQ(0.12)-0.15	< LOD	< LOD	< LOD, < LOQ(0.07)	< LOD-< LOQ(0.08)	< LOD-< LOQ(0.09)	< LOD	< LOD

For 11-oxoTTX, 4-*epi*-11-oxoTTX and 4,9-anhyydro-11-oxoTTX: LOD = 0.04 μg/g (*S/N* > 3), LOQ = 0.14 μg/g (*S/N* > 10), for other analogues: LOD = 0.01 μg/g (*S/N* > 3), LOQ = 0.03 μg/g (*S/N* > 10). 5,6,11-TrideoxyTTX was measured as the mixture with its 4-*epi* form

Table 2-20. TTX and its analogues (μg/g) in the organs of *A. nigropunctatus* No.1 from Okinawa, Japan.

Organ	Skin	Liver	Testis	Stomach	Intestine	Flesh	Spleen
TTX	134.06	0.29	3.94	3.13	1.22	0.19	1.93
4-*epi*TTX	17.19	<LOD	0.55	0.42	0.25	<LOD	0.33
4,9-anhydroTTX	64.81	0.11	1.82	1.42	0.95	0.04	1.05
11-deoxyTTX	10.55	0.08	0.50	0.65	0.18	<LOD	0.34
5-deoxyTTX	<LOD	<LOD	0.11	<LOD	<LOD	<LOD	<LOD
6,11-dideoxyTTX	1.77	<LOD	<LOD	0.10	<LOD	<LOD	<LOD
5,11-dideoxyTTX	1.80	<LOD	0.12	0.03	<LOD	<LOD	<LOD
5,6,11-trideoxyTTX	100.34	<LOD	1.40	1.06	<LOD	0.04	0.79
4,4a-anhydro-5,6,11-trideoxyTTX	178.41	0.37	3.03	3.19	0.92	0.34	2.03
4,9-anhydro-5,6,11-trideoxyTTX	266.39	0.30	6.76	5.26	0.93	0.10	3.74
11-norTTX-6(*S*)-ol	4.61	<LOD	0.13	0.10	<LOD	<LOD	0.08
11-oxoTTX	106.11	0.21	3.48	1.74	0.51	0.07	1.33
4-*epi*-11-oxoTTX	27.92	0.06	0.69	0.62	0.15	0.03	0.48
4,9-anhydro-11-oxoTTX	22.34	0.04	0.69	0.51	0.20	0.02	0.47

Table 2-21. TTX and its analogues (μg/g) in the organs of *A. nigropunctatus* No.2 from Okinawa, Japan.

Organ	Skin	Liver	Testis	Stomach	Intestine	Flesh	Spleen
TTX	254.99	0.31	10.16	2.10	4.51	4.26	4.19
4-*epi*TTX	27.90	<LOD	2.64	0.14	0.35	0.92	0.62
4,9-anhydroTTX	96.63	0.08	6.13	1.13	2.41	1.82	2.26
11-deoxyTTX	14.94	<LOD	3.03	0.30	0.65	0.88	0.76
5-deoxyTTX	4.03	0.03	3.80	0.22	0.54	0.62	0.80
6,11-dideoxyTTX	1.70	<LOD	1.31	0.14	0.27	<LOD	0.43
5,11-dideoxyTTX	2.92	<LOD	0.94	0.06	0.12	0.18	0.14
5,6,11-trideoxyTTX	275.51	0.12	22.28	6.03	8.40	3.92	10.02
4,4a-anhydro-5,6,11-trideoxyTTX	127.84	0.34	15.28	3.23	5.31	3.32	5.69
4,9-anhydro-5,6,11-trideoxyTTX	438.03	0.87	26.93	9.29	10.95	4.79	10.10
11-norTTX-6(*S*)-ol	9.72	0.00	0.32	0.11	0.19	0.11	0.15
11-oxoTTX	181.13	0.44	1.88	1.08	2.26	0.45	1.97
4-*epi*-11-oxoTTX	21.54	<LOD	0.25	0.20	0.42	0.13	0.32
4,9-anhydro-11-oxoTTX	25.02	0.04	0.25	0.26	0.41	0.35	0.09

Table 2-22. TTX and its analogues (μg/g) in the organs of *A. nigropunctatus* No.3 from Okinawa, Japan.

Organ	Skin	Liver	Testis	Stomach	Intestine	Flesh	Spleen
TTX	12.57	7.46	0.26	25.62	1.36	0.32	2.76
4-*epi*TTX	1.19	0.49	<LOD	2.05	0.07	<LOD	0.24
4,9-anhydroTTX	5.39	2.75	0.13	9.65	0.52	0.08	1.26
11-deoxyTTX	1.25	0.54	0.02	2.19	0.15	<LOD	0.31
5-deoxyTTX	2.61	0.23	0.10	5.41	0.35	0.04	0.53
6,11-dideoxyTTX	0.40	0.07	0.05	0.84	0.04	<LOD	<LOD
5,11-dideoxyTTX	0.52	0.06	0.10	1.03	<LOD	<LOD	0.09
5,6,11-trideoxyTTX	15.32	3.69	0.61	25.18	0.56	0.14	2.88
4,4a-anhydro-5,6,11-trideoxyTTX	6.81	2.69	0.45	10.24	0.74	0.35	1.13
4,9-anhydro-5,6,11-trideoxyTTX	43.00	8.28	2.05	77.04	2.81	0.70	10.46
11-norTTX-6(*S*)-ol	0.11	0.30	<LOD	<LOD	<LOD	<LOD	0.02
11-oxoTTX	16.80	3.58	0.31	42.61	0.67	0.23	3.79
4-*epi*-11-oxoTTX	2.17	0.69	0.02	7.74	0.12	0.04	0.69
4,9-anhydro-11-oxoTTX	2.57	0.50	0.05	4.15	0.22	0.04	0.53

Table 2-23. TTX and its analogues (μg/g) in the organs of *A. nigropunctatus* No.4 from Okinawa, Japan.

Organ	Skin	Liver	Testis	Stomach	Intestine	Flesh	Spleen
TTX	49.78	1.45	1.02	0.57	1.38	2.05	0.85
4-*epi*TTX	8.45	0.13	0.09	0.07	0.17	0.09	0.18
4,9-anhydroTTX	27.41	0.54	0.50	0.24	0.88	0.78	0.85
11-deoxyTTX	4.84	0.09	0.10	0.06	0.16	0.19	0.10
5-deoxyTTX	3.55	0.06	0.09	0.03	0.11	0.08	0.08
6,11-dideoxyTTX	0.94	<LOD	0.05	0.02	0.05	0.01	<LOD
5,11-dideoxyTTX	1.18	0.04	0.02	0.01	0.02	0.01	<LOD
5,6,11-trideoxyTTX	31.47	0.46	0.39	0.28	0.58	0.44	0.74
4,4a-anhydro-5,6,11-trideoxyTTX	37.27	0.63	0.56	0.39	1.06	1.04	1.01
4,9-anhydro-5,6,11-trideoxyTTX	115.93	2.15	3.48	1.42	3.90	2.87	3.94
11-norTTX-6(*S*)-ol	0.44	0.00	<LOD	<LOD	<LOD	<LOD	<LOD
11-oxoTTX	42.85	0.67	0.49	0.23	0.51	0.42	0.52
4-*epi*-11-oxoTTX	6.63	0.19	0.09	0.05	0.25	0.15	0.23
4,9-anhydro-11-oxoTTX	11.89	0.22	0.15	0.11	0.24	0.23	0.24

Table 2-24. Collective data of TTX and its analogues (μg/g) in the organs of *A. nigropunctatus* from Okinawa, Japan.

Organ	Skin *(n=4)*	Liver *(n=4)*	Ovary *(n=1)*	Testis *(n=3)*	Stomach *(n=4)*	Intestine *(n=4)*	Flesh *(n=4)*	Spleen *(n=4)*
TTX	12.6–255	0.29–7.46	1.02	0.26–10.1	0.57–25.5	1.22–4.51	0.19–4.26	0.85–4.19
4-*epi*TTX	1.19–27.9	< LOD-0.49	0.09	< LOD-2.64	0.07–2.05	0.07–0.35	< LOD-0.92	0.18–0.62
4,9-anhydroTTX	5.39–96.6	< LOD-2.75	0.50	0.13–6.13	0.24–9.65	0.52–2.41	< LOD-1.82	0.85–2.26
11-deoxyTTX	1.25–14.9	< LOD-0.54	0.10	0.02–3.13	0.06–2.19	0.15–0.65	< LOD-0.88	0.10–0.76
5-deoxyTTX	< LOD-4.03	< LOD-0.23	0.09	0.10–3.80	< LOD-5.41	< LOD-0.54	< LOD-0.62	< LOD-0.80
6,11-dideoxyTTX	0.40–1.77	< LOD-0.07	0.05	< LOD-1.31	0.02–0.84	< LOD-0.27	< LOD	< LOD-0.43
5,11-dideoxyTTX	0.52–2.92	< LOD-0.06	< LOQ(0.02)	0.10–0.94	< LOD-1.03	< LOD-0.12	< LOD-0.18	< LOD-0.14
5,6,11-trideoxyTTX	15.3–275	< LOD -3.69	0.39	0.61–22.3	0.28–25.2	< LOD-8.40	0.04–3.92	0.74–10.0
4,4a-anhydro-5,6,11-tri-deoxyTTX	6.81–178	0.34–2.69	0.56	0.45–15.3	0.39–10.2	0.74–5.31	0.34–3.32	1.01–5.69
4,9-anhydro-5,6,11-trideoxyTTX	43–438	0.30–8.28	3.48	2.05–26.9	1.42–77.0	0.93–11.0	0.70–4.79	3.74–10.5
11-norTTX-6(*S*)-ol	0.11–9.72	< LOD-0.30	< LOD	< LOD-0.32	< LOD-0.11	< LOD-0.19	< LOD-0.11	< LOD-0.15
11-oxoTTX	3.94–42.4	< LOQ(0.05)-0.84	< LOQ(0.12)	< LOQ(0.07)-0.82	< LOQ(0.05)-9.98	< LOQ(0.12)-0.53	< LOD-< LOQ(0.11)	0.12–0.46
4-*epi*-11-oxoTTX	0.51–6.54	< LOD-0.16	< LOD	< LOD-0.16	< LOD-1.81	< LOD-< LOQ(0.10)	< LOD	0.05–0.16
4,9-anhydro-11 oxoTTX	2.57–25.0	< LOQ(0.04)-0.5	0.15	< LOQ(0.05)-0.69	< LOQ(0.11)-4.15	0.20–0.41	< LOD-0.35	0.09–0.53

For 11-oxoTTX, 4-*epi*-11-oxoTTX and 4,9-anhyydro-11-oxoTTX: LOD = 0.04 μg/g (*S/N* > 3), LOQ = 0.14 μg/g (*S/N* > 10), for other analogues: LOD = 0.01 μg/g (*S/N* > 3), LOQ = 0.03 μg/g (*S/N* > 10). 5,6,11-TrideoxyTTX was measured as the mixture with its 4-*epi* form

2-3.3 TTXs distribution profile in A. hispidus and A. nigropunctatus from the Solomon Islands and Okinawa, Japan

Figures 2-6 to 2-12 displayed the TTX distribution profiles of all the toxic pufferfish been investigated in this study as well as the TTXs profile of pufferfish *Takifugu pardalis* from previous study.[45] A general comparison of the average TTX concentrations in *Arothron* specimens from the Solomon Islands and Okinawa, Japan (Figure 2-10 and 2-11) revealed a marked variation in the TTX accumulated in the skin. Results showed that Solomon Islands *A. hispidus* contained more TTX than the *A. hispidus* from Okinawa, Japan, while the skin of *A. nigropunctatus* from Okinawa, Japan, accumulated more TTX than the same species from the Solomon Islands.[69] This highlights the fact that although *Arothron* species accumulates more TTX in the skin, the overall TTX content in the skin or other organs of an individual species depends on each individual species.

Likewise, a significant difference was also observed in the profiles of *Arothron* species from Solomon Islands and Okinawa (which are tropical regions) with that of the *T. pardalis* collected off the coast of Miyagi Prefecture, Japan, situated in a more temperate region. The consistency displayed by high TTX accumulation in the skin of *Arothron* species from the tropical region proved to be very different when compared to the higher accumulation of TTX in the reproductive organ and liver of *T. pardalis* collected in the temperate region (Figure 2-12). Although a large number of data focusing on size, gender, breeding seasons or the ecological environment these pufferfish strive in may be needed for a valid conclusion, the present study highlights an important finding that may address the relationship between TTX profiles and pufferfish species collected in at least two different regions. Moreover, this comparison shows that the role of TTXs in these species may be more complex than the obvious and speculated role as part of the organisms' defense strategy.

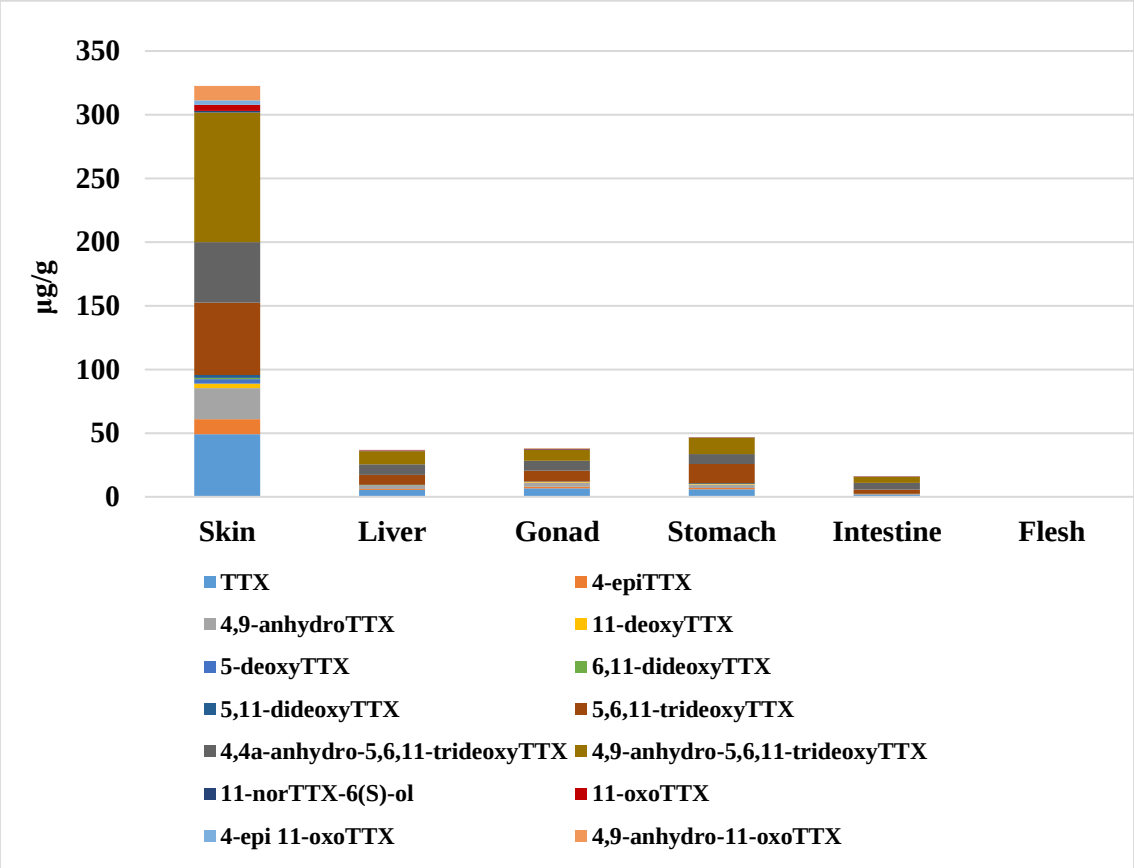

Figure 2-6. Average TTX distribution profile of *A. hispidus* (No.1-3) from Solomon Islands.

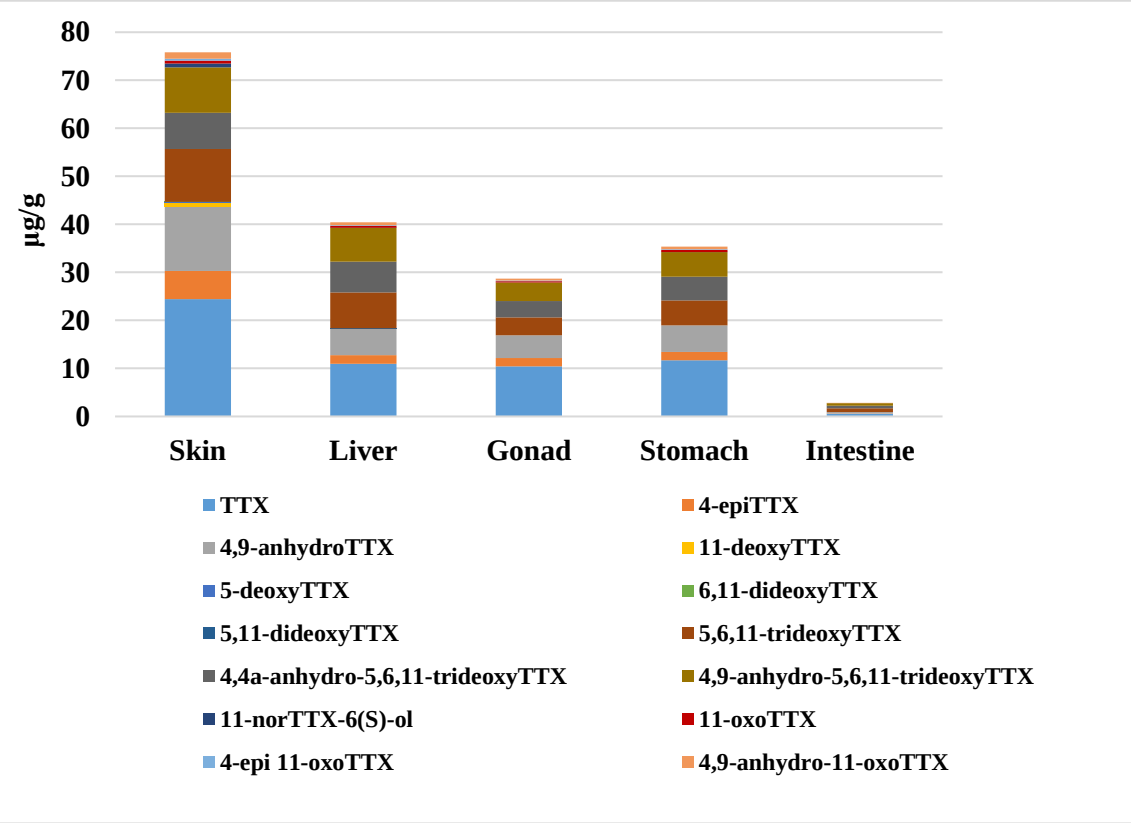

Figure 2-7. Average TTX distribution profile of *A. nigropunctatus* (sample No.1-3) from Solomon Islands.

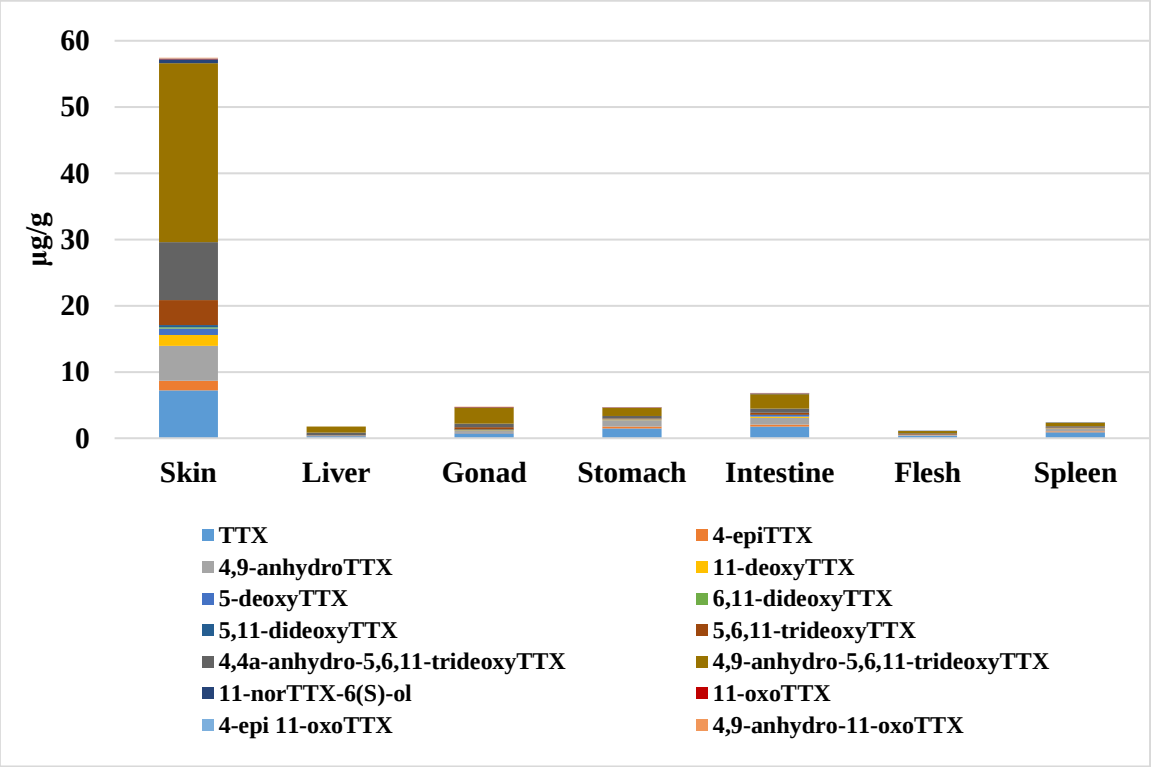

Figure 2-8. Average TTX distribution profile of *A. hispidus* (sample No.1-3) from Okinawa, Japan.

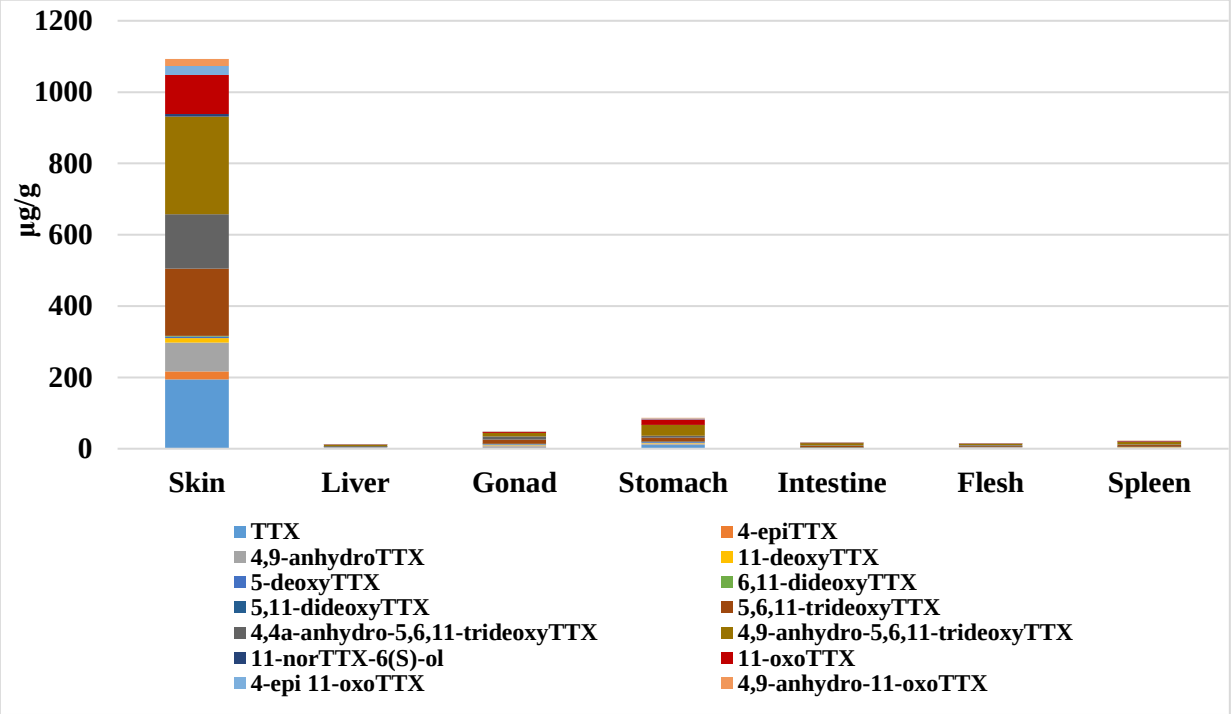

Figure 2-9. Average TTX distribution profile of *A. nigropunctatus* (sample No.1-3) from Okinawa, Japan.

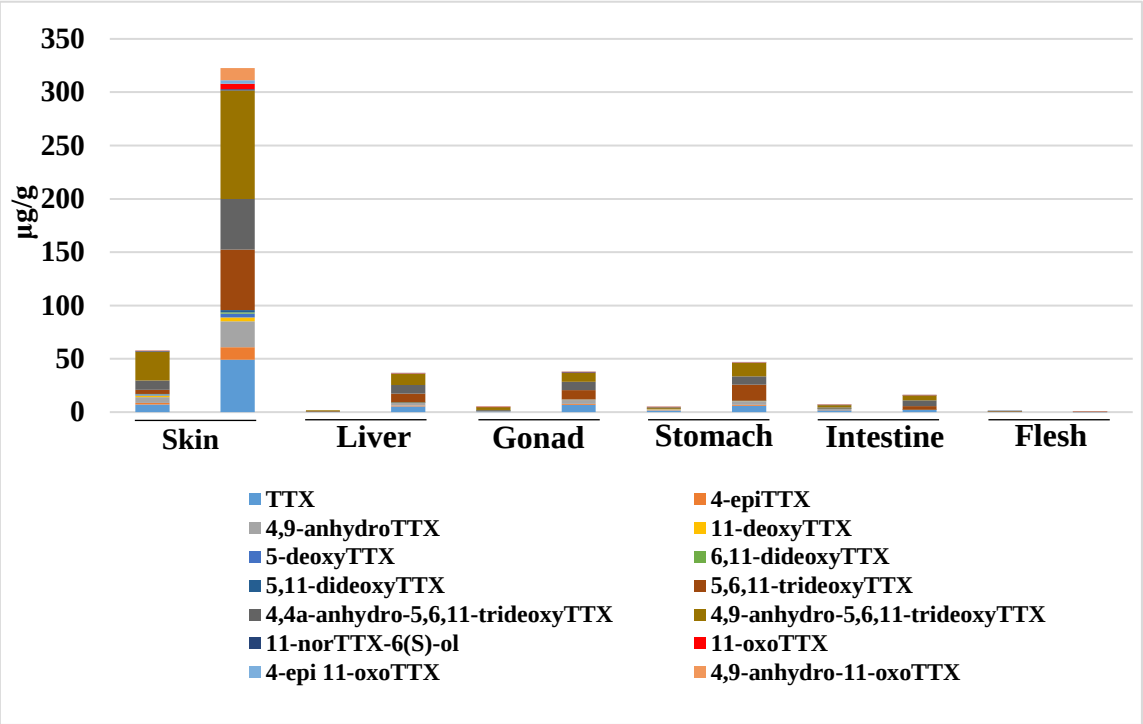

Figure 2-10. A comparison of the average TTX distribution profile of *A. hispidus* (sample No.1-3) from the Solomon Islands and *A. hispidus* (sample No.1-3) from Okinawa, Japan.

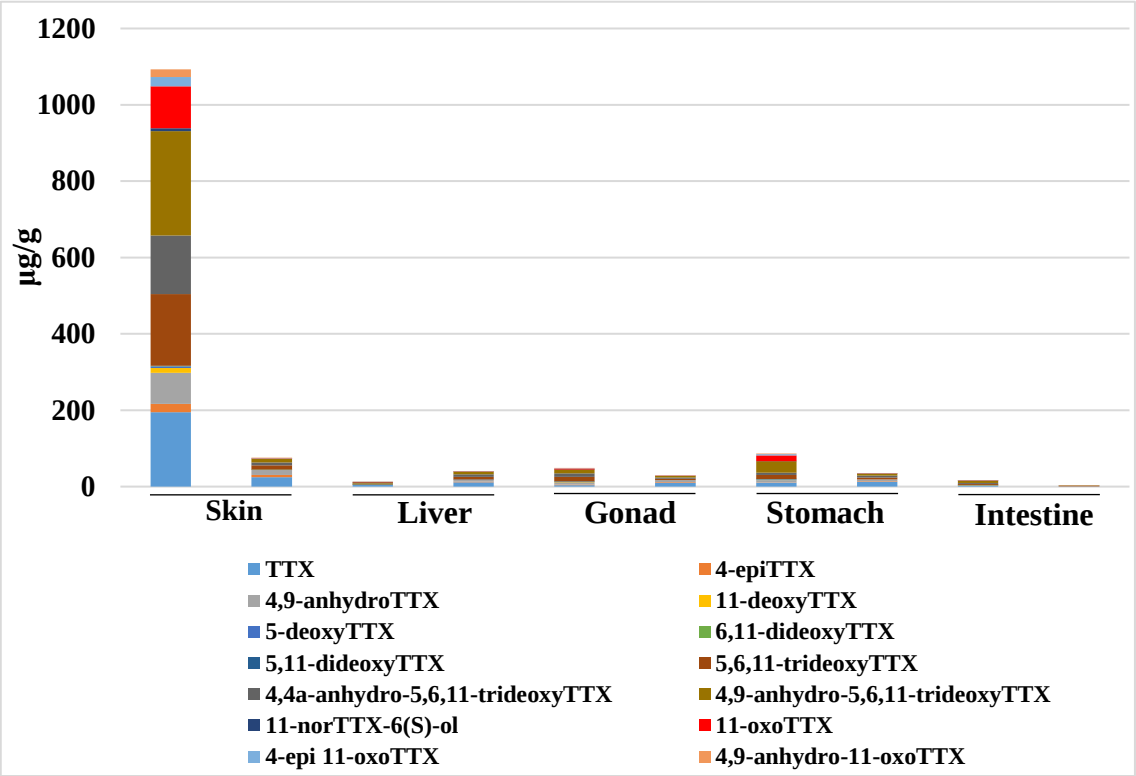

Figure 2-11. A comparison of the average TTX distribution profile of *A. nigropunctatus* (sample No.1-3) from the Solomon Islands and *A. nigropunctatus* (sample No.1-4) from Okinawa, Japan.

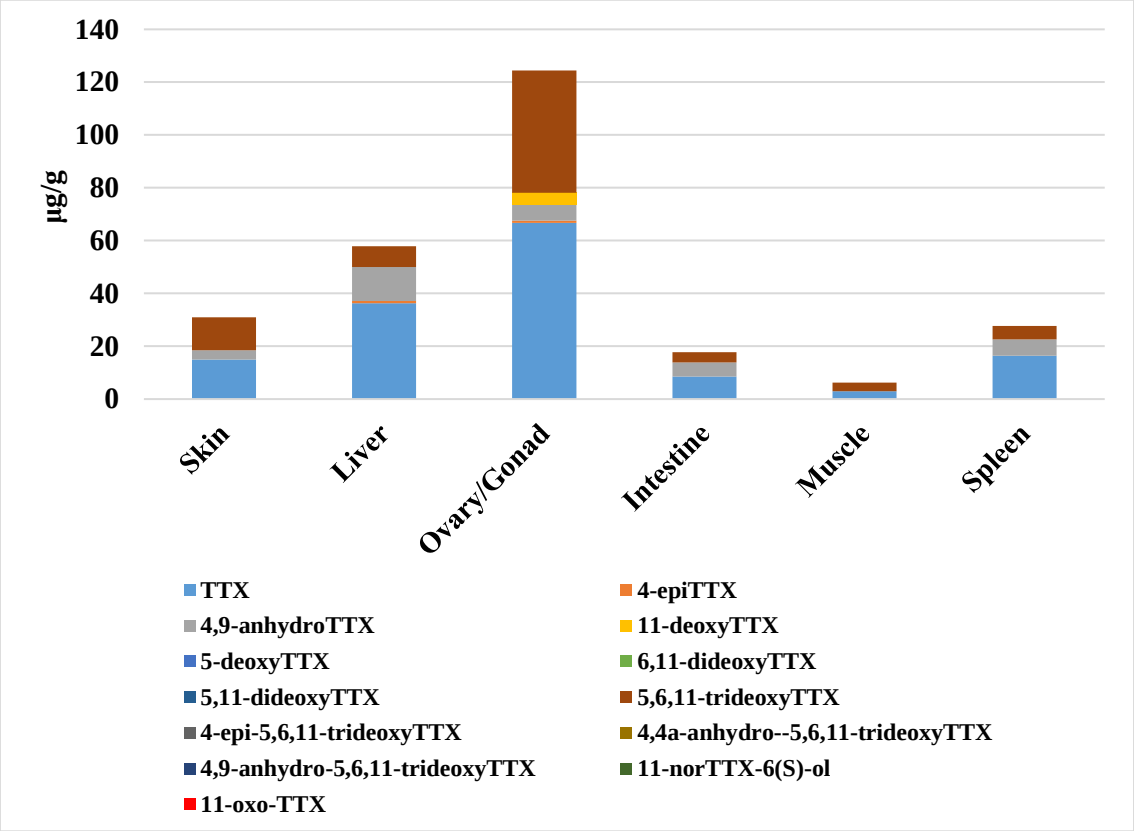

Figure 2-12. TTX distribution profile of *T. pardalis* collected off the coast of Miyagi Prefecture, Japan.[45)]

2-3.4 TTXs distribution profile in the skin of Solomon Islands pufferfish samples.

As previously mentioned, the distribution of TTXs in all toxic *Arothron* species varied among each species and their respective organs, with the highest TTX accumulation detected in the skin. However, the extent of TTXs distribution in each skin also showed different toxic profiles. As seen in Figure 2-13, the TTX concentration in the skin of *A. hispidus* is lower than the less toxic analogues such as 5,6,11 trideoxyTTX and its anhydro forms. On the other hand, TTX in the skin of *A. nigropunctatus* seems to show relatively higher levels although the overall quantity of toxins is still much lower. The analysis of the skin of two *D. holocanthus* specimen showed very low levels of TTX, presumably much lower than the limit of detection (LOD) (Figure 2-13). An example of the mass chromatograms of the skin of *D. holocanthus* No.1 is displayed in the appendix p.93.

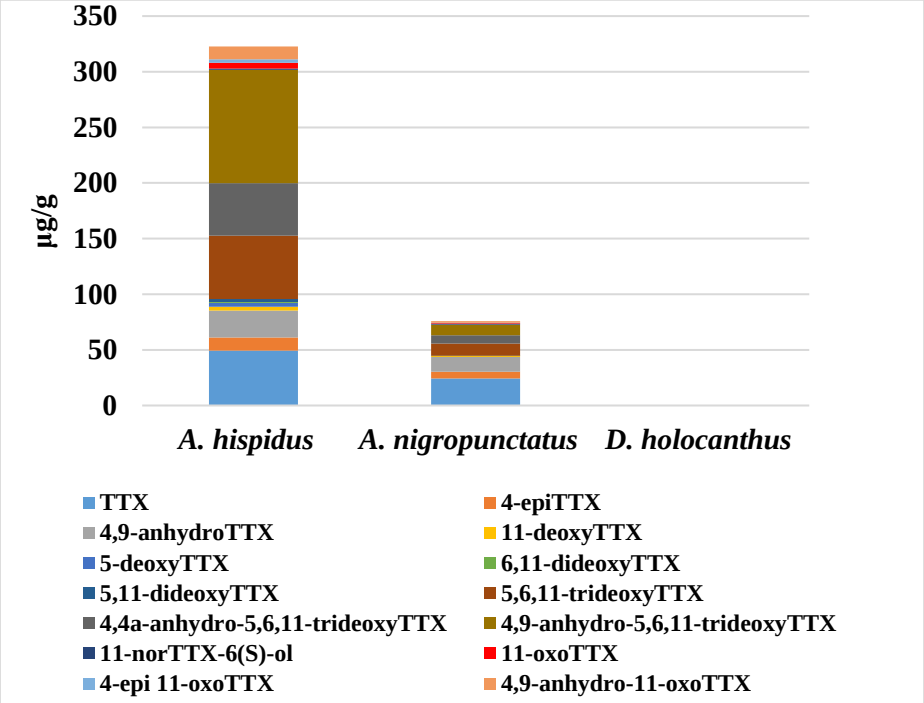

Figure 2-13. TTX distribution profile in the skin of *A. hispidus* (Sample No.1-3) and *A. nigropunctatus* (Sample No.1-3) compared to *D. holocanthus* (Sample No.1-2).

Since the skin of the toxic species showed interesting variations of toxin profiles, an investigation was conducted to see if certain areas of the skin accumulate more TTX than others. Analysis were conducted on *A. hispidus* No.3 and *A. nigropunctatus* No.1 respectively. For *A. hispidus* No.3, a part of skin samples was obtained from slightly darker spotted regions, plain white regions, greyish regions and the thin epidermial layer just beneath the skin (skin flesh) and were analyse using HR-LC-MS. The TTXs concentrations are presented in Table 2-25 and Figure 2-14. Though the greyish region showed a slightly higher TTX level (48 μg/g), all regions seem to show the same toxic profiles which suggested that TTXs in the skin of this species are evenly distributed in all areas of the skin and that the extent of intoxication in predators or humans presumably from skin is not dependent on skin regions but on the ingestion of the quantity of skin tissue.

Table 2-25. TTX and its analogues (μg/g) in the skin of *A. hispidus* No.3 from the Solomon Islands.

Organ	Dark Area	White Area	Grayish white Area	Skin Flesh
TTX	42	45	48	40
4-*epi*TTX	7.2	8.0	8.7	6.9
4,9-anhydroTTX	20	20	23	21
11-deoxyTTX	4.0	4.5	4.3	4.3
5-deoxyTTX	4.9	5.8	5.5	5.3
6,11-dideoxyTTX	1.3	1.3	1.5	1.4
5,11-dideoxyTTX	2.8	2.8	3.2	2.7
5,6,11-trideoxyTTX	86	81	84	95
4,4a-anhydro-5,6,11-trideoxyTTX	70.	67	70	79
4,9-anhydro-5,6,11-trideoxyTTX	127	126	133	148
11-norTTX-6(*S*)-ol	<LOD	<LOD	<LOD	<LOD
11-oxoTTX	6.1	6.1	7.1	7.6
4-*epi*-11-oxoTTX	2.6	3.1	3.5	3.3
4,9-anhydro-11-oxoTTX	11	12	14	15

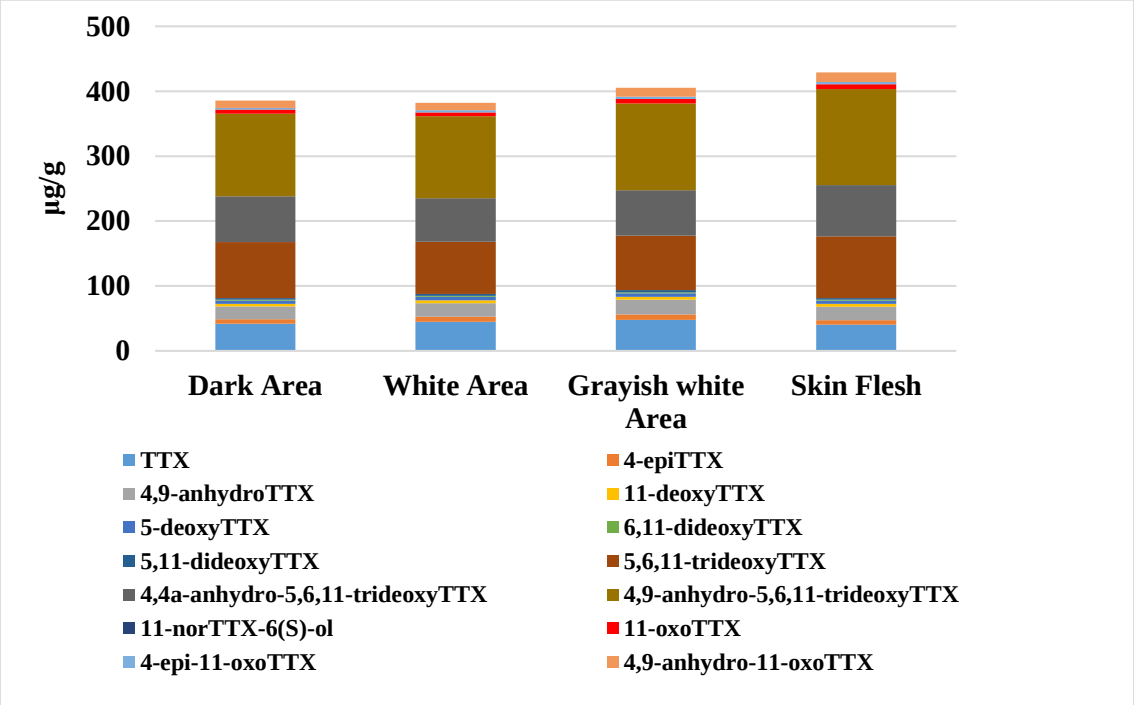

Figure 2-14. TTX distribution profile of in the skin of *A. hispidus* No.3 from the Solomon Islands.

In the *A. nigropunctatus* No.1 skin sections, the dorsal regions, underside regions and the back regions were evaluated for a possible TTX- specific area of accumulation. Results showed that both the underside and back areas contained slightly higher TTX level (20 and 20 μg/g respectively) compared to the dorsal area (17 μg/g) (Table 2-26 and Figure 2-15). However, each analogue from these skin regions seemed to show a consistent level of concentration, indicating that all analogues are evenly distributed throughout the skin tissue. The 5,6,11-trideoxyTTX and its anhydro forms which are often higher in some organs were relatively low in this skin specimen. Whether the regional skin texture of *A. nigropunctatus* species contributed differently to its toxin distribution profiles is a matter of further analysis and/or debate, however from this results it seems that toxins' distribution in the skin depends entirely on the individual specimen.

Table 2-26. TTX and its analogues (μg/g) in the skin of *A. nigropunctatus* No.1 from the Solomon Islands.

Organ	Dorsal Area	Underside Area	Back Area
TTX	17	20	20
4-*epi*TTX	4.5	5.1	6.4
4,9-anhydroTTX	8.9	11	12
11-deoxyTTX	<LOD	<LOD	<LOD
5-deoxyTTX	<LOD	<LOD	<LOD
6,11-dideoxyTTX	<LOD	<LOD	<LOD
5,11-dideoxyTTX	<LOD	<LOD	<LOD
5,6,11-trideoxyTTX	3.0	4.0	3.00
4,4a-anhydro-5,6,11-trideoxyTTX	2.0	2.4	2.3
4,9-anhydro-5,6,11-trideoxyTTX	3.3	3.9	4.2
11-norTTX-6(*S*)-ol	<LOD	0.1	<LOD
11-oxoTTX	0.5	0.5	0.6
4-*epi*-11-oxoTTX	0.4	0.5	0.7
4,9-anhydro-11-oxoTTX	7.2	7.2	9.3

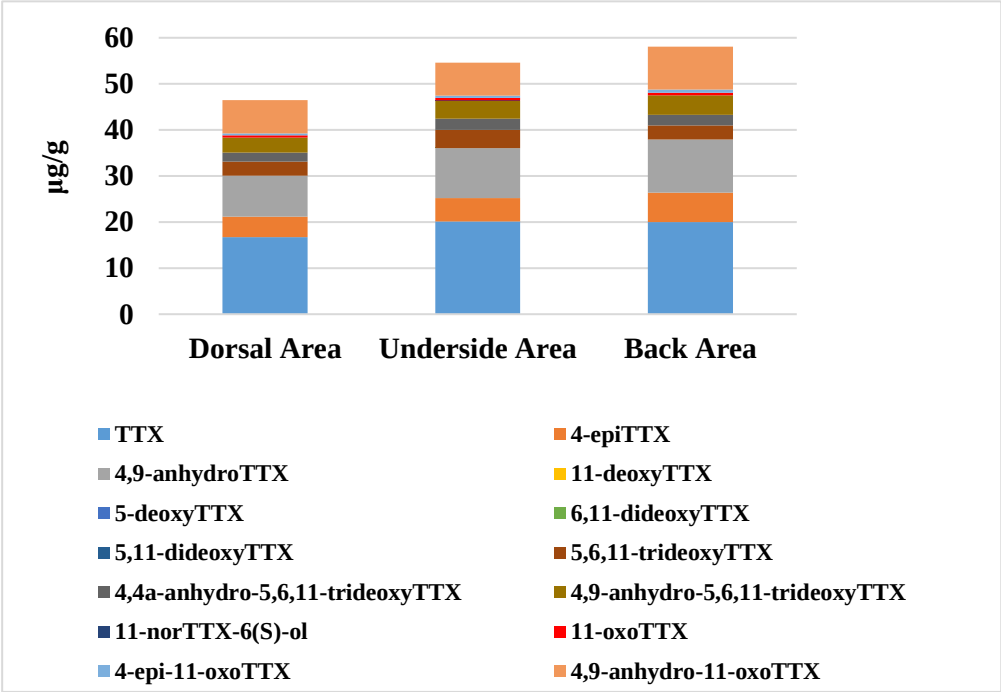

Figure 2-15. TTX distribution profile of in the skin of *A. nigropunctatus* No.1 from the Solomon Islands.

2-3.5 Investigation of STX and its analogues in A. hispidus and A. nigropunctatus from the Solomon Islands and Okinawa, Japan

Since a few pufferfish species usually possess both TTXs and STXs, the current study was also extended to investigate possible existence of STX, neoSTX, and dcSTX in the ovary and the skin of toxic pufferfish species from both the Solomon Islands and Okinawa, Japan, using HR-LC-MS and the conditions in section 2-2.7. The choice of organs in this section were based on the fact that ovary was previously known to accumulate STXs[61] and skin in this study possess a markedly higher level of TTX whereby their toxin tolerance state may also accumulate STX compounds. The results of this study are shown in Tables 2-27 to 2.30.

Table 2-27. STX analysis of the skin from the Solomon Islands pufferfish.

Species/Types	*A hispidus* No.1	*A hispidus* No.2	*A hispidus* No.3	*A nigropuntatus* No. 1	*A nigropuntatus* No. 2	*A nigropuntatus* No. 3
STX	<LOD	<LOD	<LOD	<LOD	<LOD	<LOD
neoSTX	<LOD	<LOD	<LOD	<LOD	<LOD	<LOD
dcSTX	<LOD	<LOD	<LOD	<LOD	<LOD	<LOD

LOD (*S/N* > 3) and LOQ (*S/N* > 10) for STX were 0.02 μg/g and 0.07 μg/g, neoSTX, 0.05 μg/g and 0.18 μg/g, and dcSTX, 0.07 μg/g and 0.25 μg/g, respectively.

Table 2-28. TTX analysis of the ovary from the Solomon Islands pufferfish.

Species/Types	*A hispidus* No.1	*A hispidus* No.2	*A hispidus* No.3	*A nigropuntatus* No. 1	*A nigropuntatus* No. 2	*A nigropuntatus* No. 3
STX	<LOD	<LOD	<LOD	<LOD	<LOD	<LOD
neoSTX	<LOD	<LOD	<LOD	<LOD	<LOD	<LOD
dcSTX	<LOD	<LOD	<LOD	<LOD	<LOD	<LOD

LOD (*S/N* > 3) and LOQ (*S/N* > 10) for STX were 0.02 μg/g and 0.07 μg/g, neoSTX, 0.05 μg/g and 0.18 μg/g, and dcSTX, 0.07 μg/g and 0.25 μg/g, respectively.

Table 2-29. STX analysis of the skin from the Okinawan pufferfish.

Species/Types	*A hispidus* No.1	*A hispidus* No.2	*A hispidus* No.3	*A nigropuntatus* No. 1	*A nigropuntatus* No. 2	*A nigropuntatus* No. 3	*A nigropuntatus* No. 4
STX	0.34	2.8	0.09	<LOD	<LOD	<LOD	<LOD
neoSTX	<LOD	<LOD	<LOD	<LOD	<LOD	<LOD	<LOD
dcSTX	<LOD	0.66	<LOD	<LOD	<LOD	<LOD	<LOD

LOD (*S/N* > 3) and LOQ (*S/N* > 10) for STX were 0.02 μg/g and 0.07 μg/g, neoSTX, 0.05 μg/g and 0.18 μg/g, and dcSTX, 0.07 μg/g and 0.25 μg/g, respectively.

Table 2-30. TTX analysis of the ovary from the Okinawan pufferfish.

Species/Types	*A hispidus* No.1	*A hispidus* No.2	*A hispidus* No.3	*A nigropuntatus* No. 1	*A nigropuntatus* No. 2	*A nigropuntatus* No. 3	*A nigropuntatus* No. 4
STX	<LOD	0.04	<LOD	<LOD	<LOD	<LOD	<LOD
neoSTX	<LOD	<LOD	<LOD	<LOD	<LOD	<LOD	<LOD
dcSTX	<LOD	<LOD	<LOD	<LOD	<LOD	<LOD	<LOD

LOD (*S/N* > 3) and LOQ (*S/N* > 10) for STX were 0.02 μg/g and 0.07 μg/g, neoSTX, 0.05 μg/g and 0.18 μg/g, and dcSTX, 0.07 μg/g and 0.25 μg/g, respectively.

STX analysis revealed that the STXs concentration in the skin and ovary of all toxic pufferfish from the Solomon Islands and the four specimens of *A. nigropunctatus* from Okinawa, Japan were below the LOD (0.02 μg/g). However, the skin of all *A. hispidus* from Okinawa contained STX (0.09, 2.80, 0.34 μg/g) including the ovary of one specimen. Interestingly, the highest STXs level obtained in the skin (STX - 2.8 μg/g) and (dcSTX - 0.66 μg/g) and ovary (STX - 0.04 μg/g: between LOD and LOQ) in this study were from *A. hispidus* No.2 of Okinawa, Japan. In other samples, dcSTX and neoSTX were not detected. LOD (*S/N* > 3) and LOQ (*S/N* > 10) for STX were 0.02 μg/g and 0.07 μg/g, neoSTX, 0.05 μg/g and 0.18 μg/g, and dcSTX, 0.07 μg/g and 0.25 μg/g, respectively.

2-4.0 Discussion

In this study, the analysis of TTX and its analogues in the pufferfish, *A. hispidus* and *A. nigropunctatus*, from the Solomon Islands and Okinawa, Japan were carried out using LC-FLD and HR-LC-MS. Preliminary analysis of the condition of TTX in all organs from Solomon Islands specimens by LC-FLD showed that tetrodonic acid peaks were approximately 60% of the TTX peaks indicating a partial decomposition in the TTX compounds. It should be noted herein that the amount of TTX in the samples from the Solomon Islands toxic pufferfish as outline in Tables 2-8 to 2-15 could be underestimated due to storage methods, duration and possibly chemical transformation of TTX and its analogues. However, we believe that the data obtained in this study holds much valuable information and facts to warn of the high toxicity in these toxic pufferfish species from the Solomon Islands.

Due to the chemical properties of TTX in nature such as its solubility to water and heat resistance, consumption of pufferfish even after being properly cooked can still cause one to suffer from pufferfish intoxication. In areas where cautionary information or research facilities are not available, the only way to avoid being intoxicated from such toxic animals has been to have the knowledge passed down through generations based on previous experiences. In most cases, this is not so reliable considering the unregulated introduction of new species into the local environment, existence of potentially merging species types, unpredictable distribution of TTX producers and for less fortunate societies the potential socioeconomic issues relating to food availability. Therefore, screening of TTXs in pufferfish through scientific methods and informing people of its proof of existence is thus far the most effective way to reduce risks of pufferfish poisoning.

In this study, not all the flesh from the Solomon Islands toxic specimens were analysed due to limited number of storage tubes and volume of ethanol solution available during pufferfish collection. For the one specimen of *A. hispidus* which was analysed, result showed that TTX concentration was 0.07 μg/g which is relatively low compared to other organs. (See appendix p.92). On the other hand, all the flesh of Okinawan toxic

specimens contained TTX concentrations of somewhat lower to much higher levels, the highest levels being from *A. nigropunctatus* No.2 and 4 with concentrations 4.26 μg/g and 2.05 μg/g respectively.

Since all species from both the tropical regions are the same and both displayed similar toxin profiles, the chances that other flesh from Solomon Islands *Arothron* species would be toxic if analyzed, is highly possible. Previous mouse bioassay studies by Khora S, *et al.*[47] and Teruya N, *et al*.[73] also revealed that flesh in *Arothron* species from Okinawa, Japan contained higher levels of toxicity. Since flesh is the tissue that usually owes much to most intoxication, the confirmed detection of TTX in *Arothron* species from the Solomon Islands and Okinawa, Japan should call for a ban on the consumption of these species from both regions.

TTX analysis of *A. hispidus* and *A. nigropunctatus* from the Solomon Islands and Okinawa, Japan, consistently revealed that skin accumulates more TTX than any other organs.[69] The highest level of TTX concentration obtained in this study was from the skin of *A. nigropunctatus* No.2 from Okinawa, Japan, at 255 μg/g with the lowest being from *A. hispidus* No.1 also from Okinawa at 4.26 μg/g. The highest TTX concentration in the skin of Solomon Islands toxic specimens is from *A. hispidus* No.1 at 51.0 μg/g while *A. nigropunctatus* No.2 contains lower TTX level at 7.20 μg/g. From this data, it is evident that TTX composition in the skin tissue is highly variable among pufferfish species.

Separate studies on *A. nigropunctatus* collected in the Philippines and Okinawan, Japan also confirmed comparable levels of TTX in the skin tissue [47,74]. An investigation of Hawaiian *A. hispidus* suggested high levels of TTX producing bacteria were isolated from the skin.[75] Studies on *Kytoccocus sedentarius* bacteria believed to be a TTX-producer isolated from the skin of *A. hispidus* also displayed modulating activities against P388 cell lines.[76] Other pufferfish species from *Arothron* genus which have shown to contain a considerable level of TTX either in their skin or in other organs are *A. immaculatus.*[77] *A. firmamentum*[78] *A. meleagris,*[78] *A. reticularis*[79] and *A. stellatus.*[52]

The very high level of TTX concentration in the skin has prompted the need to investigate the potential distribution of TTXs in the skin tissue. Exemplary analysis was carried out in different skin regions of *A. hispidus* No.3 and *A. nigropunctatus* No.1 from the Solomon Islands (Tables 2-25 and 2-26). The TTX analysis of the slightly darker spotted regions, plain white regions, greyish regions and the thin epidermal layer just beneath the skin (skin flesh) of *A. hispidus* No.3 showed a TTX concentration range of 40-48 μg/g (Table 2-25) which was assumed to be an even distribution of TTXs throughout the regions of the skin tissue. On the other hand, *A. nigropunctatus* No.1 showed a TTX concentrations of 17 μg/g, (dorsal regions), 20 μg/g (underside regions) and 20 μg/g (back regions) (Table 2-26). As a matter of physical observation, smooth and glossy skin textures are distinctively observed around the dorsal region while a rough texture with few small spikes uniformly covers the other regions from the base of the dorsal end, throughout the mid-body and reaches the base of the tail and fins. Whether these skin textures or their function play a role in TTX accumulation levels is yet to be fully confirmed due to limited samples used in the analysis of this species. Moreover, since different species contains different TTX profiles, speculative assumptions based on a single specimen cannot be used to fully verify the exact TTX accumulation in each species. However, despite the slight variation of TTX content, the profile of all the other analogues in these areas showed a similar pattern which seemingly accounts for an equal distribution of these analogues which at this point would also include the TTX.

When comparing the TTX distribution in this study to the Japanese pufferfish *T. pardalis*, a significant difference can be observed (Figure 2-12). *T. pardalis* contains higher levels of TTX in the liver and gonads,[80] but in *Arothron* species, these organs have a much lower TTX compared to the skin. From this study, it is highly possible that different regions together with their different biotic and abiotic factors, may play a leading role in the TTX accumulation ability of the various dominant pufferfish species in each region. Moreover, few important factors that may contribute a lot to the difference in TTX accumulation and distribution are the size of individual specimen, gender, breeding seasons and the immediate ecological interaction faced by each pufferfish species in their environment.

On a molecular level, proteins which are implicated in the TTX accumulation system may contribute to variations in toxins profile among species. Studies showed that these glycoproteins, named as PSTBP (puffer fish saxitoxin and tetrodotoxin binding protein), bind to TTX and STX in the blood plasma of *Takifugu pardalis.*[81-83)] Though parallel PSTBP screening studies should also be done for the blood plasma of *Arothron* species, the underlying question of how pufferfish directs TTX accumulation to specific organs is an interesting study with potential application in biomolecular sciences and toxicology. Moreover, to properly verify the TTX distribution profile in pufferfish species from the tropical regions, more specimen collections and analysis are required.

Other analogues with significant concentrations in this study were the 4,9-anhydroTTX, 5,6,11-trideoxyTTX, 4,4a-anhydro-5,6,11-trideoxyTTX and 4,9-anhydro-5,6,11-trideoxyTTX. Due to the structural proximity of TTX and 4,9-anhydroTTX, it is highly possible that chemical equilibrium between the two may have resulted in its higher concentration.[60,80)] An analogue that frequently surpass the TTX concentration in few organs is the 4,9-anhydro-5,6,11-trideoxyTTX (Tables 2-11, 2-19 and 2-24). Analogue 5,6,11-trideoxyTTX on the other, proves to be a major analogue not only in this study but in many pufferfish species including Japanese *T. pardalis,*[80)] *T. Oblongus,*[84)] *T. nigroviridis,*[85)] *Lagocephalus sceleratus,*[86)] *Fugu poecilonotos* [87)] and gastropod such as *Charonia lampas*[88)] and *Nassarius* spp.[89)] Previous experiment showed that 5,6,11-trideoxyTTX has a relatively low toxicity (LD_{99} 720 μg/kg, mice, i.p.)[46)] compared to TTX and other toxic analogues.

As previously highlighted, 11-oxoTTX a rare but very potent analogue was detected in *A. nigropunctatus* and *A. hispidus* from the Solomon Islands and Okinawa, Japan (Tables 2-11, 2-15,2-19 and 2-24). Studies by Yotsu-Yamashita M, *et al.*[49)] on the TTXs structural affinity to rat brain membrane showed that C-6 and C-11 are hydrogen bond donors and are vital in binding toxins to sodium channels. Since 11-oxoTTX contains an additional OH group in C11, probably its binding affinity to sodium channels is more high and efficient than TTX thus increasing its potency. Since the first isolation of 11-oxoTTX from a Micronesian *A. nigropunctatus,*[47)] few other occurrences were detected in Brazilian frog,[90)] the red spotted newt,[91)] the blue-ringed octopus,[92)] the marine

snail[93] and the xanthid crab.[94] The detection of 11-oxoTTX in *A. hispidus* from Solomon Islands is the first to be recorded in this species. Due to the higher potency of 11-oxoTTX (4-5 times potent than TTX) as revealed by some authors,[48,49] its presence in *A. hispidus* and *A. nigropunctatus* are indeed a potential risk to pufferfish poisoning.

Analysis of two specimen of *D. holocanthus* from Solomon Islands showed no TTX level or a negligible level of TTX concentration at LOD 0.01 μg/g ($S/N > 3$) (appendix p.93). Whether there are physio-ecological reasons for such results, it is not confirmed. However, when comparing the physical appearance of *D. holocanthus* to the *Arothron* species, it is evident that the skin textures of each species type varies significantly. *D. holocanthus* consists of a rough, rugged spiky-like skin texture while *Arothron* species are composed of few coarse but fairly smooth skin texture. Theoretically, if TTX is really a part of their defense strategy to void off predators than for ecological reasons it is likely that *Arothron* species would need to accumulated more TTX to protect itself whereas for *D. holocanthus*, it has adapted a more obvious method of defense.

Moreover, results displaying low or no TTX level in *D. holocanthus* may also support the very reason why some genus of *Diodon* species are a part of food source in some regions. According to the Ministry of Health, Labour and Welfare of Japan, the skin, flesh, and testis of *D. holocanthus* collected in Japan region are officially allowed for consumption.[63] Nevertheless, since the producers of TTX in marine environment such as *Vibrio* spp.[95] *Aeromonas* spp.[96] *Pseudomonas* spp.[97] cannot be tracked instantly and along with fewer to no analytical toxicology research on genus of *Diodon* species in the Solomon Islands, a possibility that intoxication from *D. holocanthus* cannot affect potential consumers in Solomon Islands or other nearby tropical regions cannot be totally ruled out. The negligible presence of TTXs (below LOD) observed in this study, needs to be supported by additional investigation of few more *D. holocanthus* from other areas of the Solomon Islands and in nearby regions to verify the status of TTX in this species.

The presence of STX and its analogues were also tested in the skin and ovary of *A. hispidus* and *A. nigropunctatus* from the Solomon Islands and Okinawa, Japan. STX was detected in the skin of all three specimens of *A. hispidus* from Okinawa (0.09, 2.80, 0.34 μg/g), as well as in the ovary of one specimen, but not detected in all *A. nigropunctatus* from Okinawa and all the pufferfish specimens from the Solomon Islands (< 0.02 μg/g). It is notable that the concentration of STX equivalents (STX + dcSTX) was 3.46 μg/g in the skin of an *A. hispidus* specimen from Okinawa.[69)] This is higher than the global regulatory limit of 800 μg of STX equivalents per kg of shellfish meat (e.g. Codex, EU, US, Japan).[98-101)] Additional analysis of STX in more specimens from both regions should be conducted because Nakashima K, *et al.*[61)] also reported that STX and dcSTX were detected in the ovary of *A. firmamentum* collected in Japan at high concentration. I hope the results obtained in this present study will help inform the citizens of Solomon Islands of the potential risks associated with the consumption of the toxic pufferfish species living within their coastal waters.

2-5.0 Conclusion

The present study showed that both *A. hispidus* and *A. nigropunctatus* specimens from the Solomon Islands and Okinawa, Japan, accumulated higher level of TTX and its analogues in the skin compared to other organs such as liver, ovary, testis, stomach, intestine, and flesh. Due to the high TTX concentration in the skin of these two species from the Solomon Islands (51.0 and 28.7 μg/g at highest) and Okinawa, Japan (12.7 and 255 μg/g at highest), a ban on their consumption should be imposed by relevant authorities. In addition, the presence of 11-OxoTTX, a rare but more potent analogue than TTX commonly detected in all toxic specimens in this study should also warn citizens of these regions of the potential risks of higher toxicity. STX was detected in the skin of all *A. hispidus* specimens from Okinawa, Japan, with one of the specimen showed presence of STX in the ovary. The level of STX equivalents (STX + dcSTX) in the skin of one specimen was 3.46 μg/g, which is more than the global regulation level. More monitoring and awareness programs as well as up-to-date toxicity studies of pufferfish species (including other *Arothron* species) and other marine natural biotoxins is recommended for these regions.

Chapter 3.0 Studies on Marine Invertebrates

Introduction of Marine Natural Products.

Natural products are intriguing sources of bioactive secondary metabolites. It was estimated that approximately 75% of antibiotic and anticancer drugs currently in use are from natural sources or are at some point derived or modified from natural product compounds.[102)] Marine environment has been a source of knowledge for centuries. With the need to survive these competitively harsh conditions, marine organisms are believed to have developed predative and/or defensive mechanisms to hunt or protect themselves and in doing so produce some of the most interesting secondary metabolites useful in combating a variety of diseases. Marine invertebrates such as marine sponges, soft and hard corals, tunicates or even marine microbes and fungi are few examples. Marine sponge in particular, has been extensively studied for the purpose of drug discovery and biomedicine.[103,104)] In this study, marine sponges collected in the Solomon Islands were screened for potential bioactive compounds using bioassay guided fractionation method. Cell-based bioassay was employed as the basis for each stages of fractionation.

Chapter 3.1.0 Minor Introduction (*Melophlus* sp.)

Steroidal glycosides such as the 30-norlanostane triterpenoidal saponin sarasinosides from marine sponges (class Demospongiae)[105] contain variable congeners[106-108] that possess various biological activities against bacteria, yeast, or fungi,[109,110] ichthyotoxicity against killifish *Poecilia reticulata* [110], and cytotoxicity against cancer cell lines.[111-114]

Since the first isolation of a sarasinoside from the Palauan marine sponge *Asteropus sarasinosum* by Kitagawa and group,[110] continuous discovery by various groups have so far been made on the marine sponge genus *Melophlus*.[109,111-114] Generally, known sarasinosides are classified according to their aglycon skeleton structures and sugar moieties which are represented by either pentaoside or tetraoside sugar types[109,114] (Figure 3-1).

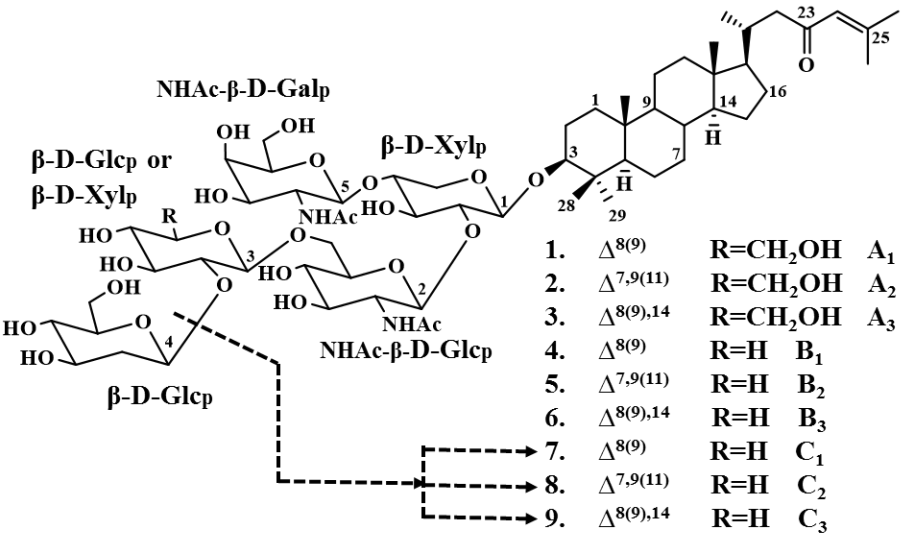

Figure 3-1. Few known sarasinosides categorized on the basis of their steroidal structures and sugar moieties.

In this study, the discovery of a new sarasinoside congener, sarasinoside M_2 (**1**; Figure 3-2), will be discussed along with known sarasinosides B_1 (**2**) and B_2 (**3**) or B_3 (**4**) (Figure 3-3), which were isolated from a marine sponge assumed to be *Melophlus* sp. collected in the Solomon Islands (Figure 3-4).

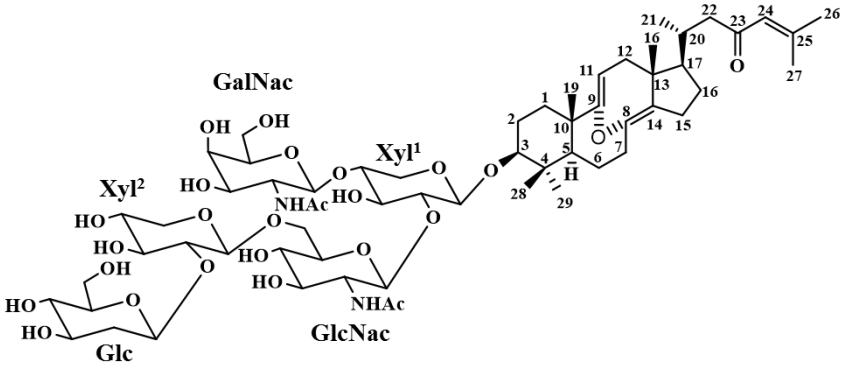

Figure 3-2. Structure of sarasinoside M_2 (**1**)

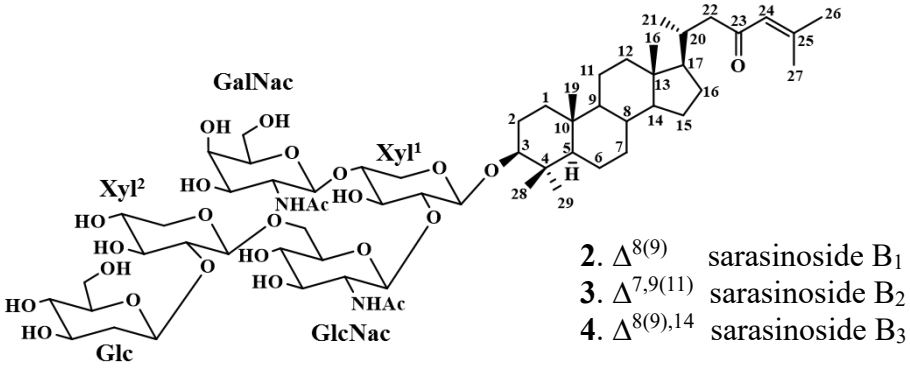

Figure 3-3. Structures of sarasinoside $B_{1\text{-}3}$ (**2**-**4**)

Figure 3-4. *Melophlus* sp. collected in the Solomon Islands.

3-2.0 Procedure [115)]

3-2.1 Isolation and purification

A marine sponge identified via the database to have shown the identical physical features of a *Melophlus* sp. (Figure 3-4) was collected in the Solomon Islands, cut into a small portion that weighed approximately 7.0 g and was transported to Tohoku University in a disposable plastic tube (TPP, Trasadingen, Switzerland) containing 20 mL of the EtOH–H_2O mixture (7:3, *v/v*) at room temperature. Upon arrival, the specimen was kept in -25^{o}C until use.

The specimen was chopped, minced, soaked in 20 mL of EtOH–H_2O (9:1, *v/v*) and left to macerate for a while. After the supernatant was remove this procedure was repeated two more times and together with the preserving solvent [EtOH–H_2O (7:3, *v/v*)], the mixture was filtered through ADVANTEC Toyo filter No.2 - 185 mm (Toyo Roshi Kaisha, Ltd., Tokyo, Japan) and vacuum dried using rotary evaporator.

The extract was then partitioned between ethyl acetate (EtOAc) and H_2O (2:1, *v/v*). The dried residue (40 mg) from the EtOAc portion was suspended in 100 µL of MeOH, which was then applied to a Sep-Pak® C-18 SPE cartridge (0.7 mL, Waters, USA) to obtain six fractions [MeOH–H_2O: 0:1, 3:7, 1:1, 8:2, 1:0 (*v/v*), and absolute acetonitrile] (F1-6). Scheme 3-1) Based on the preliminary cell-base assay from mouse neuroblastoma 2a cell line with a concentration of 100 ug/mL, the fractions MeOH–H_2O (8:2/1:0) showed a high cytotoxicity (Figure 3-5) which was the focus of the next stage of purification procedure.

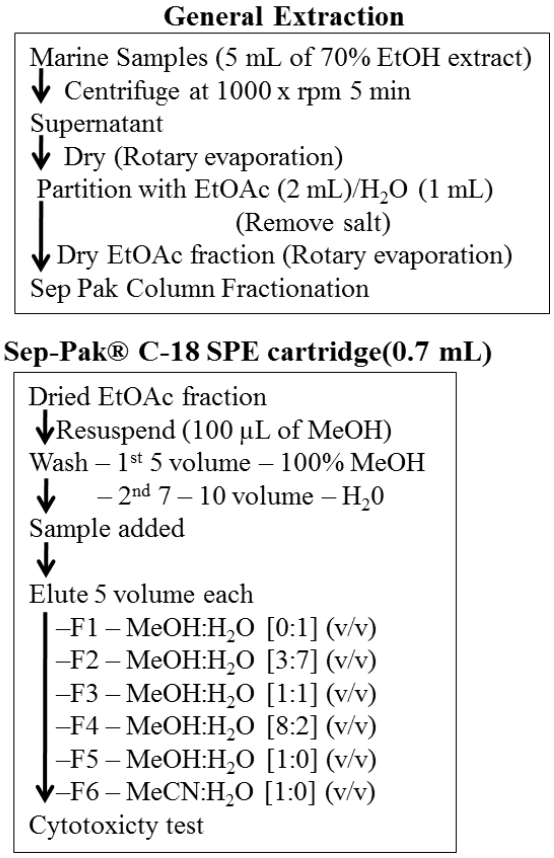

Scheme 3-1. General extraction procedure and Sep Pak fractionation method.

3-2.2 Cytotoxicity bioassay

Compounds **1** and **2** were tested for their toxicity against mouse neuroblastoma (Neuro-2a) and human hepatocyte carcinoma (HepG2) cell lines. The cells were cultured in RPMI 1640 medium (Sigma-Aldrich, St. Louis, MO, USA) supplemented with 10% fetal bovine serum and 100 µg/mL streptomycin and 100 U/mL penicillin in 96-well plates and incubated at 37 °C in 5.0% of CO_2 /air. The test compounds were solubilized in DMSO and were added to the cells (DMSO final conc. 0.50%, *v/v*) after a preincubation of 12 h. After a 24 h, Cell Count Reagent SF (Nacalai Tesque) was added, and the cells were re-incubated for 2.5 h. Rotenone was used as the positive control, while a separate 0.5% *v/v* DMSO was the negative control. The cytotoxicity was evaluated by means of absorbance at 405 nm on a Bio-Rad 680 Microplate reader.

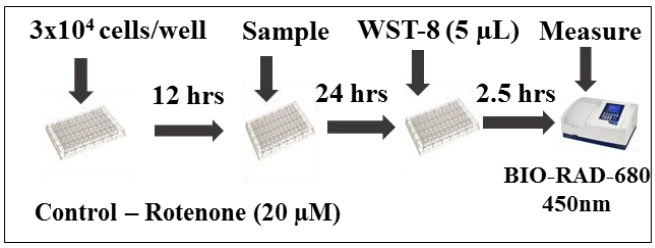

Scheme. 3-2. Flow diagram of cytotoxicity bioassay.

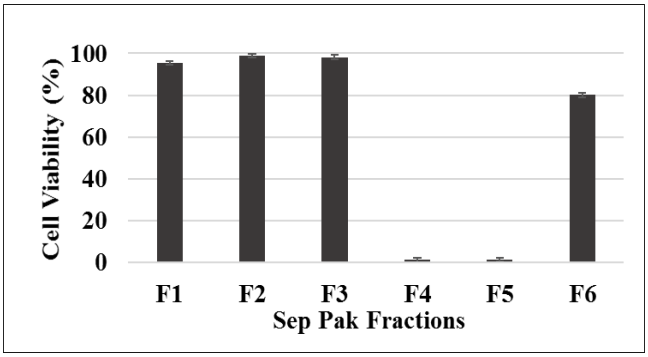

Figure 3-5. Preliminary cytotoxicity result after the Sep Pak fractionation of *Melophlus* sp.

3-2.2 HPLC Purification

The residues from the MeOH–H_2O (8:2/1:0) fractions were combined (5.4 mg) and was then subjected to a Mightysil RP-18GP II column chromatography (10 × 250 mm, 5 µm, Kanto Chemical, Tokyo, Japan) with a condition set as stepwise elution: MeOH–H_2O 1:1, 8:2, 9:1, and 1:0 (*v/v*). The parameter for UV detection was set at 240 nm and was observe using a diode array detector (DAD) (Hitachi Chromaster 5430, Hitachi, Japan) (Figure 3-6)

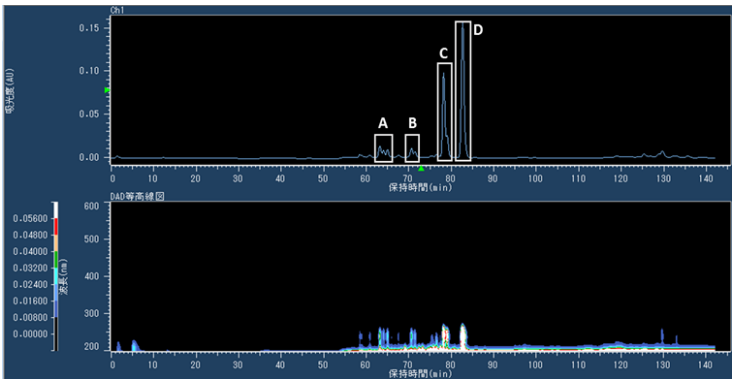

Column: Mighysil RP-18 GPII 250 mm, (5 µm). Kanto Chemical)
Mobile Phase: A: MeOH, B: H_2O. Initial 50% A, 80% A, 90% A, 100% A (0-100 min). 1.0 mL/min

Figure 3-6. LC-DAD chromatogram of Sep Pak fraction (F4-5). A) Mixture of C and D. B) is the new sarasinoside M_2, C) is sarasinoside B_2 or B_3, D) is sarasinoside B_1

The screening of compounds in fractions correlating the peaks observed in the UV-DAD were first performed using API 2000 AB SCIEX. From each fraction 2 µL was diluted tenfold and 5 µL was injected into the API 2000 AB SCIEX by direct injection. General parameters were set as a positive mode, 2 min run time with a target range of *m/z* 400 – 1500. This gave the specific candidate compounds which ultimately helped narrowed the focus of the search. To further verify the candidate compounds, 2 µL from each fraction was diluted one hundred-fold and 1 µL (1-2 ng) of each fraction was applied to the high-resolution (HR) electrospray mass spectrometry (ESI-MS; MicrOTOF QII, Bruker Daltonics, Billerica, MA, USA).

The screening result led to the identification of the new sarasinoside congener (sarasinoside M_2, (**1**), along with other known sarasinosides B_1 (**2**)[110] and B_2 (**3**) or B_3 (**4**). The weight of **1** was approximately 0.8 mg, **2** approximately 1.4 mg while **3** or **4** was at least 1.0 mg. The fraction containing the new sarasinoside was further purified using a Cosmosil Cholester column (4.6 × 250 mm, 5 μm, Nacalai Tesque, Kyoto, Japan), with gradient elution of MeOH–H_2O (8:2, *v/v*) : MeOH–formic acid (99.9:0.1, *v/v*). Figure 3-7.

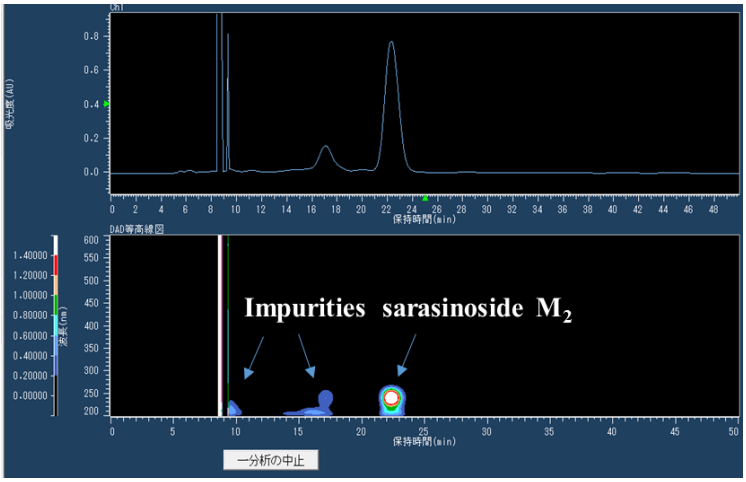

Cholester (Cosmosil) (4.6 x 250 mm. Nacalai tesque)
Gradient Elution; MeOH–H_2O (8:2, *v/v*): MeOH–formic acid (99.9:0.1 *v/v*), (100 min), 0.5 mL/min

Figure 3-7. LC-DAD after further purification of the fraction containing the new compound; sarasinoside M_2 (**1**).

3-2.2 LC-MS Analysis by API 2000 SCIEX ™

Prior to drying the new compound, 2 µL of the fraction containing the new compound was diluted tenfold and was analysed using the API 2000 AB SCIEX LC-MS to check for its purity. The Cosmosil Cholester column (4.6 × 250 mm, 5 µm, Nacalai Tesque, Kyoto, Japan) was used on a positive selected ion monitoring (SIM) mode, with a mixture of MeOH-H_2O (8:2) *v/v* and a flow rate of 2 mL/min at a duration of 95 min (Figure 3-8). The major (SIM) ion chromatogram was set at *m/z* 1295 along with other additional minor target ions.

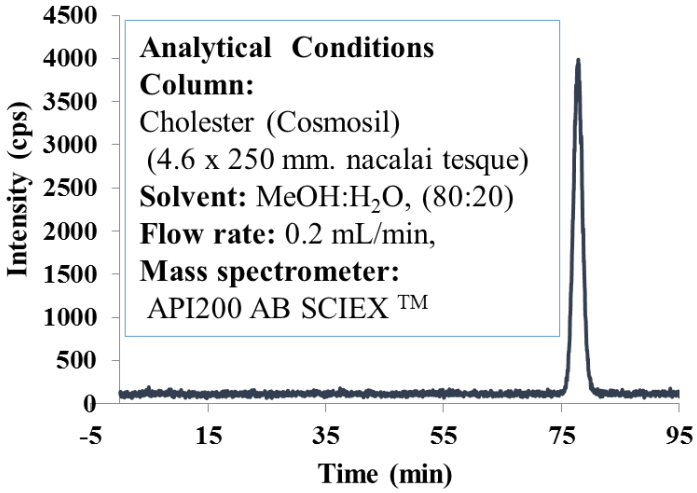

Figure 3-8. SIM chromatogram of a more purified form of the new sarasinoside M_2 (**1**)

SIM chromatogram displayed a single peak at approximately 80 min which indicated that the compound was at least much closer to pure. The fraction containing the new sarasinoside was dried to an extent where a colorless powder was obtained, weighed (approximately 0.5 mg) and suspended in CD_3OD (0.4 mL) for NMR spectral analysis. The new sarasinoside was named sarasinoside M_2 which is a congener of the sarasinoside group of compounds.

3-3.0 Results/Discussion

3-3.1 Structure Determination

From the HR-ESI-MS peak spectrum of **1**, its molecular formula was determined to be $C_{61}H_{96}N_2O_{26}$ and showed $[M + Na]^+$ *m/z* 1295.6128 (calcd. for $C_{61}H_{96}N_2O_{26}Na$ 1295.6144; and $[M + H]^+$ *m/z* 1273.6305 (calcd for $C_{61}H_{97}N_2O_{26}$ 1273.6309). (Figure 3-9 (A)). The negative mode also supported the existence of **1** with precursor ions $[M – H]^-$ *m/z* 1271.6062, (calcd for $C_{61}H_{97}N_2O_{26}$ 1271.6068), $[M + Cl]^-$ *m/z* 1307.5846 and $[M + HCOOH – H]^-$ *m/z* 1317.6124 (Figure 3-9 (B)).

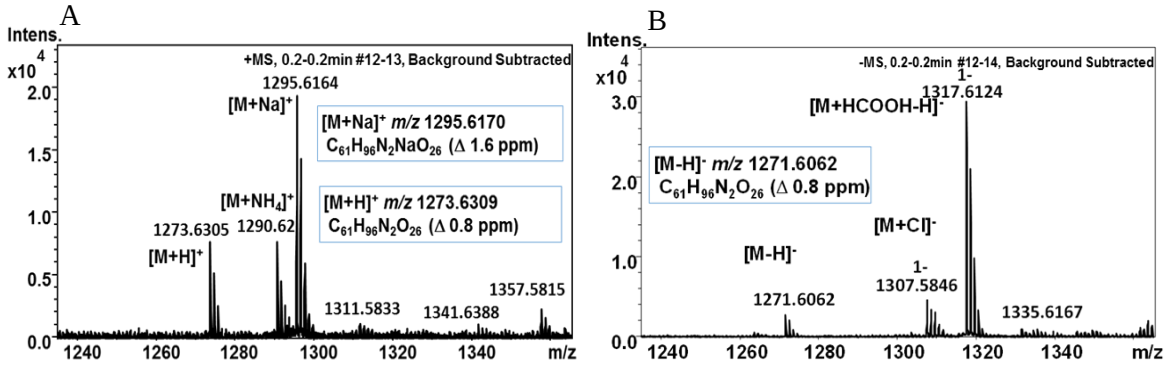

Figure 3-9. HR-ESI-MS spectrum of **1** in both A) positive and B) negative ion modes.

Partial assignment of the ^{1}H NMR (Figure 3-10) signals and ^{13}C NMR signals of **1** were performed on the basis of gradient COSY, TOCSY, TOCSY1D, and gradient HSQC spectra as shown in the appendix p.94-98, 104-109.

The assignment of the ^{1}H NMR signals and ^{13}C NMR signals are listed in Table 3-1.

Table 3-1. NMR spectroscopic data of sarasinoside M_2 (**1**) in CD_3OD.

No.	δ^{13}C	δ^{1}H	(mul. *J* in Hz)	No.	δ^{13}C	δ^{1}H	(mul. *J* in Hz)
1	ND	1.68	brt 10.5	Xyl^{1}-1'	107.2	4.35	d, 7.4
		1.45	m	Xyl^{1}-2'	ND	3.93	m
2	ND	1.81	m	Xyl^{1}-3'	ND	3.56	t 8.5
		1.81	m	Xyl^{1}-4'	ND	3.72	m
3	92	3.18	q 8.0	Xyl^{1}-5'	63.7	3.15-3.20	m
4	ND			GlcNAc-1"	102.7	4.87	d 8.5
5	ND	1.96	m	GlcNAc-2"	ND	3.72	t 8.2
6	ND	1.68	m	GlcNAc-3"	ND	3.43	t 10.3
		1.45	m	GlcNAc-4"	ND	3.18	t 7.2
7	ND	2.72	d 11.0	GlcNAc-5"	ND	3.72	t 8.6
		2.14	m	GlcNAc-6"	70.7	3.71/4.11	t 8.6, d 10.8
8	ND			GlcNAc-Ac	23.6	1.98*	s
9	171.2			Xyl^{2}-1'''	103.3	5.05	d 7.5
10	ND			Xyl^{2}-2'''	83.4	3.41	t 8.8
11	ND	5.21	t 6.4	Xyl^{2}-3'''	ND	3.68	t 10.0
12	ND	3	dd 13.0, 6.4	Xyl^{2}-4'''	72.1	3.52	m
		2.12	m	Xyl^{2}-5'''	62.7	3.68/ND	t 10.0, ND
13	ND			Glc-1''''	106.1	4.65	d 7.0
14	ND			Glc-2''''	77.3	3.44	m
15	ND	1.45	m	Glc-3''''	ND	3.31-3.38	m
16	ND	2.3	m	Glc-4''''	ND	3.31-3.38	m
		2.05	m	Glc-5''''	ND	3.31-3.38	m
17	ND	1.23	m	Glc-6''''	63.6	3.7	m
18	18.1	0.95	s	GalNAc-1'''''	103	4.53	d 10.3
19	23.2	1.22	s	GalNAc-2'''''	ND	3.92	t 9.0
20	ND	2.1	m	GalNAc-3'''''	ND	3.65	dd 9.0, 1.2
21	21.3	0.95	d 5.9	GalNAc-4'''''	ND	3.83	m
22	52.3	2.59	brd 15.3	GalNAc-5'''''	ND	ND	
		2.18	m	GalNAc-6'''''	63.7	3.92/ND	t 8.0, ND
23	ND			GalNAc-Ac	23.6	1.99*	s
24	125.6	6.21	s				
25	ND						
26	21.5	2.11	s				
27	28	1.9	s				
28	17.8	0.96	s				
29	29.6	1.21	s				

^{1}H NMR (600 MHz), ^{13}C NMR (151 MHz). ND represents “not determined”. *interchangeable assignment.

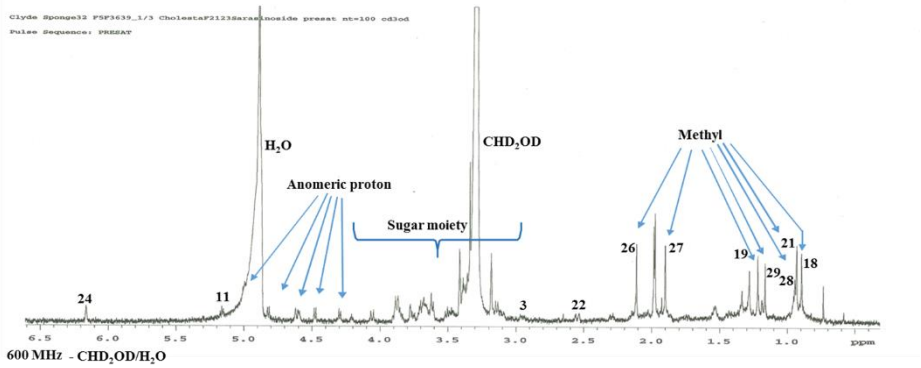

Figure 3-10. ^{1}H NMR spectrum of **1** with major signals of structural assignment.

Compound **2** was identified using HR-ESI-MS at $[M + Na]^+$ *m/z* 1281.6310, calcd. for $C_{61}H_{98}N_2O_{25}Na$ 1281.6351, and $[M + H]^+$ *m/z* 1259.6498 calcd for $C_{61}H_{99}N_2O_{25}$ 1259.6531 (Figure 3-11 (A)). The negative mode also supported the likely presence of **2** by displaying precursor ions $[M - H]^-$ *m/z* 1257.6058, $[M + Cl]^-$ *m/z* 1293.6183 and $[M + HCOOH - H]^-$ *m/z* 1303.6105 (Figure 3-11 (B)). SciFinder database search and spectral comparison from NMR data in literature showed that **2** corresponded to a known sarasinoside B_1 which was first isolated by Kobayashi and Kitagawa group.[110,114)] The ^{1}H NMR signals and ^{13}C NMR signals assignment of **2** which resembled the literature value are listed in Table 3-2.

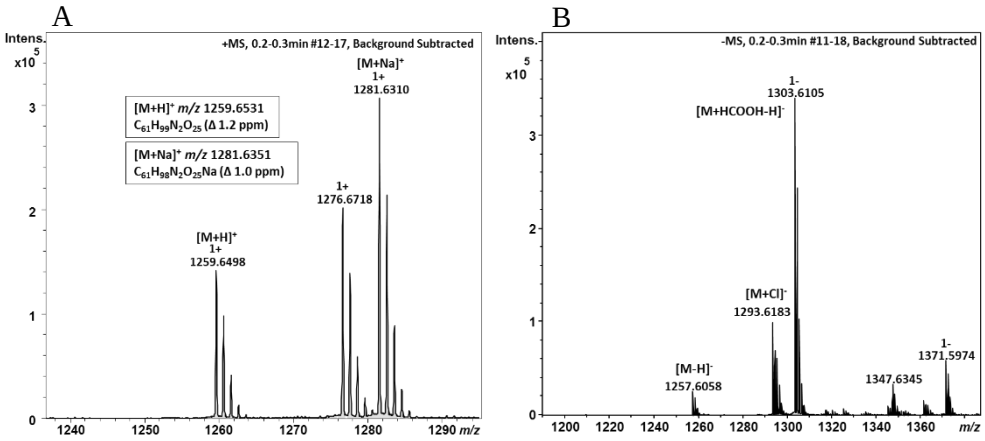

Figure 3-11. HR-ESI-MS chromatogram of **2** in both A) positive and B) negative ion modes.

Assignment of the ^{1}H NMR signals and ^{13}C NMR signals of **2**[110] were performed on the basis of gradient COSY, TOCSY, TOCSY1D, and gradient HSQC spectra as shown in appendix p.99-103, 104-109. This NMR spectral assignment were almost the same as the one in the literature[110, 114] except that additional signals were detected in **2** from the Solomon Islands marine sponge.

Table 3-2. NMR spectroscopic data of sarasinoside B_1 (**2**) in CD_3OD.

No.	δ^{13}C	δ^{1}H	(mul. *J* in Hz)	no.	δ^{13}C	δ^{1}H	(mul. *J* in Hz)
1	ND	1.69	brt 10.5	Xyl^{1}-1'	107.5	4.35	d, 7.2
		1.40	m	Xyl^{1}-2'	ND	3.95	m
2	ND	1.82	m	Xyl^{1}-3'	ND	3.51	t 8.4
		1.82	m	Xyl^{1}-4'	ND	3.70	m
3	92	3.20	q 8.0	Xyl^{1}-5'	63.7	3.18-3.21	m
4	ND			GlcNAc-1"	102.2	4.89	d 8.4
5	ND	1.96	m	GlcNAc-2"	ND	3.74	t 8.0
6	ND	1.65	m	GlcNAc-3"	ND	3.42	t 10.4
		1.45	m	GlcNAc-4"	ND	3.20	t 7.0
7	ND	2.72	d 11.0	GlcNAc-5"	ND	3.70	t 8.5
		2.14	m	GlcNAc-6"	70.7	3.73/4.13	t 8.5, d 10.9
8	ND			GlcNAc-Ac	23.6	2.00*	s
9	171.2			Xyl^{2}-1'"	103.5	5.08	d 7.6
10	ND			Xyl^{2}-2'"	83.1	3.40	t 8.9
11	23	2.1	m	Xyl^{2}-3'"	ND	3.70	t 9.9
12	ND	2.0	m	Xyl^{2}-4'"	72.0	3.54	m
		1.4	m	Xyl^{2}-5'"	63	3.65/ND	t 9.9, ND
13	ND			Glc-1""	106.4	4.67	d 7.0
14	ND			Glc-2""	77.1	3.42	m
15	ND	1.48	m	Glc-3""	ND	3.33-3.40	m
16	ND	2.1	m	Glc-4""	ND	3.33-3.39	m
		2.05	m	Glc-5""	ND	3.33-3.40	m
17	ND	1.20	m	Glc-6""	63.2	3.71	m
18	18.5	0.90	s	GalNAc-1""	103.2	4.55	d 10.4
19	23.0	1.20	s	GalNAc-2""	ND	3.90	t 9.2
20	ND	2.2	m	GalNAc-3""	ND	3.62	dd 9.2, 1.4
21	21.3	0.95	m	GalNAc-4""	ND	3.85	m
22	52.3	2.58	brd 15.3	GalNAc-5""	ND	ND	
		2.18	m	GalNAc-6""	63.3	3.9/ND	t 8.2, ND
23	ND			GalNAc-Ac	23.2	2.00*	s
24	125.5	6.22	s				
25	ND						
26	21.5	2.10	s				
27	28	1.8	s				
28	18.0	0.96	s				
29	29	1.21	s				

^{1}H NMR (600 MHz), ^{13}C NMR (151 MHz). ND represents 'not determined".

HR-ESI-MS of compounds **3** or **4**[110,114] revealed $[M + H]^+$ *m/z* 1257.6373; calcd for $C_{61}H_{97}N_2O_{25}$, 1257.6375, $[M + Na]^+$ *m/z* 1279.6205; calcd for $C_{61}H_{96}N_2O_{25}Na$, 1279.61.94. (Figure 3-12. Both **3** and **4** have the same molecular formula $[M + H]^+$ *m/z* 1257.6373 however due to low recovery of this compound, the NMR spectral data which would identify the assumed known compound was not obtained.

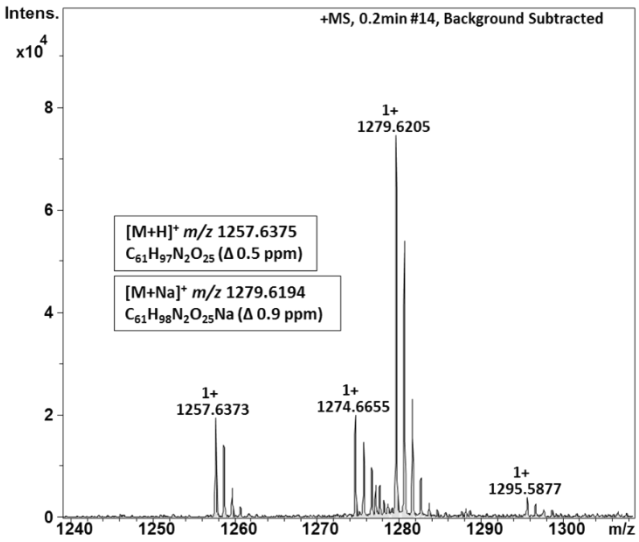

Figure 3-12. HR-ESI-MS spectrum of **3** or **4** in a positive ion mode.

By comparing the chemical shifts and coupling constants of ^{1}H NMR signals of the sugar moiety of **1** and **2**, results showed that all values detected were similar for both compounds although few coupling constants of the ^{1}H signals of the sugars of **1** were not completely determined as can be seen in Table 3-1 and 3-2. To confirm that **1** and **2** possess the same sugar moiety, which is a sarasinoside B-type, an additional measurement of the TOCSY1D spectra of **1** and **2** were performed. (See appendix p.104-109). The two compounds were irradiated at the anomeric proton signals on each of the five sugars and independent H-6 signals of GlcNAc. Result showed a similarities between the irradiated targets of **1** and **2**, indicating that both possess the same sugar moiety. Additional comparison suggested that the sugar moiety of **1** is 3β-O-[β-Glcp (1→2) β-Xylp (1→6) β-GlcNAcp (1→2) (β-GalNAcp (1→4)) β-Xylp], which is the same as **2**[110] except that the absolute configuration to verify their stereochemistry was not determined.

Similarly, the HR-ESI-MS/MS fragmentation pattern of **1**, **2** and **3** or **4** all displayed a sarasinoside B type sugar moiety. The HR-ESI-MS/MS spectra of **1**, **2** and **3** or **4** were recorded by setting the precursor $[M + Na]^{+}$ ions at *m/z* 1295.6128, *m/z* 1281.6178 and *m/z* 1279.6170 respectively. Although each compound has a different molecular weight (except for **3** and **4**), the fragmented ions that were gradually decomposed were very similar and corresponded to the same group of sugars they all possess. For instance, HR-ESI-MS/MS peaks of **1** detected at *m/z* 1295.6128 (calcd. for $C_{61}H_{96}N_2O_{26}Na$ 1295.6130, *m/z* 1092.5309 (calcd. for $C_{43}H_{83}NO_{21}Na$ 1092.5309) and *m/z* 798.4380 (calcd. for $C_{32}H_{65}NO_{12}$ 798.4380) represented the molecule of **1** and its degrading fragment ions after a sequential loss of GalNAc, Glc, and Xyl^2 sugars respectively. Similarly, the lower fragment ions of **1** detected at *m/z* 498.1826, 336.1306, and 204.0883 (Figure 3-13 (A)) indicated that Glc-Xyl^2-GlcNAc, is also present in the molecule of **1** which is apparently the same for **2** and **3** or **4** (Figure 3-13 (B, C)).

A) sarasinoside M_2 (**1**)

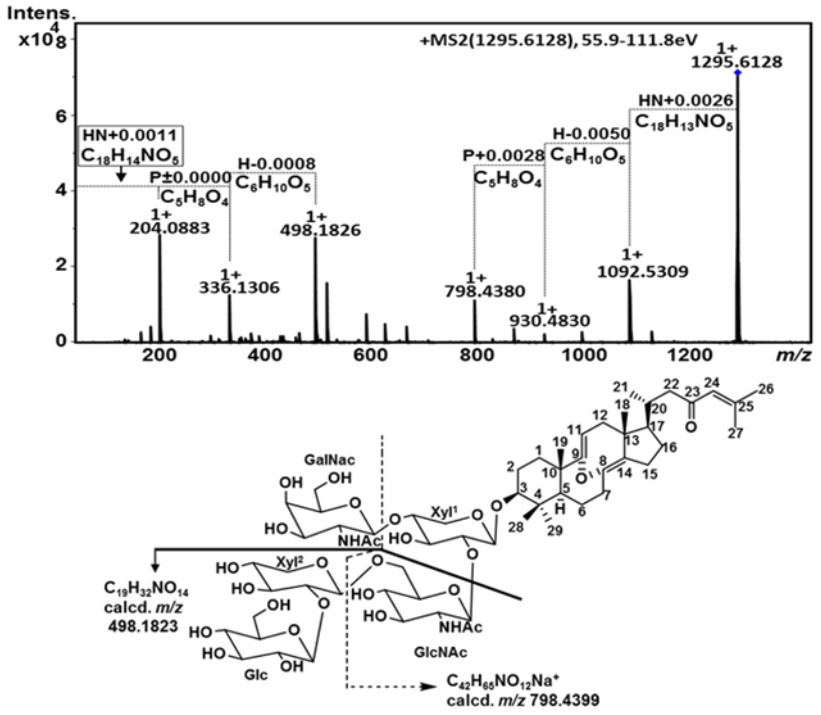

B) Sarasinoside B_1 (**2**)

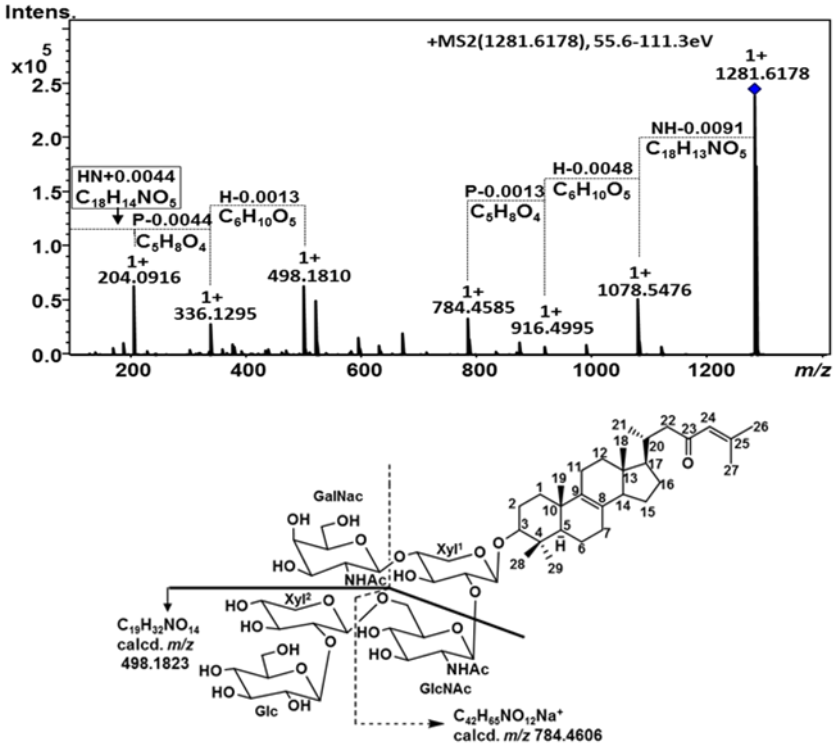

C) sarasinoside $B_{2\text{-}3}$ (**3-4)**

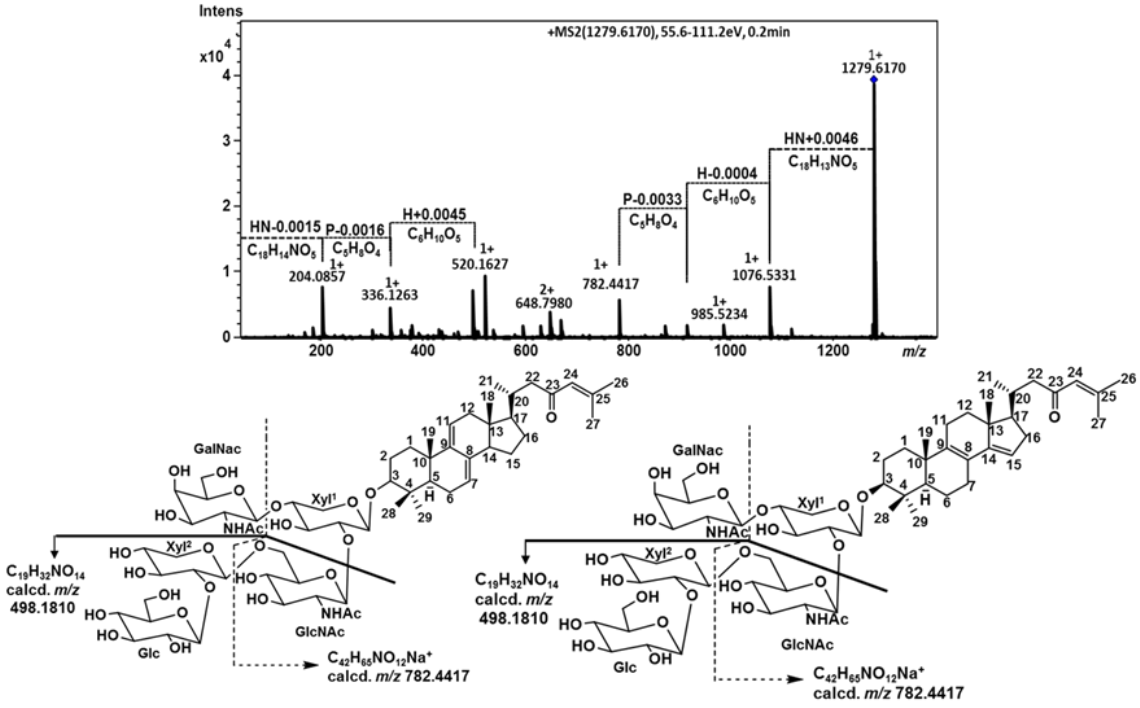

Figure 3-13. HR-ESI-MS/MS with the fragmented ions of A) **1**, B) **2** and C) **3** or **4**. Acronyms HN, H, and P represent *N*-acetyl hexose, hexose, and pentose, respectively.

Among other similar structural features that are present in the structures of **1** and **2**, ^{1}HNMR data signals at 6.21 ppm in **1** and 6.22 ppm in **2** corresponding to C24–C26, 27 (Figure 3-14) along with other signals suggested that both compounds possessed the same side chain structure which is a dimethyl substituted enone moiety at carbon positions C20–C27. Therefore, the difference between **1** and **2** is likely to be observed in their steroidal structures. By comparing their molecular formulas, the similarities in their distribution patterns and the side chain structure, it is apparently clear that the difference only exist in the molecular formula of the core steroidal structure which excluded the side chain at positions C20–C27. The core steroidal structure of **1** is proposed to be $C_{21}H_{32}O$, while that of **2** is $C_{21}H_{34}$. Moreover, the presence of oxygen in **1** would account for the additional 18 amu (one oxygen and absent of two hydrogen due to ether bond) calculated in the molecular weight of **1**.

^{1}H NMR data comparison of the aglycon of **1** (Table 3-1) with the known sarasinosides that also possessed $C_{21}H_{32}O$ as a steroidal structure showed a similarity in the aglycon structures of **1** and sarasinoside M (**5**)[115] (Figure 3-15). Both contained a rare ether bond between two olefin carbons (C8 and C9). The existence of the ether bond in **1** was supported by the presence of the characteristic coupling signals of H-11 (δ 5.21, t 6.4 Hz) and H2-12 (δ 3.00, dd 13.0, 6.4 Hz; δ 2.12, m) shown in COSY and TOCSY spectra of **1** (S3, S4). This is very similar to the coupling signals of **5** at H-11 δ 5.21, t 6.9 Hz and H2-12 δ 3.00, dd, 13.2, 6.9 Hz; δ 2.12, dd, 13.2, 6.9 Hz) as described by Dai HF, *et al.*[116] An evidence that showed the natural existence of the seemingly unstable C8-C9 ether bond can be seen in the structure of tylopiol A[117] (Figure 3-16 (A)), along with its crystal structure (Figure 3-16 (B)) and plastic model of sarasinoside M_2 to show the α-orientation (stereochemistry) of the ether bond at position C8-C9 (Figure 3-16 (C)).

Due to the limited amount of **1** (0.5 mg), a sufficient ^{13}C NMR cannot be fully assigned. However, a coupling correlation in the HMBC spectrum of **1** which proved the presence of ether bond in **1** was observed in C9 (δ 171.2)/H3-19. This greatly supported the structure of **1** since **5** also displayed a similar chemical shift at position C9 (δ 172.7).[115] It is worth noting that the difference of the chemical shift between the aglycon of **1** and **5** was less than 0.1 ppm in the ^{1}H NMR spectrum and less than 1.5 ppm (C9) in the ^{13}C NMR spectrum, which supported a structural resemblance in their aglycon. The absolute configuration of the aglycon of **1** was not determined due to the limited sample obtained.

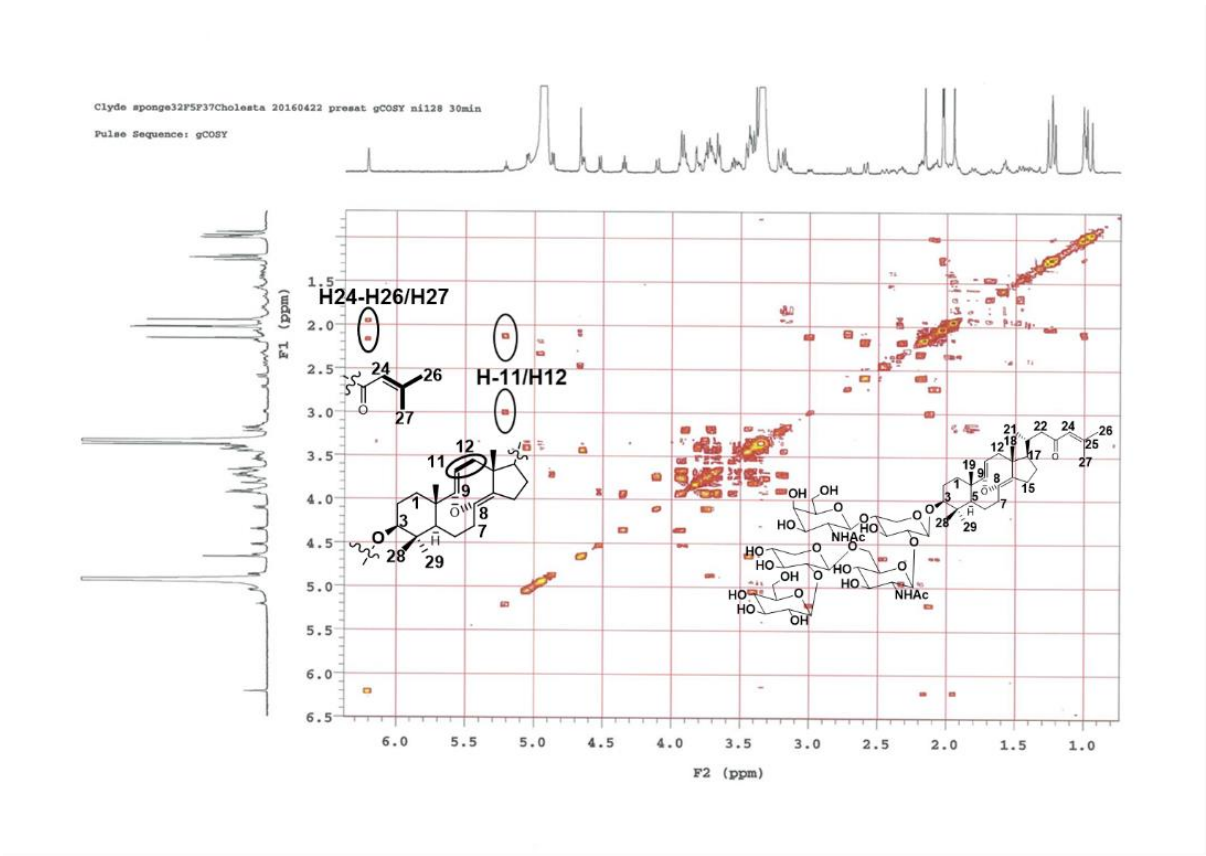

Figure 3-14. COSY spectrum (CD_3OD, 600 MHz) of sarasinoside M_2 (**1**) with the characteristic cross peaks.

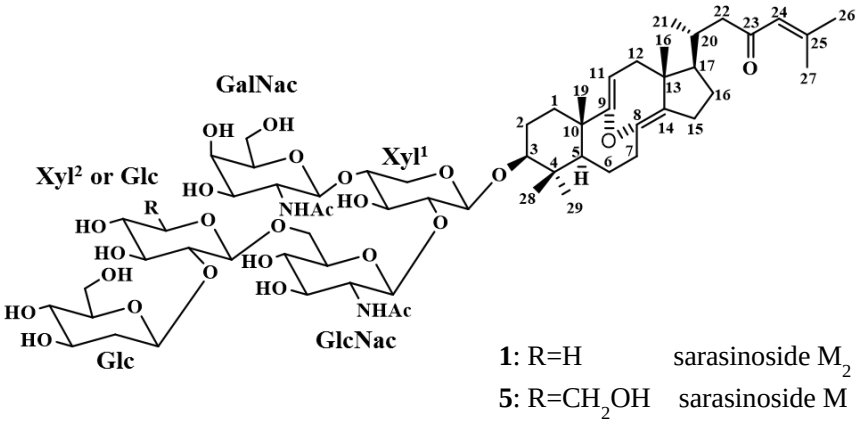

Figure 3-15. Structures of sarasinoside M_2 (**1**) and M (**5**).

Therefore, the difference between **1** and **5** would likely to be found only in a sugar moiety which would suggest that the internal Glc present in **5** is replaced by Xyl in **1**. The difference in the hydroxymethyl substituent of **1** and **5** along with the structural difference in ether bond between C8-C9 of **1** and double bond in C8-C9 of **2** agrees well with each of their molecular formula, molecular weight and other structural features, thus, making **1** a new sarasinoside congener. Since **5** contained a sarasinoside A type sugar moiety, the presence of Glc of **5** compared to Xyl of **1** (both located in the third sugar of the sugar moiety group) categorizes **5** to be a sarasinoside A type compound. Other reported steroidal congeners with a characteristic ether bond between two olefin carbons included tylopiol A,[117] sarasinoside A_4,[118] and jereisterol A.[119]

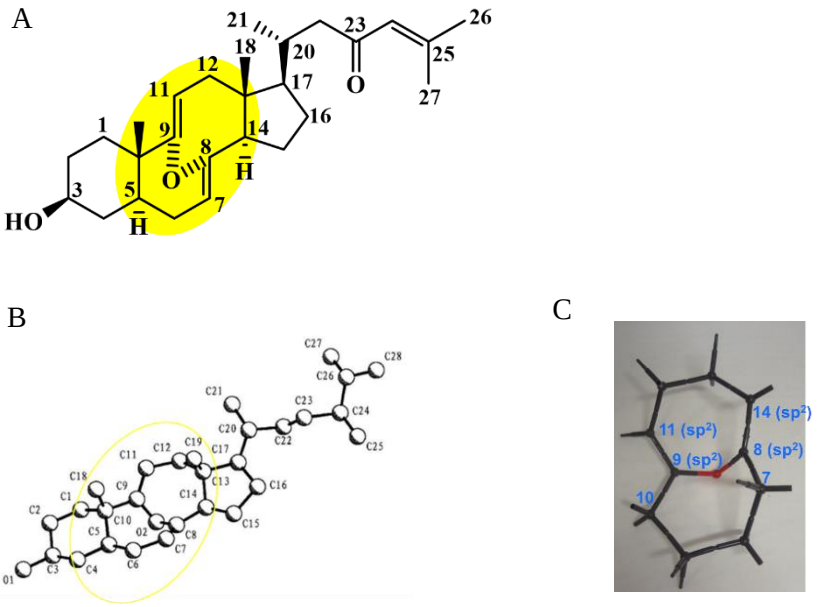

Figure 3-16. A) Stereochemistry of tylopiol A. B) A crystal structure of tylopiol A obtained by X-ray analysis. C) A model structure of sarasinoside M_2 that supports the α-orientation of the ether bond.

3-3.2 Cytotoxic Activity Test

Compounds **1** and **2** were tested for their cytotoxic activity using the procedure outlined in the methodology section 3-2.2. The IC_{50} values (half maximal [50%] inhibitory concentrations, mean ± SD, n = 3) for **1** and **2** toward Neuro-2a cells were approximately 21.5 ± 1.6 and 7.3 ± 0.3 μg/mL respectively (Figure 3-17 (A, C). For the cytotoxicity bioassay using HepG2 cells, the incubation period was extended to 48 h due to their slow growth rate. The cytotoxic activity against HepG2 cells revealed IC_{50} for **1** as approximately 20.4 μg/mL and 26.7 μg/mL with the average IC_{50} of 24 μg/mL (n = 2, due to limited sample amount) and for **2** as 7.4 ± 1.2 μg/mL (mean ± SD, n = 3; Figure 3-17 (B, D)). Although the cytotoxicity of **1** and **2** markedly displayed different cytotoxic strengths, both compounds are categorized as possessing a moderate activity towards Neuro 2a and HepG2 cell lines. These values also correlated the reported cytotoxicity of other sarasinosides against K562 leukemia and A549 lung carcinoma cell lines.[120)]

According to Kalinin V, *et al*.[108)] the decrease in the biological activities of sarasinoside type compounds can be a result of the modifications in C and D rings. These may include the migration of double bond into C8(14)-position, the presence of introduced oxygen-bearing substituents and various occurrences of oxidative transformations in cyclic systems of aglycons. In relation to this study, the difference in the cytotoxic activities displayed by **1** and **2** seemed to support the structural changes and their biological properties highlighted by Kalinin V, *et al*.[108)]

A) **Cytotoxicity of sarasinoside M_2 against Neuro-2a cells**

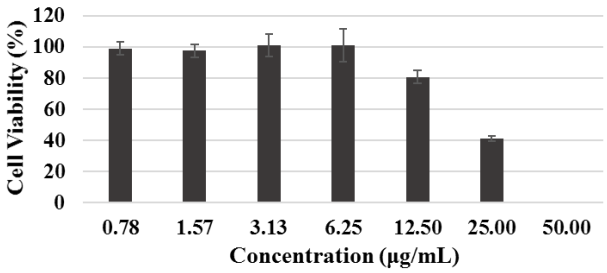

Sarasinoside M_2 displayed IC_{50} at 21.5 ± 1.6 µg/mL. Cytotoxicity bioassay carried out in triplicate (n=3).

B) Cytotoxicity of sarasinoside M_2 against HepG2 liver cells

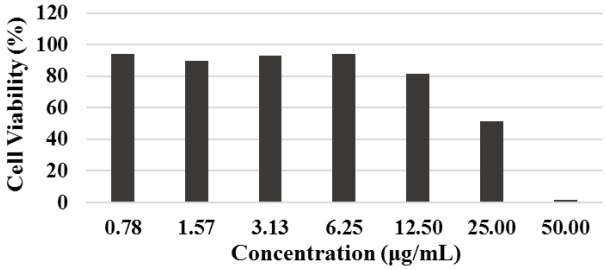

Sarasinoside M_2 displayed IC_{50} at 24 µg/mL (mean of two data). Cytotoxic bioassay carried out in duplicate (n=2).

C) Cytotoxicity of sarasinoside B_1 against Neuro-2a cells

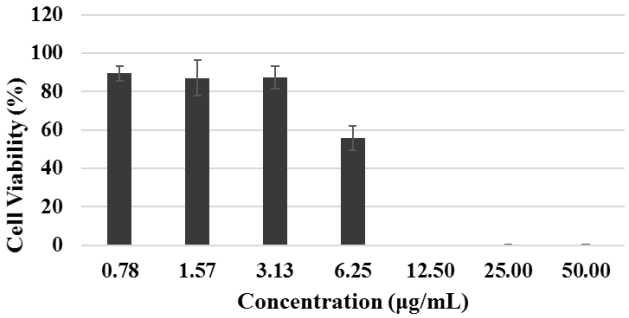

Sarasinoside B_1 displayed IC_{50} at 7.3 ± 0.3 µg/mL. Cytotoxicity bioassay carried out in triplicate (n=3).

D) Cytotoxicity of sarasinoside B_1 against HepG2 liver cells

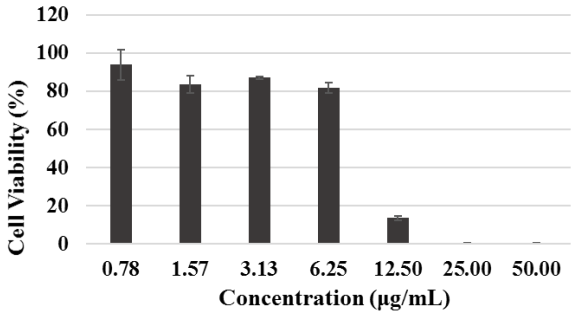

Sarasinoside B_1 displayed IC_{50} at 7.4 ± 1.2 µg/mL. Cytotoxicity bioassay carried out in triplicate (n=3).

Figure 3-17. Cytotoxicity activity of sarasinosides M_2 (**1**) and B_1 (**2**) against Neuro-2a and HepG2 cell lines.

3-3.0 Conclusion

Our chemical studies on *Melophlus* sp. have isolated a new sarasinoside congener, sarasinoside M_2 (**1**) along with other known sarasinosides B_1 (**2**), B_2 (**3**) or B_3 (**4**). The HR-LC-MS/MS fragmentation pattern analysis showed that all the isolated compounds possessed a sarasinoside B-type sugar moiety. The aglycon structure of **1** was the same as the aglycon of sarasinoside M (**5**), however the difference between **1** and **5** was the presence of xylose in **1** as opposed to a glucose in **5** at third sugar position. Biological evaluation showed that **1** and **2** displayed moderate cytotoxic activity against both Neuro 2a and HepG2 cell lines.

Chapter 4.0 Studies on Marine Invertebrates

4-1.0 Minor Introduction (*Haliclona* sp.)

Marine sponge *Halichlona* sp. belongs to the Order Haplosclerida and family Chalinidae.[121)] Research on various *Haliclona* species have resulted in the isolation of numerous compounds, most of which included the alkaloids, macrolides, steroids, peptides and polyketides.[122-126)] Among many of the bioactive compounds isolated from genus *Haliclona* were antibacterial activities,[127)] anti-parasitic activities [127)] and anticancer activities, [128,129).] In this section, the isolation studies of a *Haliclona* sp. (Figure 4-1) collected in the Solomon Islands is being discussed.

.

Figure 4-1. Marine sponge *Haliclona* sp. collected in the Solomon Islands.

4-2.0 Procedure

4-2.1 Isolation and purification

A portion (6.0 g) of a marine sponge identified as a *Haliclona* sp. (Figure 4-1) through a marine sponge database was collected in the Solomon Islands, preserved in 20 mL of a disposable plastic tube (TPP, Trasadingen, Switzerland) containing 20 mL of the EtOH–H_2O mixture (7:3, *v/v*) and transport to Tohoku University at room temperature. After arrival, the specimen was kept in -25 °C until use. The specimen was minced and soaked in the 20 mL of EtOH–H_2O (9:1, *v/v*) and left to macerate for few hours.

After the maceration period, the supernatant was collected and the same procedure was repeated two more times, after which all the supernatant and the the preserving solvent [EtOH–H_2O (7:3, *v/v*)] were combined and filtered through a ADVANTEC Toyo filter No.2 - 185 mm (Toyo Roshi Kaisha, Ltd., Tokyo, Japan). The filtrate was collected into an evaporating flask and was dried using the rotary evaporator.

Like the procedure in section 3-2.1 of chapter 3, the extract was partitioned between ethyl acetate (EtOAc) and H_2O (2:1, *v/v*). The EtOAc portion was dried (28 mg yield) and suspended in 100 μL of MeOH, which was then applied to an already equilibrated Sep-Pak® C-18 SPE cartridge (0.7 mL, Waters, USA) to obtain six fractions [MeOH–H_2O: 0:1, 3:7, 1:1, 8:2, 1:0 (*v/v*) and absolute acetonitrile] (F1-6). A preliminary cell-base assay from mouse neuroblastoma 2a cell line was performed where a test concentration of 100 ug/mL was applied into each well. Fractions MeOH–H_2O (8:2, 1:0 *v/v*) and absolute acetonitrile (F4, F5 and F6) showed cytotoxic activities with the highest bioactivities displayed by F4 and F5 (Figure 4-2).

4-2.2 Cytotoxicity Bioassay

The same procedure described in section 3-2.2 of chapter 3 was performed in this section, except that extracts and compounds were obtained from *Haliclona* sp. and that only Neuro 2a cell line was used in the cell bioassay. Briefly, the test compounds or extract mixture (for preliminary test) were solubilized in DMSO and were added to the cells (DMSO final conc. 0.50%, *v/v*). The cells were cultured in the RPMI 1640 medium (Sigma-Aldrich, St. Louis, MO, USA) supplemented with 10% fetal bovine serum and 100 µg/mL streptomycin and 100 U/mL penicillin in 96-well plates and incubated at 37 °C in 5.0% of CO_2 /air. The remaining procedure was outlined in the scheme below.

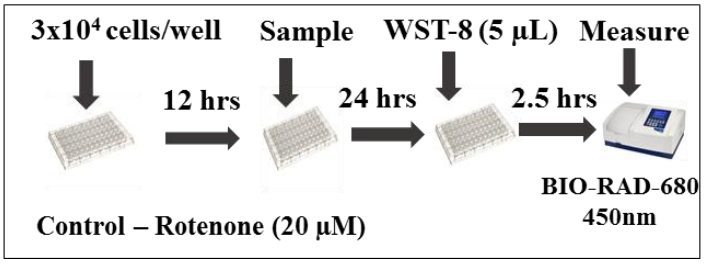

Scheme 4-1. Flow diagram of the cytotoxicity test procedure.

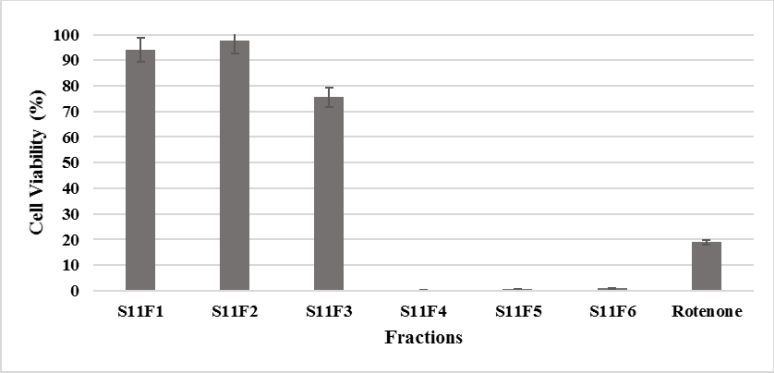

Figure 4-2. Cytotoxicity test after Sep Pak fractionation. The concentration of each fraction was 100 µg/mL.

4-2.3 HPLC Purification

Based on the cytotoxicity result, the fractions eluted with MeOH–H_2O (8:2/1:0) were combined (8.8 mg) and then subjected to a Mightysil RP-18GP II column chromatography (10 × 250 mm, 5 µm, Kanto Chemical, Tokyo, Japan) with a stepwise condition: MeOH–H_2O 1:1, 8:2, 9:1, and 1:0 (*v/v*). The UV detection (240 nm) was performed using a diode array detector (DAD) (Hitachi Chromaster 5430, Hitachi, Japan) (Figure 4-3).

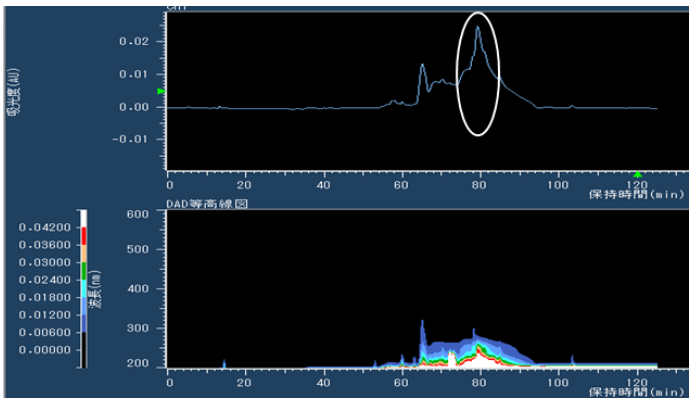

Column: Mighysil RP-18 GPII 250 mm, (5µm). Kanto Chemical)
Mobile Phase: A: MeOH, B: H_2O. Initial 50% A, 80% A, 90% A, 100% A (0-100 min). 1.0 mL/min

Figure 4-3. LC-DAD chromatogram of the elution with MeOH–H_2O (8:2/1:0) (F4–5) fractions.

The bioactive fractions were screened using HR-LCMS. Upon identifying the potential candidates, the fractions were dried and dissolved in CD_3OD (0.4 mL) for NMR analysis.

4-3.0 Results/Discussion

4-3.1 Structure Identification

HR-ESIMS (MicrOTOF QII, Bruker Daltonics, Billerica, MA, USA) screening of the active fractions in the cell-based assay revealed two known stereo chemically related compounds corresponding to the major peak observed in the LC DAD (UV absorbance 240 nm) (Figure 4-3). The molecular formula of **6** (S11F4F40) was determined as $[M + H - H_2O]^+$ $C_{27}H_{47}O_5$; *m/z* 451.3420, and $[M + Na]^+$ *m/z* 491.3341 (calcd. for $C_{27}H_{48}O_6Na$ 491.3343 (Figure 4-4) while **7** (S11F4F42) gives $[M + H - H_2O]^+$ $C_{27}H_{47}O_5$; *m/z* 451.3405 and $[M + Na]^+$ *m/z* 491.3334 (calcd. for $C_{27}H_{48}O_6Na$ 491.3343. (Figure 4-5). FABMS analysis also confirmed the identical molecular formula of the two compounds as $[M + Na]^+$ *m/z* 491.9827 (est. for $C_{27}H_{48}O_6Na$) (See appendix p.110).

^1H NMR data comparison between **6** and **7** showed similar proton peaks except for the protons which accounts for their difference in stereochemistry (Figure 4-6). The ^1H NMR signals and ^{13}C NMR signals of **6** and **7** were comparably assigned on the basis of gradient COSY, TOCSY, TOCSY1D, and gradient HSQC (Figure 4-7 and 4-8) and HMBC spectra (See appendix p.111-118). The NMR spectral assignment of **6** and **7** are listed in Table 4-1. Comparison with known polyoxygenated 9-11 *seco*sterol compounds revealed that **6** (although now with more precise assignment) was identified as herbasterol previously isolated from *Dysidea herbacea.*[130] and **7** was identified as stellettasterol isolated from *Stelletta* sp.[131]

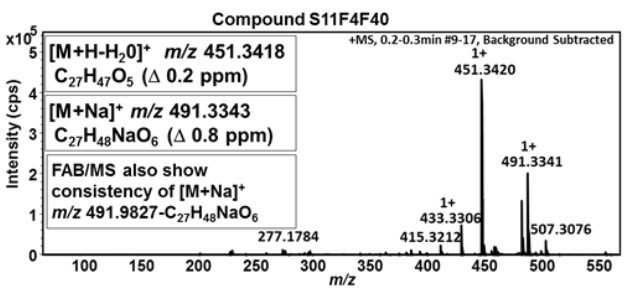

Figure 4-4. HR-ESI-MS of compound **6** (S11F4F40).

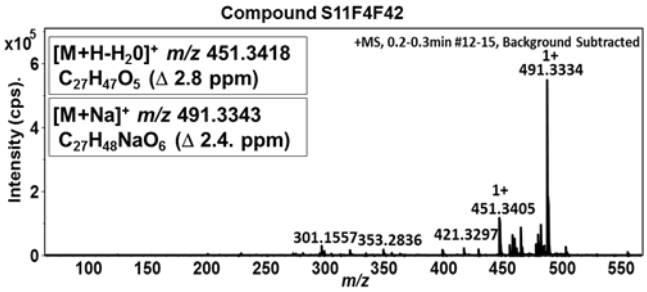

Figure 4-5. HR-ESI-MS of compound **7** (S11F4F42).

Among other major signals, ^{13}C NMR of four methyl groups in **6** and **7** were observed at C18 (18.5/17.6), C21 (20/19.9), C26 (22/22.6), C27 (22/22.8). The ^{1}H NMR spectrum also revealed the corresponding protons of these four methyl groups at H-3 (0.75, s, 3H/0.77, s, 3H), H-21 (1.02, d, 3H/1.0, d, 3H) and H-26 (0.88, d, 3H/0.88, d, 3H). The only different characteristic point observed in HSQC data of **6** and **7** is the coupling at position C3 which accounts for their stereochemistry. NMR spectral data of **6** via gradient HSQC revealed coupling at C3/H3 (73/3.22) (Figure 4-7) while that of **7** was C3/H3 (69/ 3.83) (Figure 4-8). The coupling assigned for methine and the oxygenated methine proton at position C3 of **6** and **7** correlate well with known compounds herbasterol and stellettasterol respectively. As suggested by Li H, *et al.*[131] referring to stellettasterol, the absolute configuration at C3 deviates from herbasterol C3 in that the coupling constant of 11.6 Hz between H1 and H2 and that of 2.9 Hz between H2 and H3 indicated that H2 and H3 are axial and equatorial respectively (Figure 4-9 and 4-10)

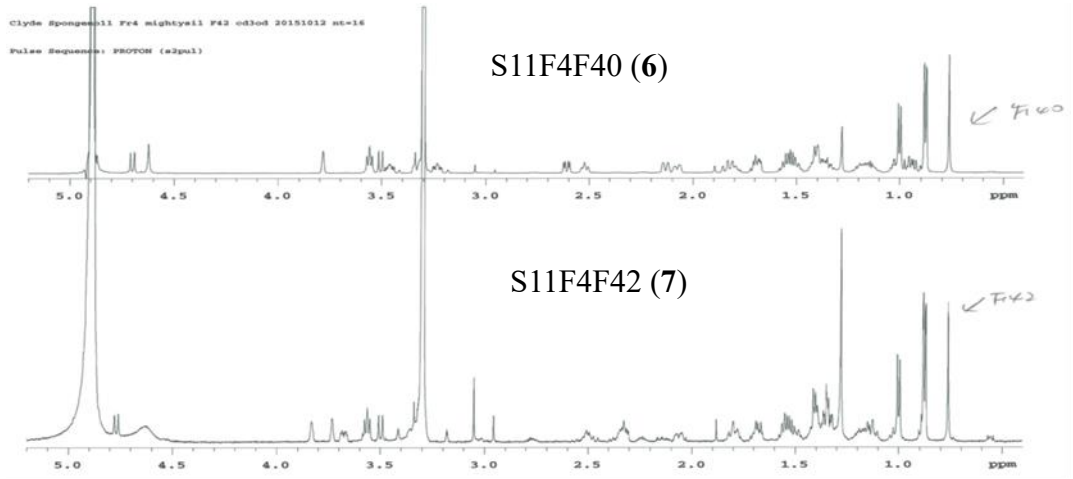

Figure 4-6. ^{1}H NMR spectra of S11F4F40 (**6**) and S11F4F42(**7**).

Table 4-1. NMR spectroscopic data of S11F4F40 and S11F4F42 in CD_3OD.

S11F4F40 (CD_3OD)				S11F4F42 (CD_3OD)			
no.	$\delta^{13}C$	$\delta^{1}H$	(mul. *J* in Hz)	no.	$\delta^{13}C$	$\delta^{1}H$	(mul. *J* in Hz)
1α	39.3	2.6	m	1α	31.7	2.31	m
1β		0.96	dd	1β		1.34	m
2	76	3.45	m	2	67.9	3.66	dd
3	73	3.22	m	3	68	3.83	br s
4α	38.2	1.68	m	4α	33.8	1.68	m
4β		0.98	m	4β		1.13	m
5	48	2.14	d	5	40.8	2.34	m
6	72	3.78	br s	6	70	3.74	br s
7α	36.9	1.83	m	7α	35.5	1.78	dd
7β		2.07	d	7β		2.05	d
8	40.8	3.35	s	8	39.5	3.34	s
9	213.6			9	215.8		
10	59			10	59		
11	59	3.55		11	57.8	3.58	t
12α	41.8	1.52	m	12α	39.8	1.55	m
12β		1.69	m	12β		1.7	m
13	59			13	45		
14	43	2.51	t	14	41	2.5	d
15α	23.9	1.35	m	15α	22	1.34	m
15β		1.46	m	15β		1.48	m
16α	27.8	1.8	m	16α	25.5	1.8	m
16β				16β		1.35	m
17	51	1.56	m	17	49.2	1.55	m
18	18.5	0.75	3H, s	18	16.5	0.77	3H, s
19α	72	3.5	d	19α	70.8	3.5	d
19β		4.69	d	19β		4.76	d
20	36	1.41	d	20	34	1.42	m
21	20	1.02	3H, d	21	19	1	3H, d
22α	37.1	1.02	d	22α			
22β		1.39	d	22β			
23α	26	1.4	m	23α	22	1.38	m
23β		1.2	m	23β			
24α	41.2	1.14	m	24α	39	1.15	m
24b				24b			
25	29.9	1.51	m	25	28	1.5	m
26	22	0.88	3H, d	26	21.5	0.88	3H, d
27	22	0.88	3H, d	27	21.7	0.88	3H, d

^{1}H NMR (600 MHz), ^{13}C NMR (151 MHz). ND represents “not determined”.

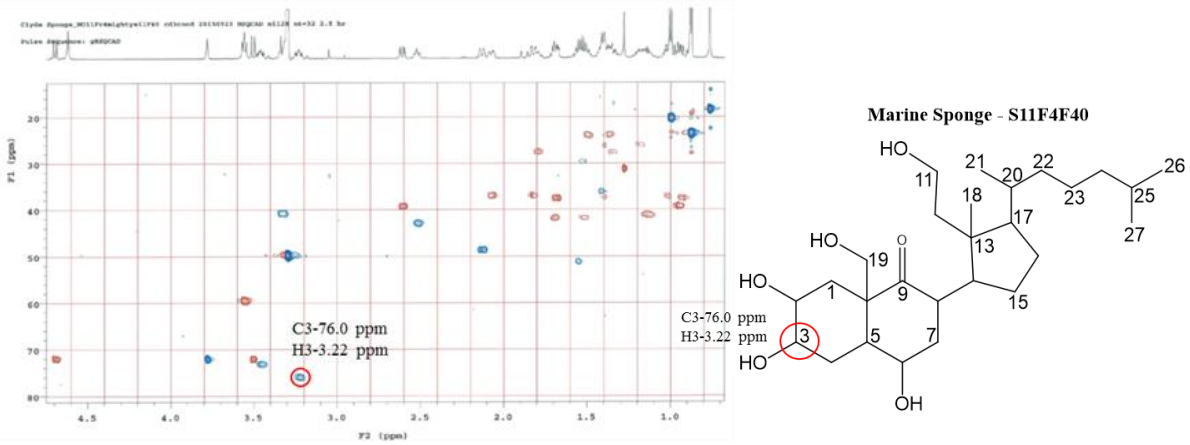

Figure 4-7. HSQC spectrum of **6**.

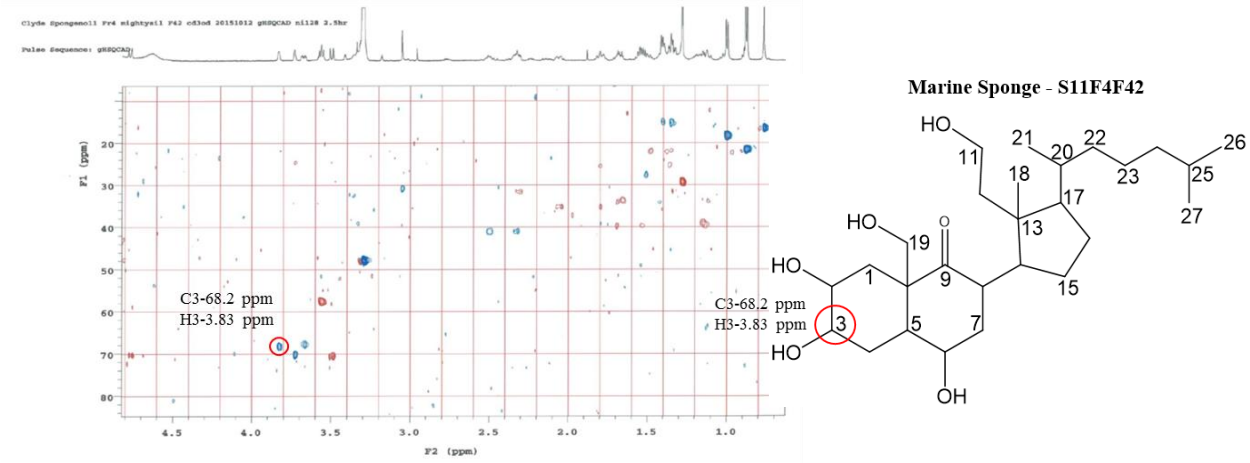

Figure 4-8. HSQC spectrum of **7**.

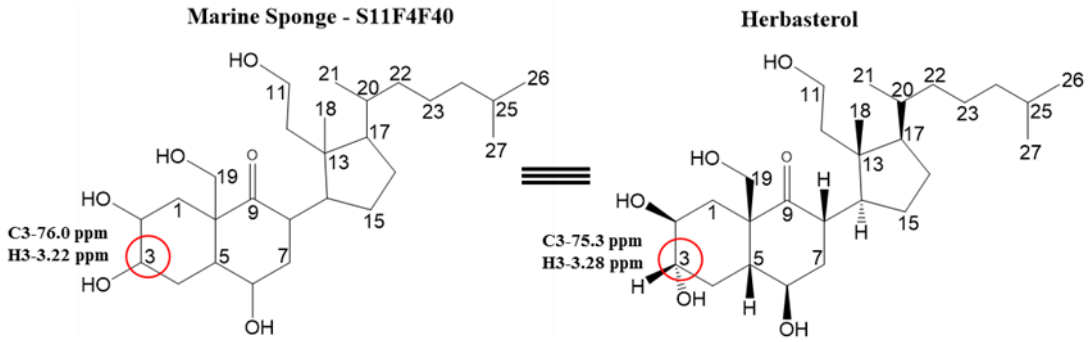

Figure 4-9. Comparison of **6** and with herbasterol.[130)]

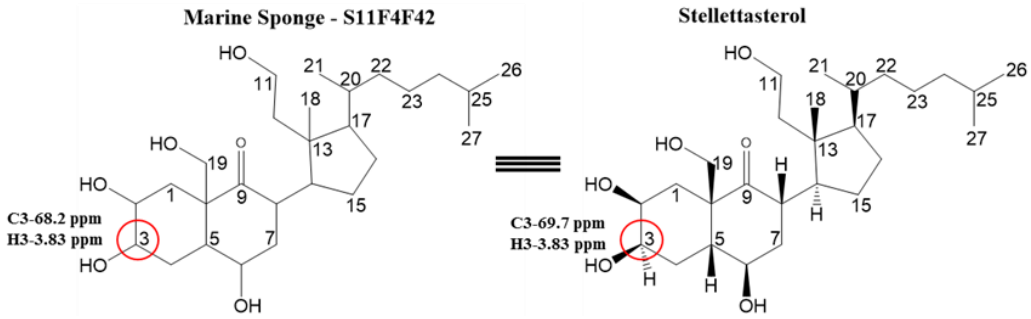

Figure 4-10. Comparison of **7** and stellettasterol.[131)]

4-3.3 Cytotoxic Activity Test

In light of the difference in stereochemistry at position C3 of **6** and **7**, assay using Neuro 2a cells cytotoxicity showed that **6** displayed slightly stronger cytotoxic effect with IC_{50} of 9.4 µg/mL compared to **7** with IC_{50} of > 9.4 µg/mL (Figure 4-11) Since both **6** and **7** were isolated from the same marine sponge (*Haliclona* sp.), while herbasterol and stellettasterol were obtained from two different marine sponges *Dysidea herbacea* and *Stelletta* sp. respectively, it would be interesting if other studies highlight their biogenetic origins and the roles these polyoxygenated 9-11 secosterol compounds play in these marine sponge species.

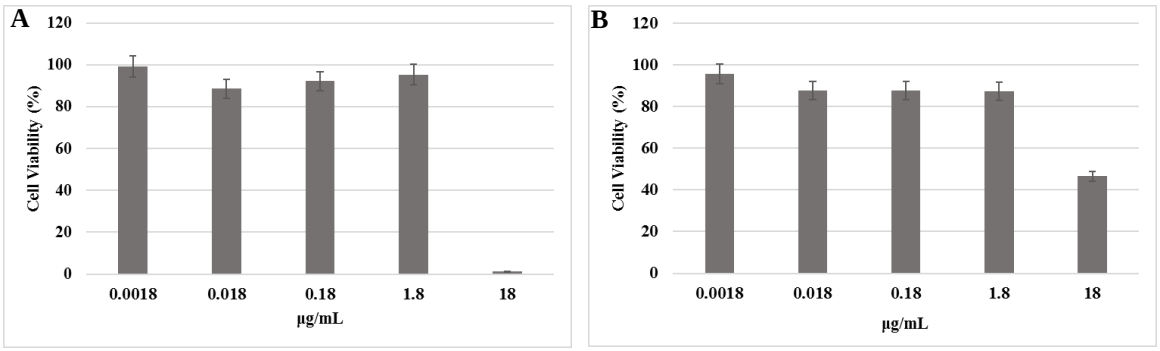

Figure 4-11. Preliminary cytotoxicity activity of **6** (A) and **7** (B).

4-4.0 Conclusion

Screening of a portion of marine sponge *Haliclona* sp. yielded compounds **6** and **7**, which (on the basis of spectral comparison) were believed to be known polyoxygenated 9-11 *seco*-steroids herbasterol and stellettasterol, respectively. A preliminary cytotoxicity studies on these two stereo chemically different isomers of **6** (herbasterol) and **7** (stellettasterol) showed an IC_{50} of almost 10 μg/mL.

Appendices

Selected Toxic Profiles from the Solomon Islands specimens

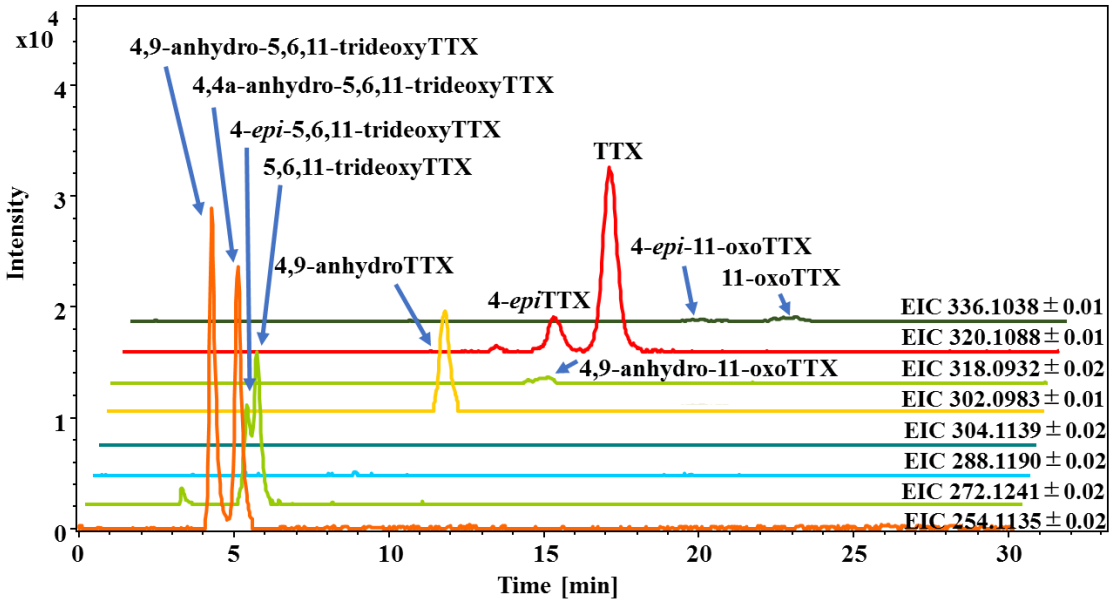

Toxic profile from EtOH extract of the skin of *A. nigropunctatus* No.3 from the Solomon Islands.

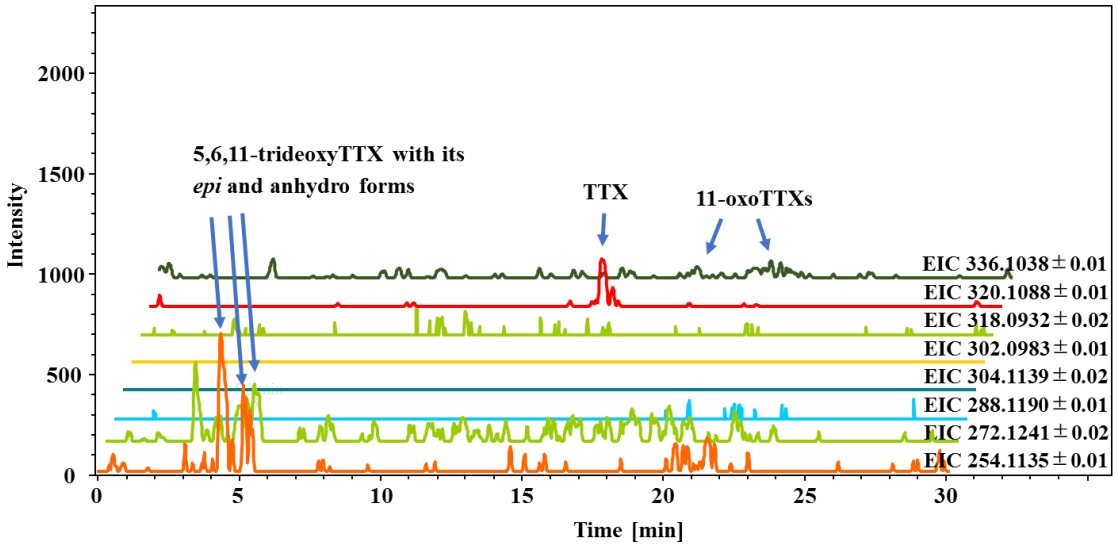

Toxic profile from flesh of *A. hispidus* No.3 from the Solomon Islands.

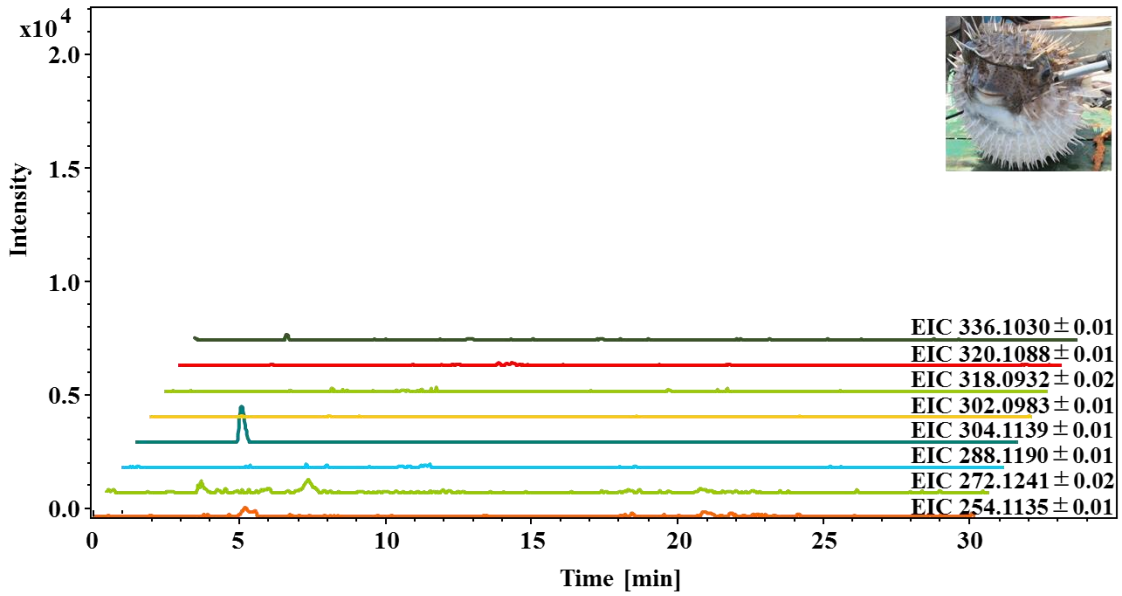

No TTX was detected in the skin of *D. holocanthus* No. 1 from the Solomon Islands.

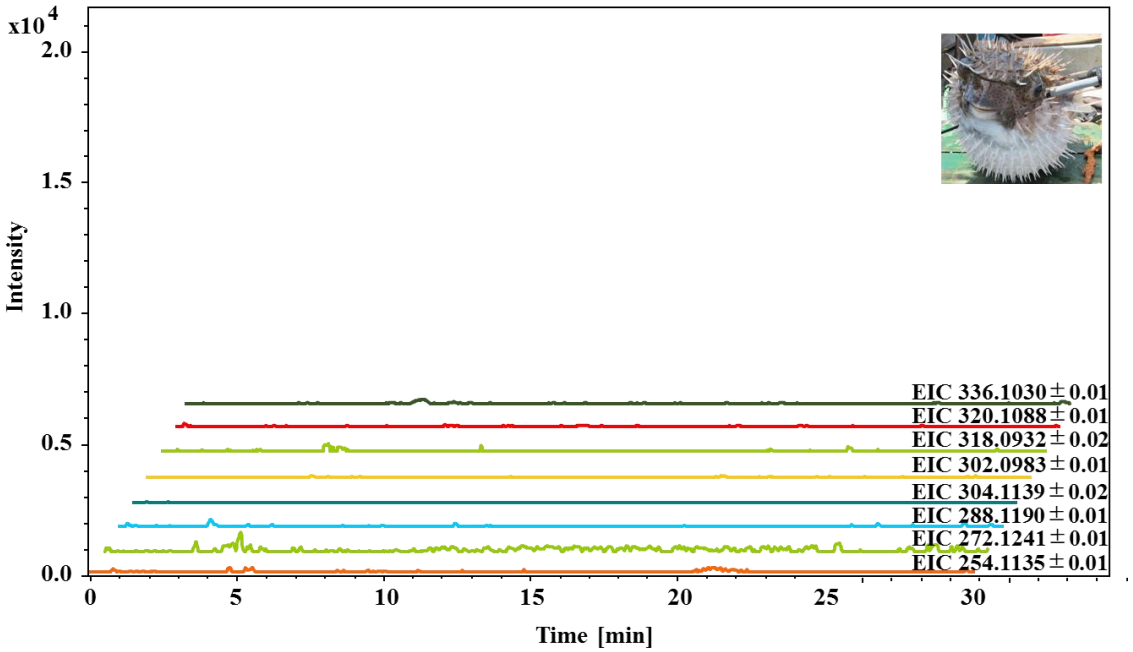

No TTX was detected in the skin of *D. holocanthus* No. 1 from the Solomon Islands.

NMR data for Chapter 3

Internal references: ^{1}H NMR spectra - CHD_2OD signal at 3.35 ppm
: ^{13}C NMR spectra - $^{13}CD_3OD$ signal at 49.8 ppm

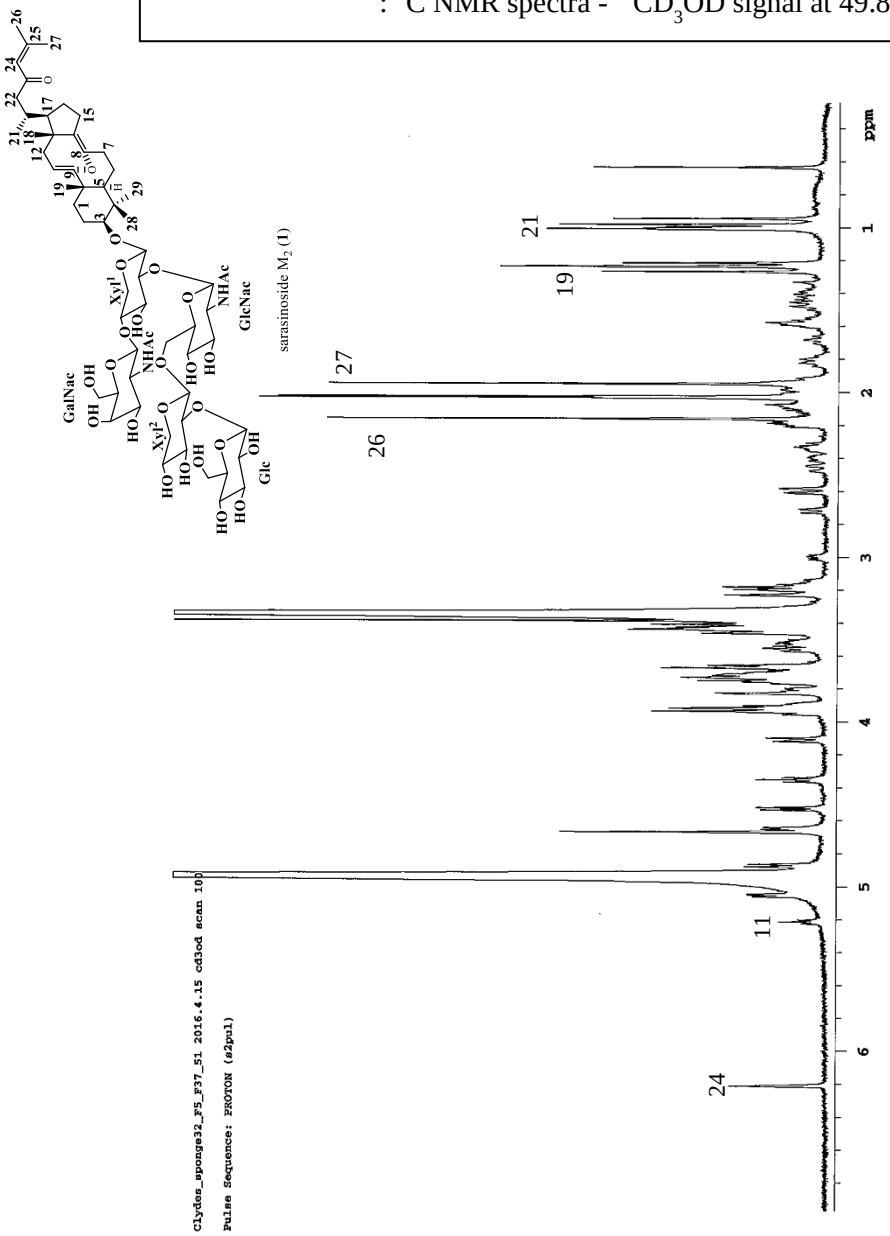

The ^{1}H NMR spectrum (CD_3OD, 600 MHz) of **1**.

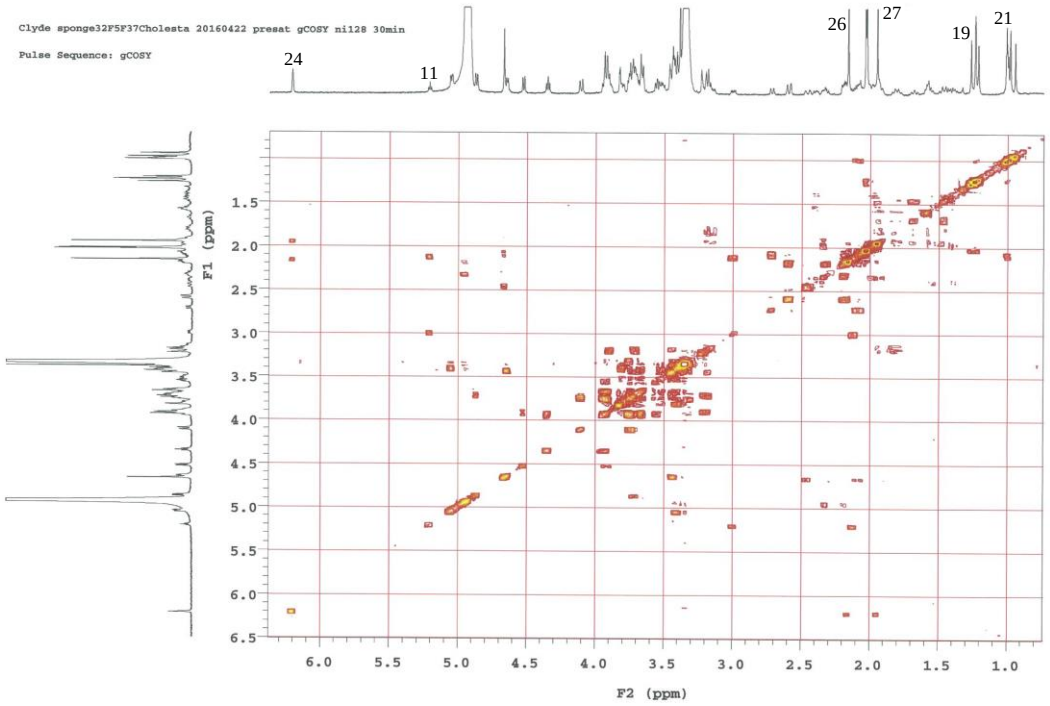

The gradient COSY spectrum (CD_3OD, 600 MHz, ni = 128) of **1**.

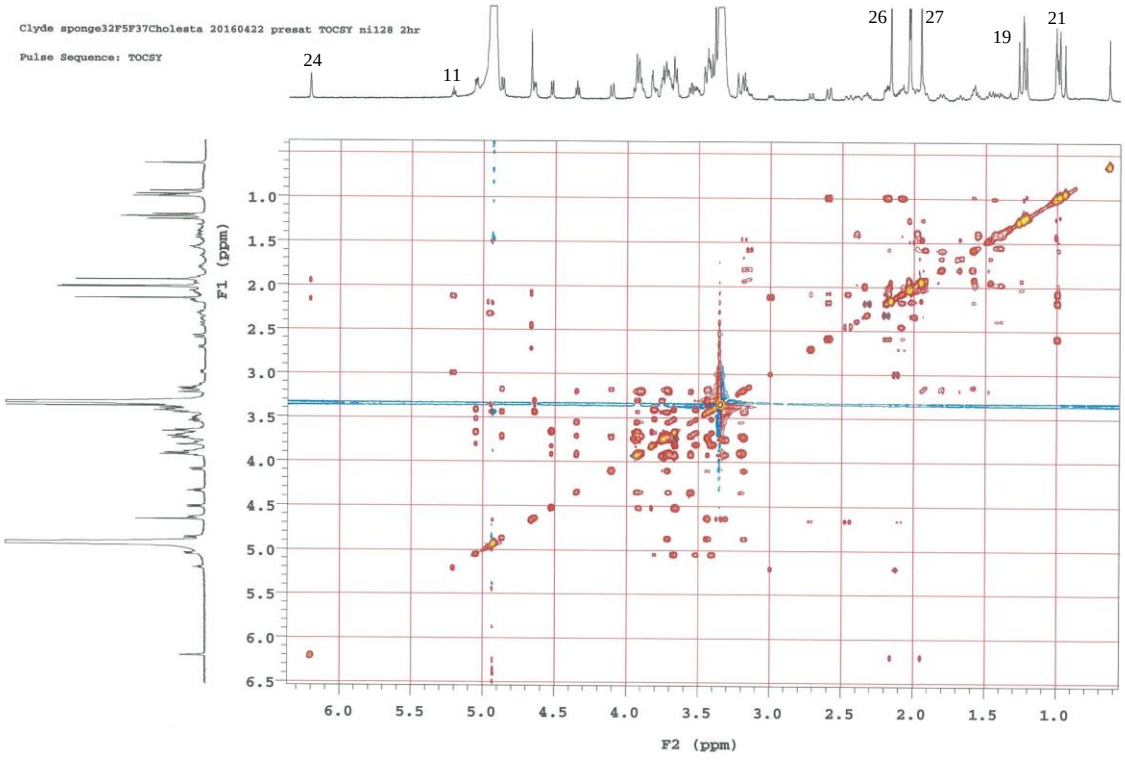

The TOCSY spectrum (CD_3OD, 600 MHz, ni = 128) of **1**.

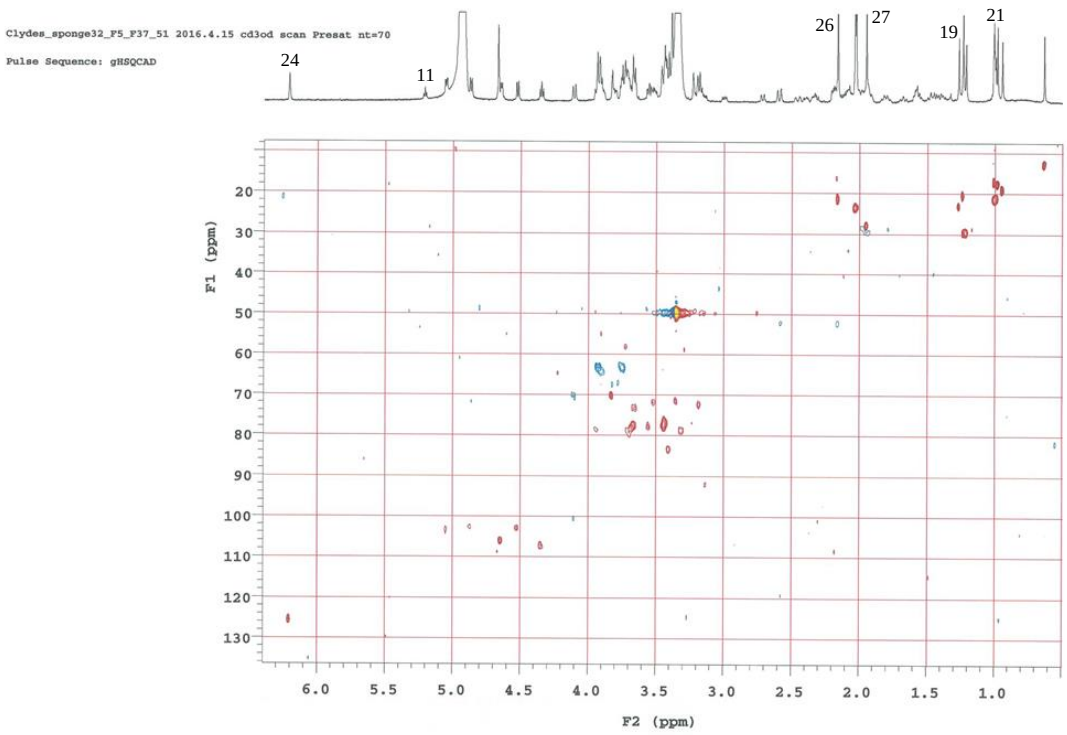

The gradient HSQC spectrum (CD_3OD, 600 MHz, ni = 128) of **1**.

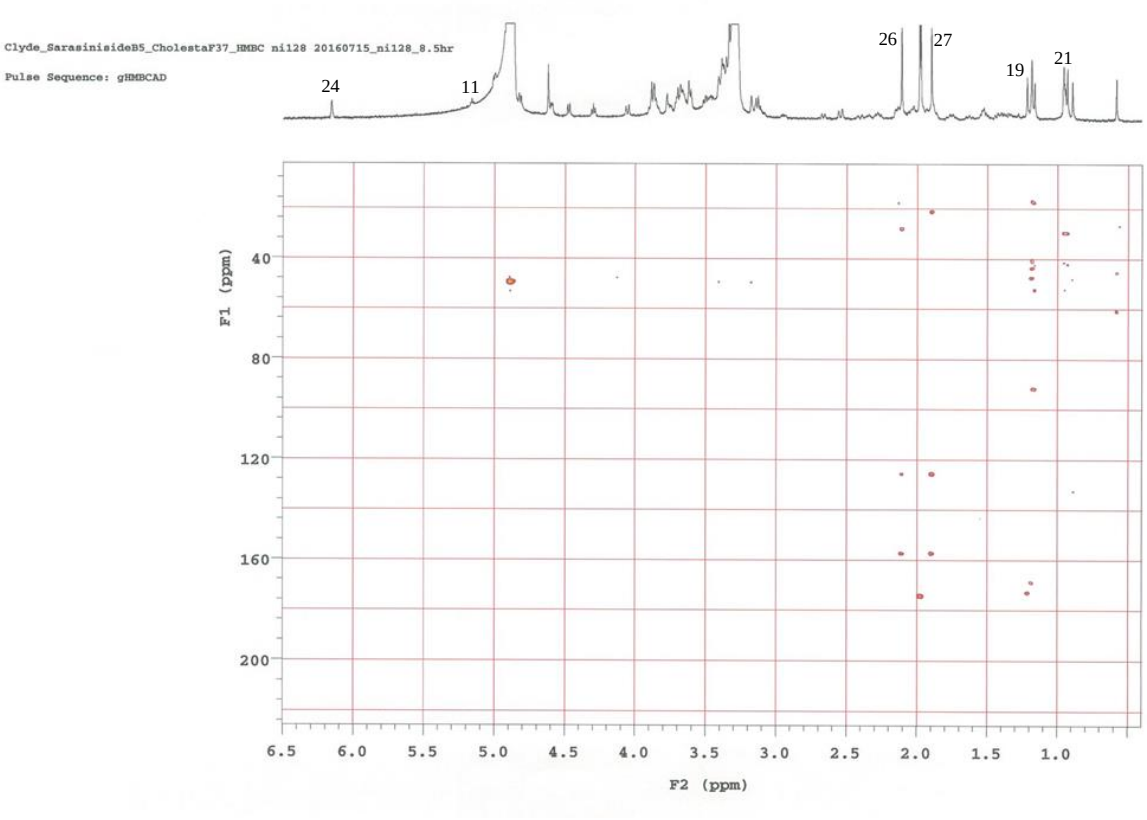

The gradient HMBC spectrum (CD_3OD, 600 MHz, ni = 128) of **1**.

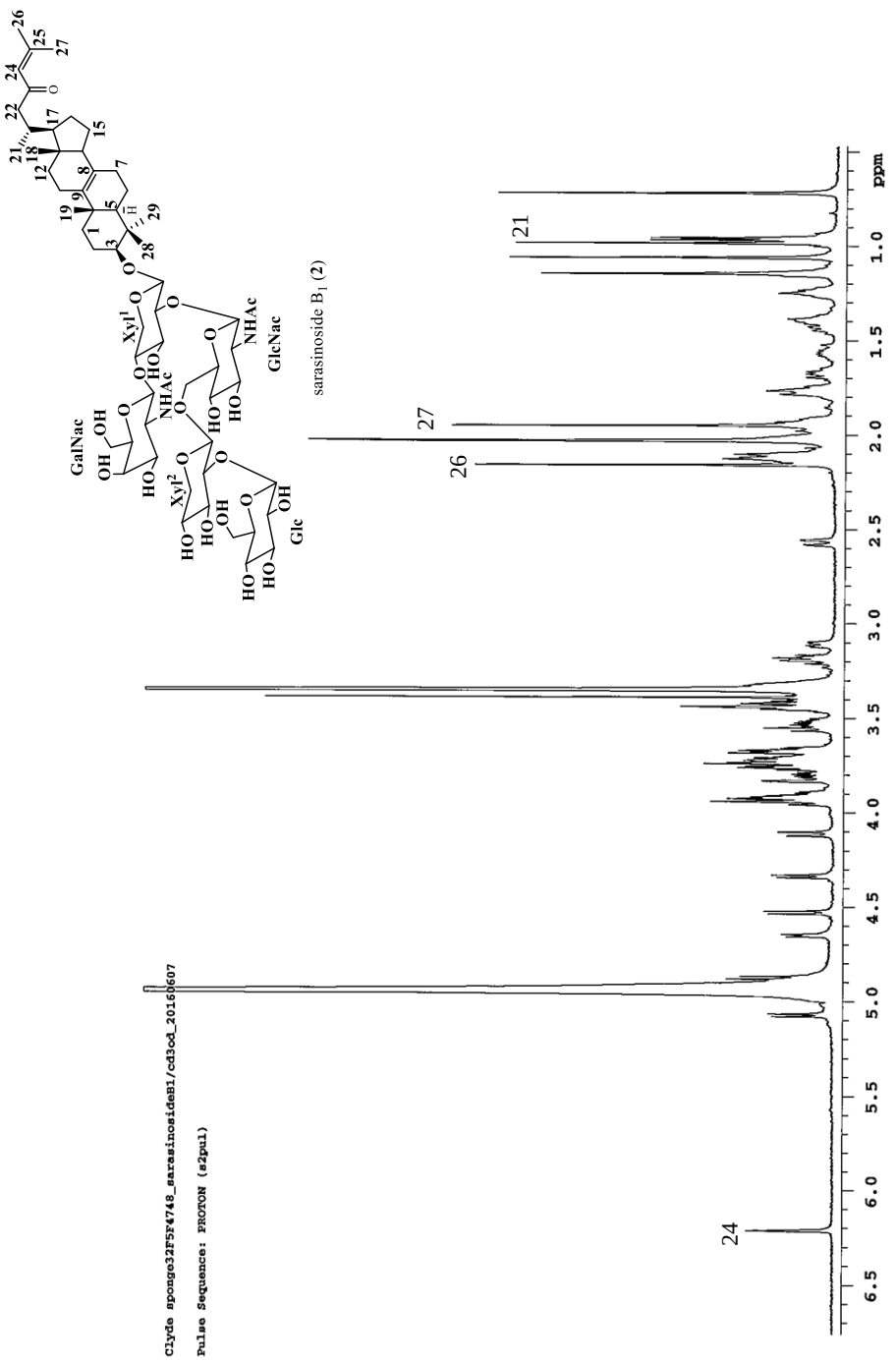

The ^{1}H NMR spectrum (CD_3OD, 600 MHz) of **2**.

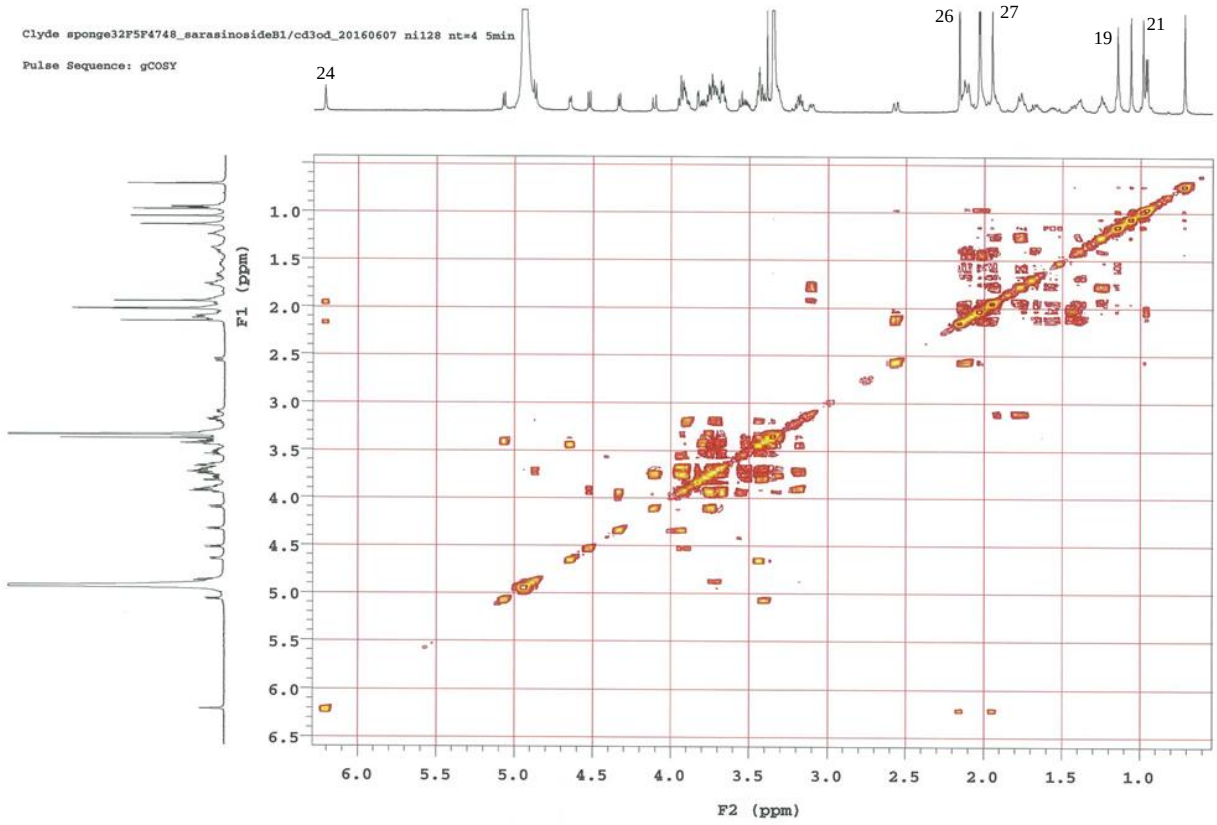

The gradient COSY spectrum (CD_3OD, 600 MHz, ni = 128) of **2**.

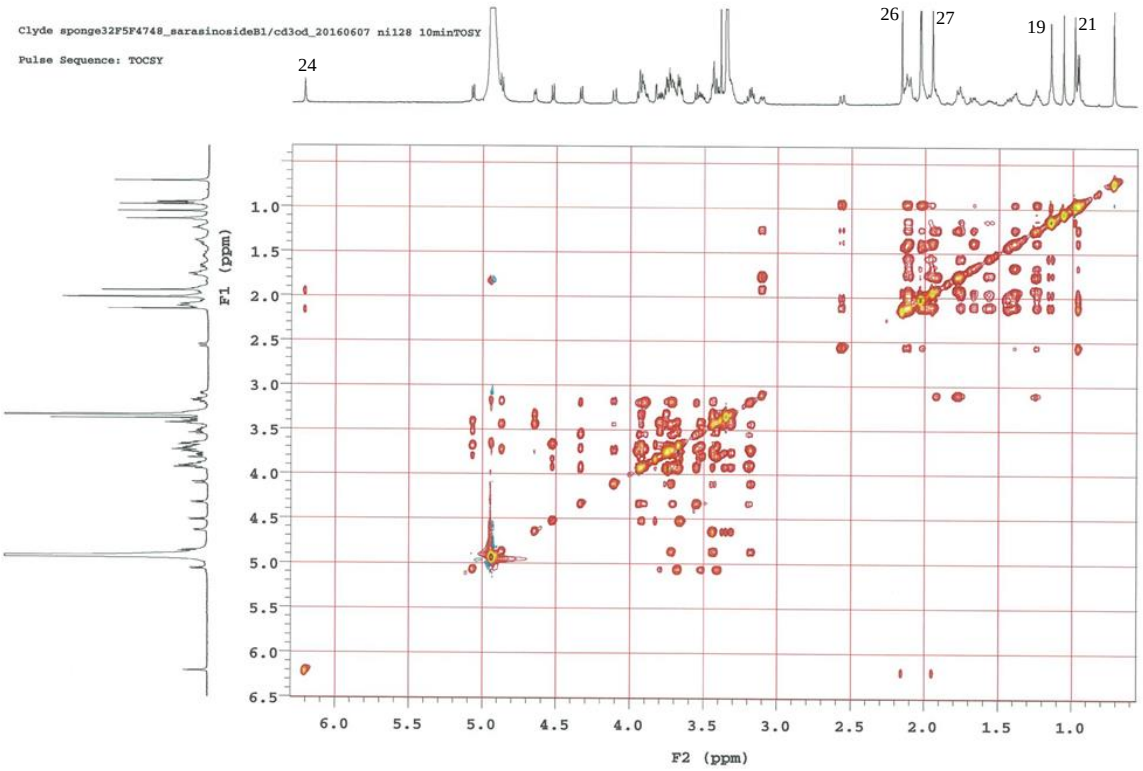

The gradient TOCSY spectrum (CD_3OD, 600 MHz, ni = 128) of **2**.

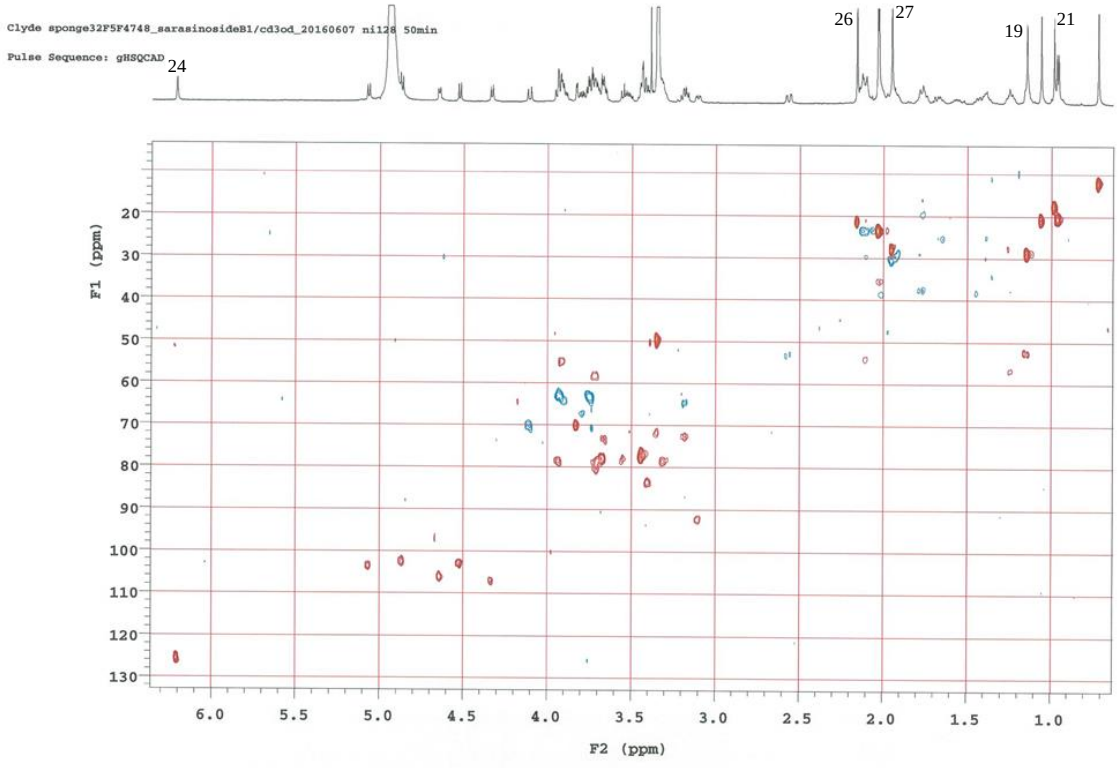

The gradient HSQC spectrum (CD_3OD, 600 MHz, ni = 128) of **2**.

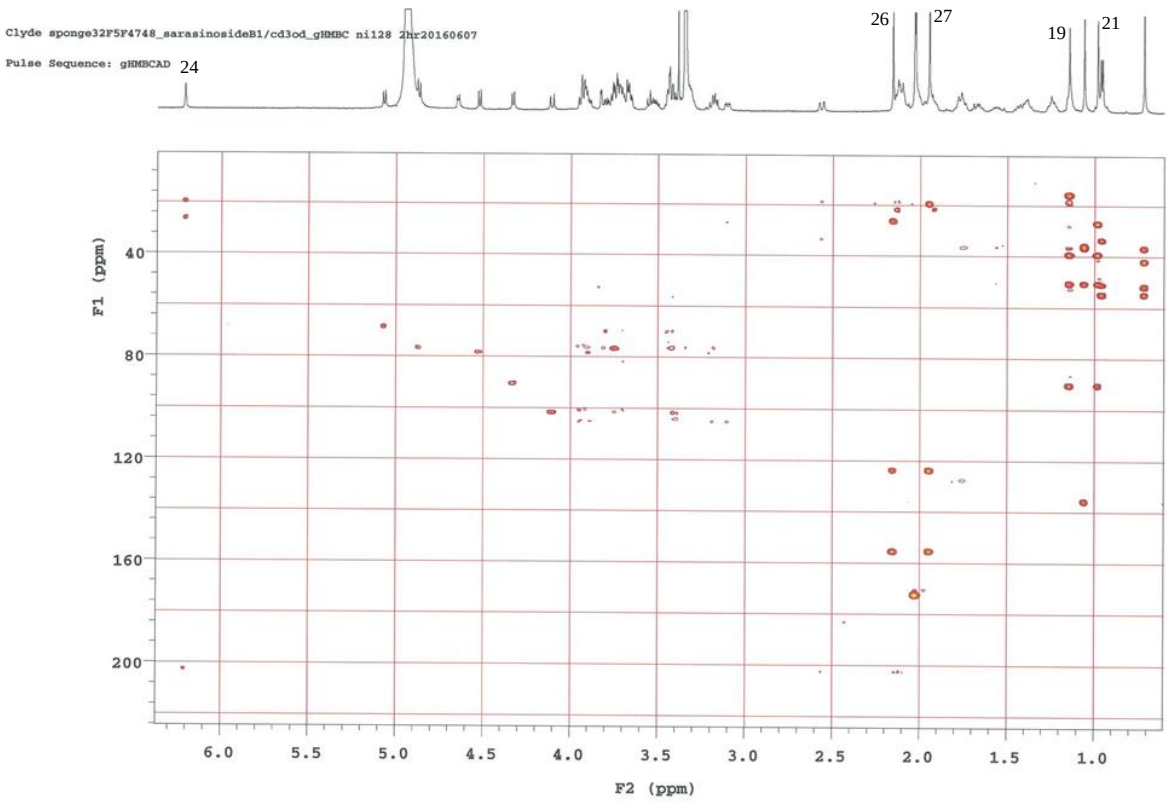

The gradient HMBC spectrum (CD_3OD, 600 MHz, ni = 128) of **2**.

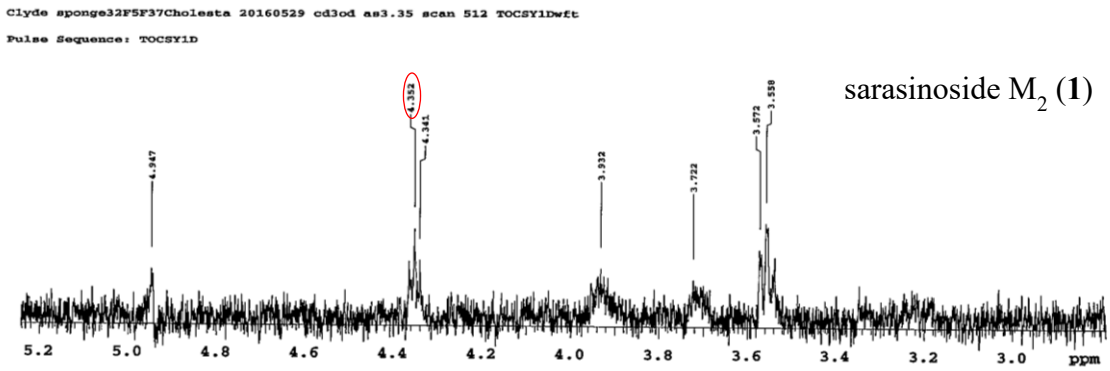

sarasinoside M_2 (**1**)

TOCSY 1D spectrum (CD_3OD, 600 MHz) irradiation of Xyl-1′ (4.35 ppm) signal of **1**.

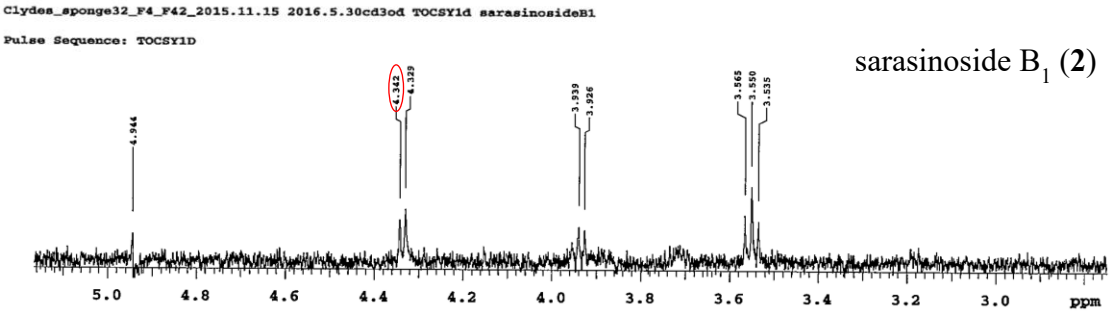

sarasinoside B_1 (**2**)

TOCSY 1D spectrum (CD_3OD, 600 MHz) irradiation of Xyl-1′ (4.35 ppm) signal of **2**.

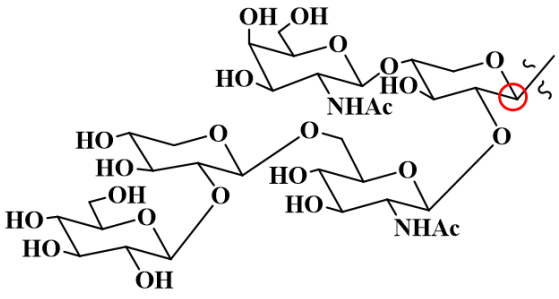

Irradiation at Xyl-1’ (4.35 ppm)

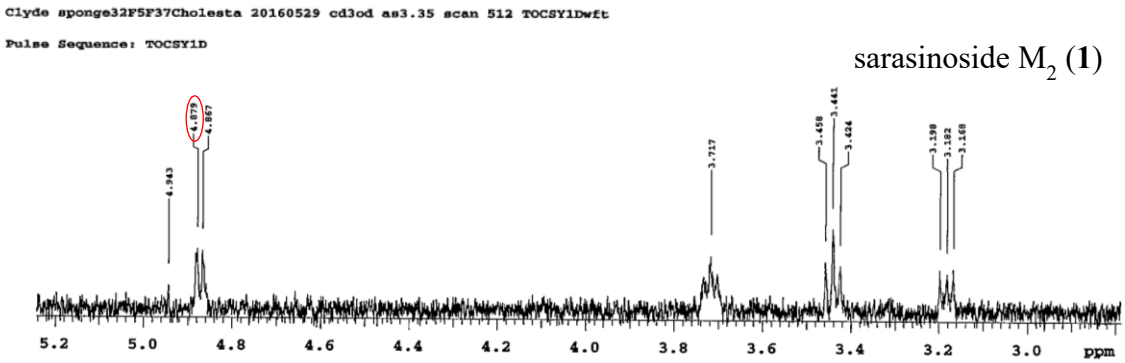

sarasinoside M_2 (**1**)

TOCSY 1D spectrum (CD_3OD, 600 MHz) irradiation of GlcNAc-1'' signal (4.87 ppm) of **1**.

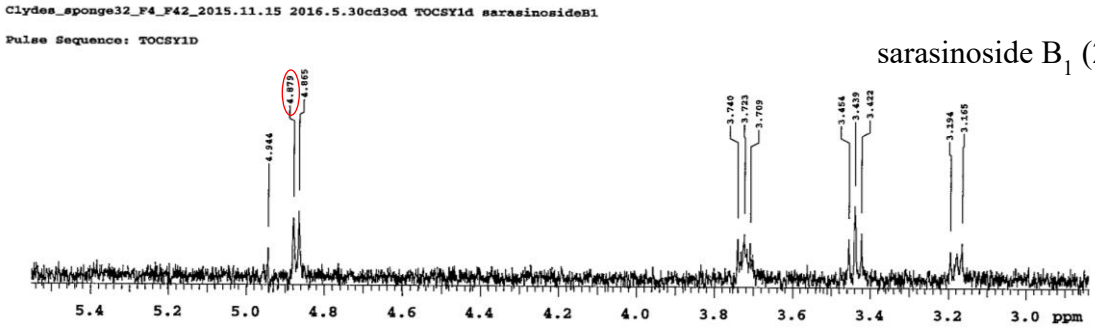

sarasinoside B_1 (**2**)

TOCSY 1D spectrum (CD_3OD, 600 MHz,) irradiation of GlcNac-1'' signal (4.87 ppm) of **2**.

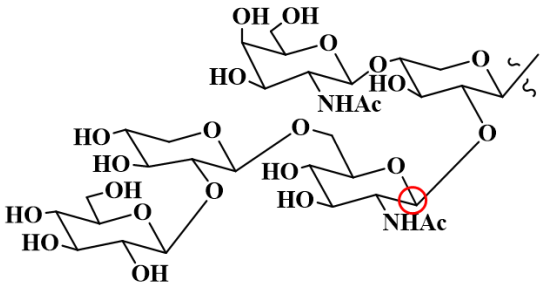

Irradiation at GlcNac-1'' (4.87 ppm)

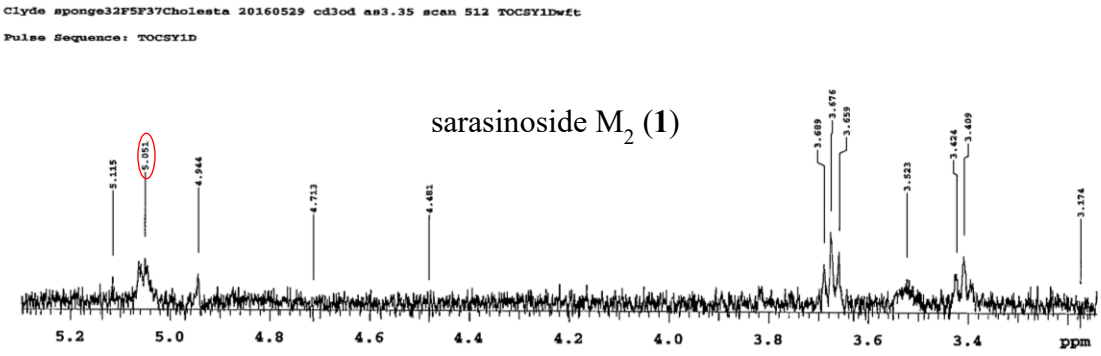

TOCSY 1D spectrum (CD_3OD, 600 MHz) irradiation of Xyl^2-1''' signal (5.05 ppm) of **1**.

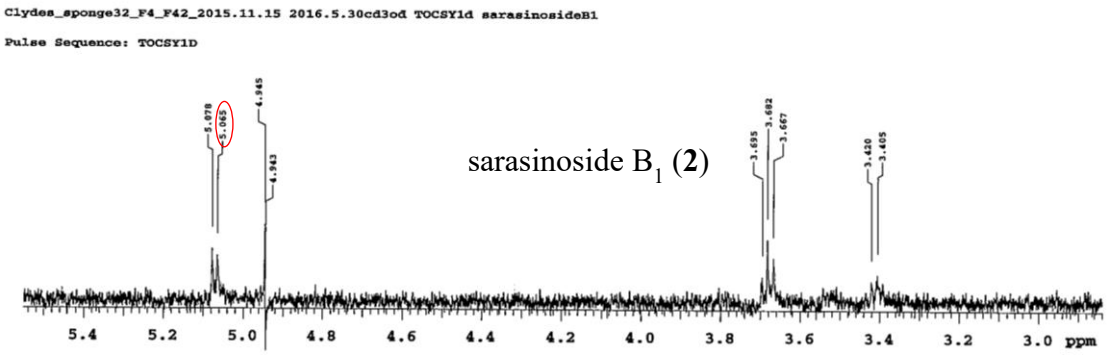

TOCSY 1D spectrum (CD_3OD, 600 MHz) irradiation of Xyl^2-1''' signal (5.05 ppm) of **2**.

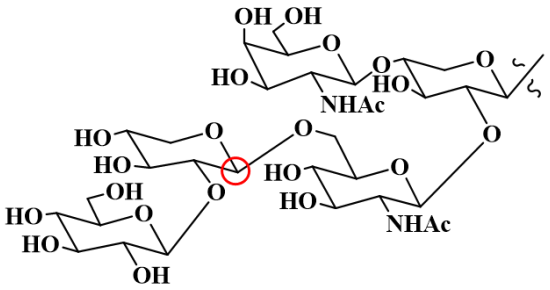

Irradiation at Xyl^2-1''' (5.05 ppm)

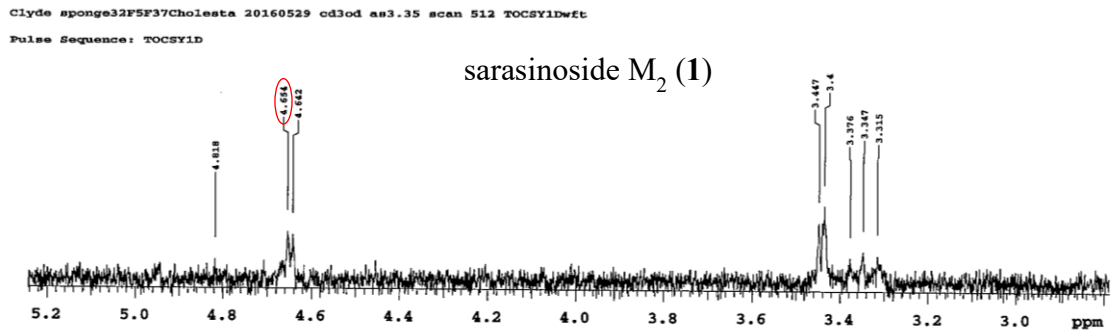

TOCSY 1D spectrum (CD_3OD, 600 MHz) irradiation of Glc-1'''' signal (4.65 ppm) of **1**.

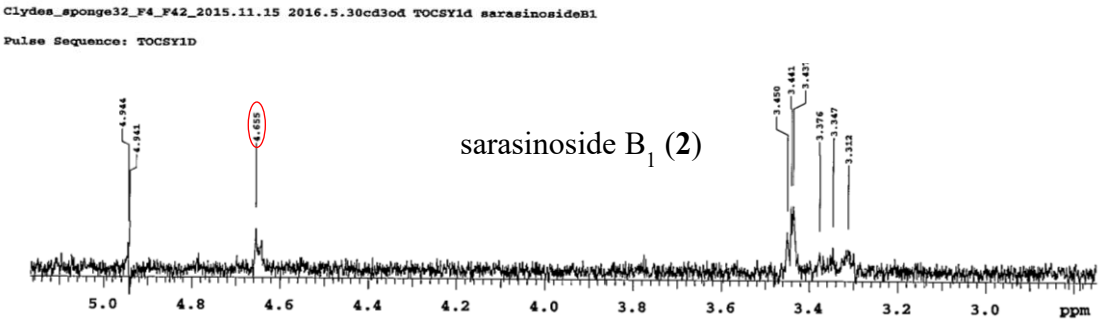

TOCSY 1D spectrum (CD_3OD, 600 MHz) irradiation of Glc-1'''' signal (4.65 ppm) of **2**.

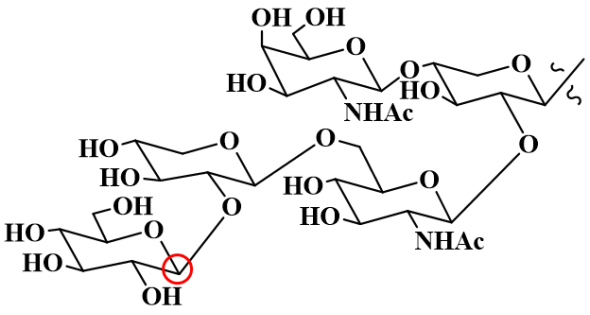

Irradiation at Glc-1'''' (4.65 ppm)

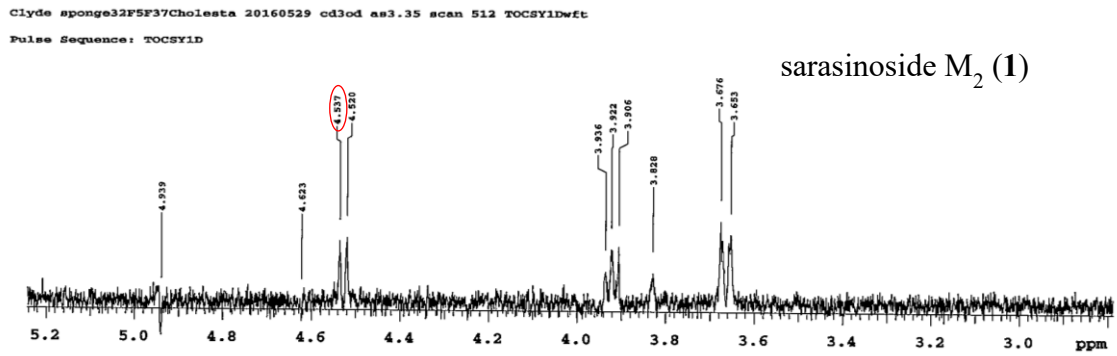

sarasinoside M_2 (**1**)

TOCSY 1D spectrum (CD_3OD, 600 MHz) irradiation of GalNAc-1’’’’’ signal (4.53 ppm) of **1**.

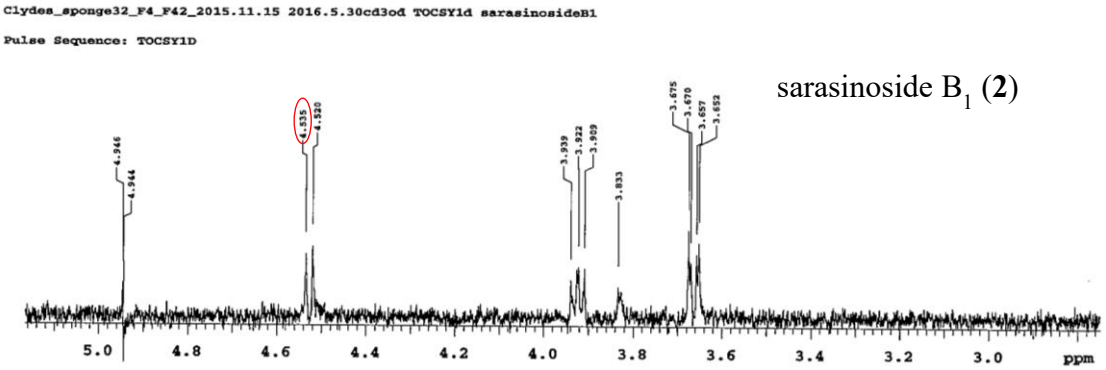

sarasinoside B_1 (**2**)

TOCSY 1D spectrum (CD_3OD, 600 MHz) irradiation of GalNAc-1’’’’’ signal (4.53 ppm) of **2**.

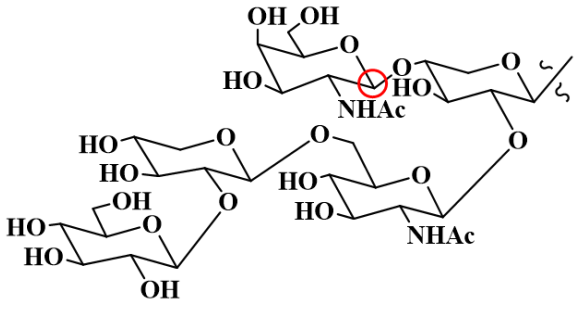

Irradiation at GalNAc-1’’’’’ (4.53 ppm)

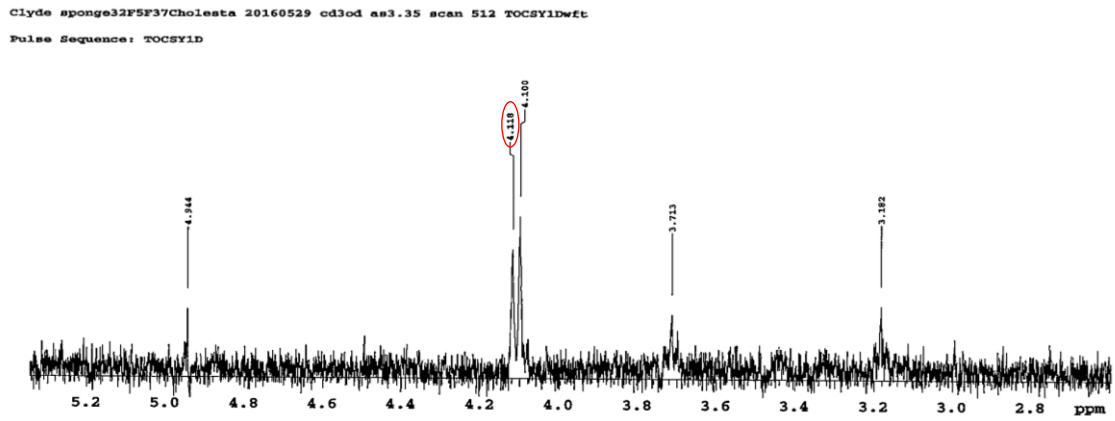

TOCSY 1D spectrum (CD_3OD, 600 MHz) irradiation of GlcNAc-6'' signal (4.11 ppm) of **1**.

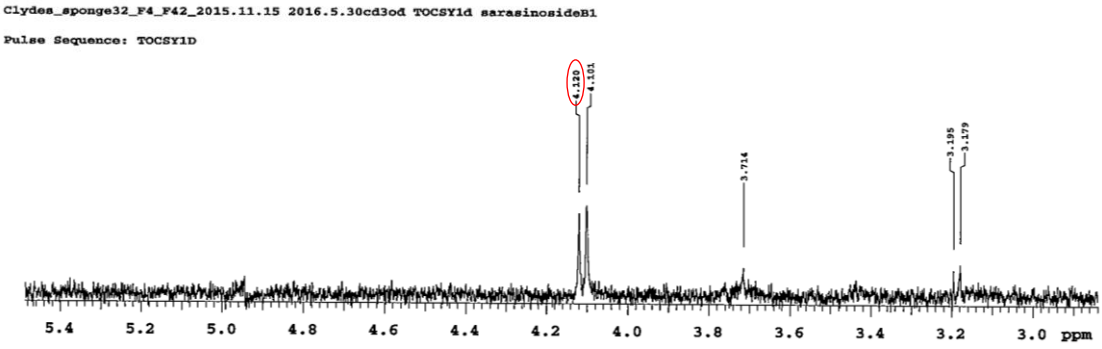

TOCSY 1D spectrum (CD_3OD, 600 MHz) irradiation of GlcNAc-6'' signal (4.11 ppm) of **2**.

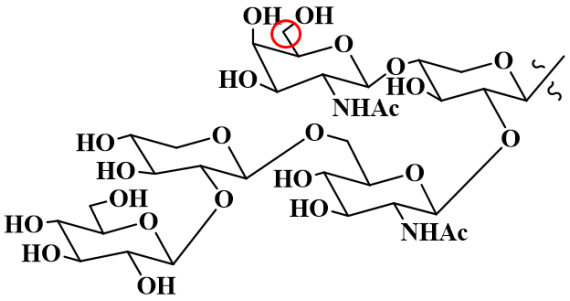

Irradiation at GlcNAc-6'' (4.11 ppm)

FABMS data for Chapter 4

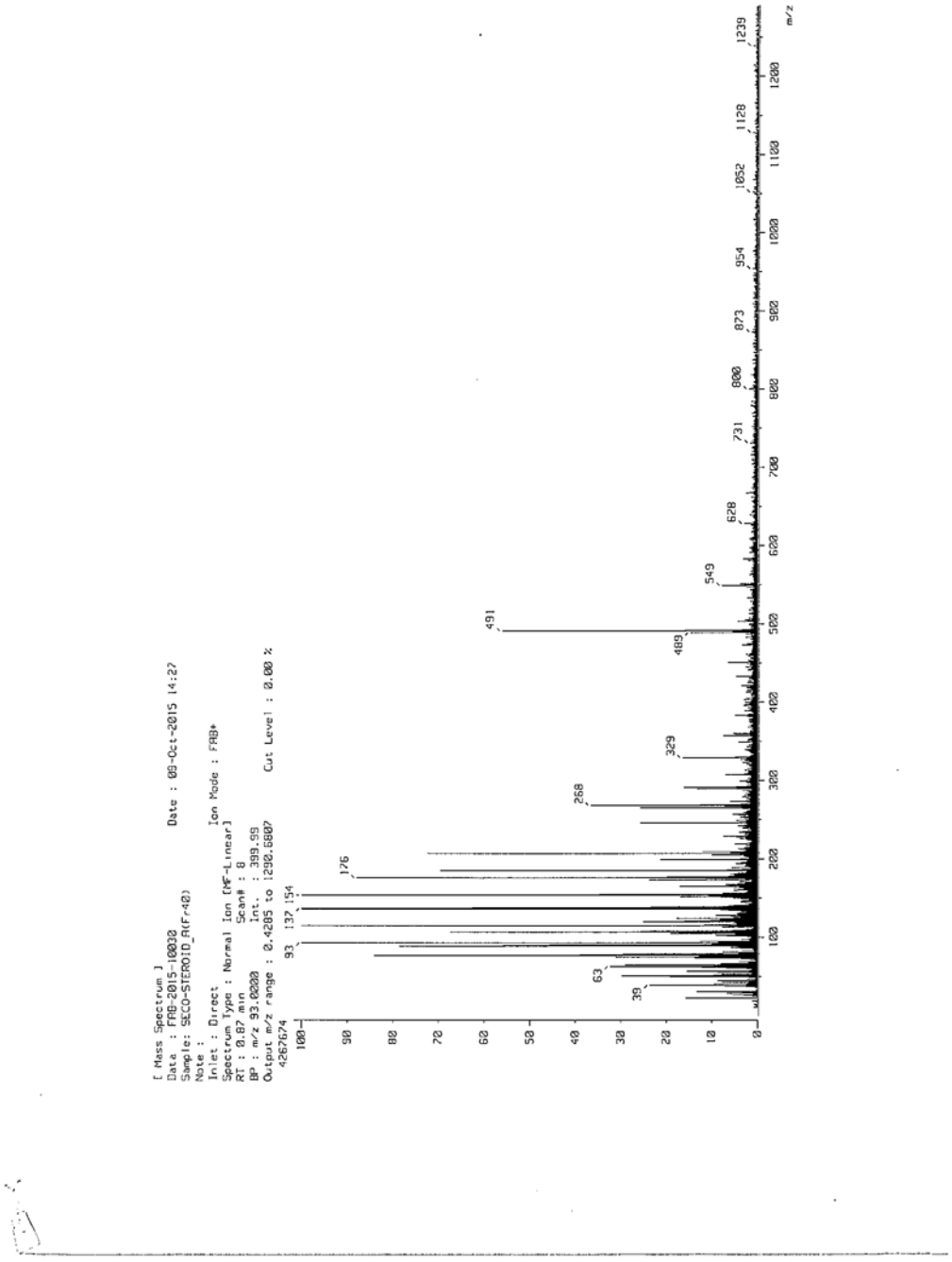

The FABMS spectrum of **6.**

NMR data for Chapter 4

Internal references: ^{1}H NMR spectra - CHD_2OD signal at 3.35 ppm
: ^{13}C NMR spectra - $^{13}CD_3OD$ signal at 49.8 ppm

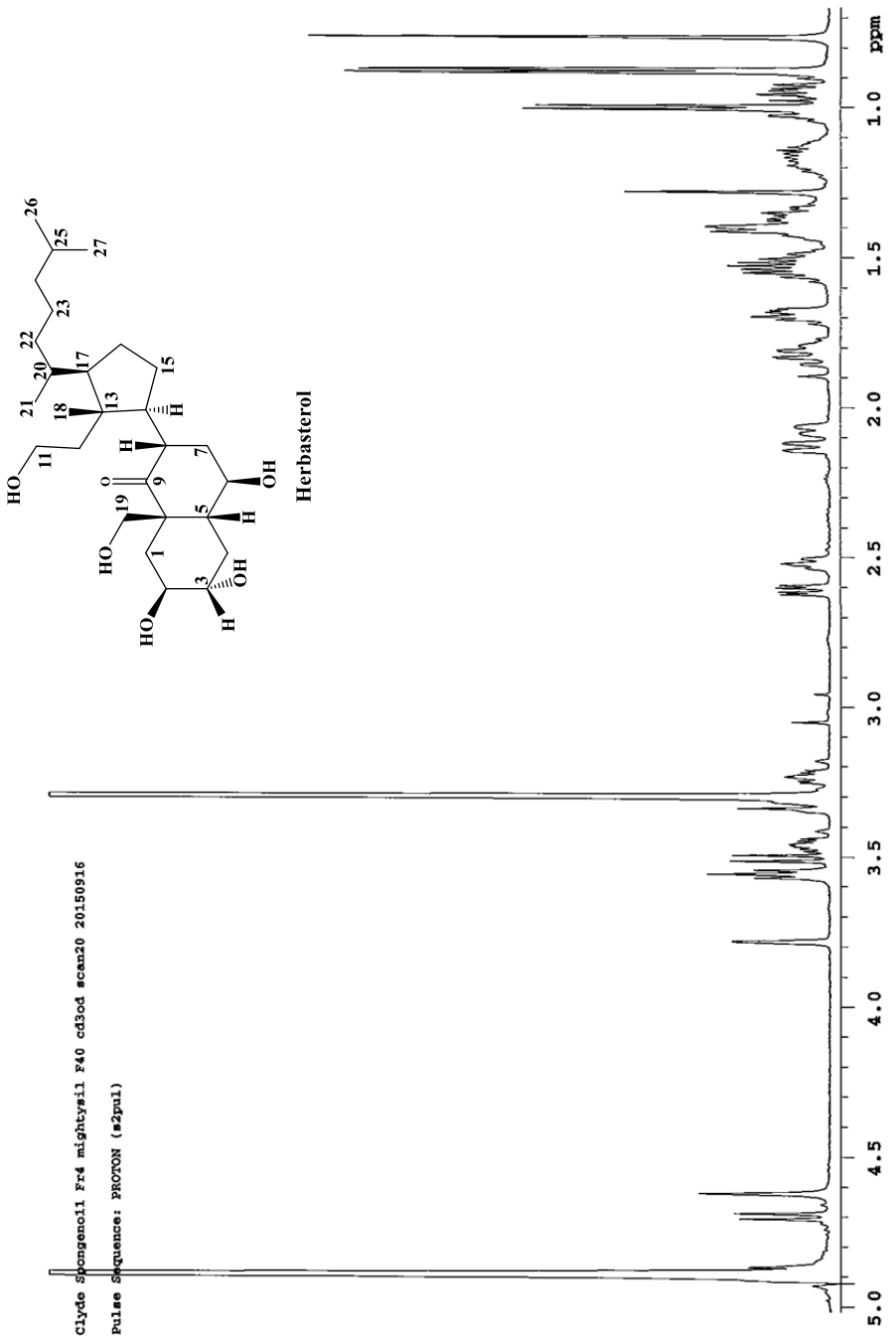

The ^{1}H NMR spectrum (CD_3OD, 600 MHz) of **6**.

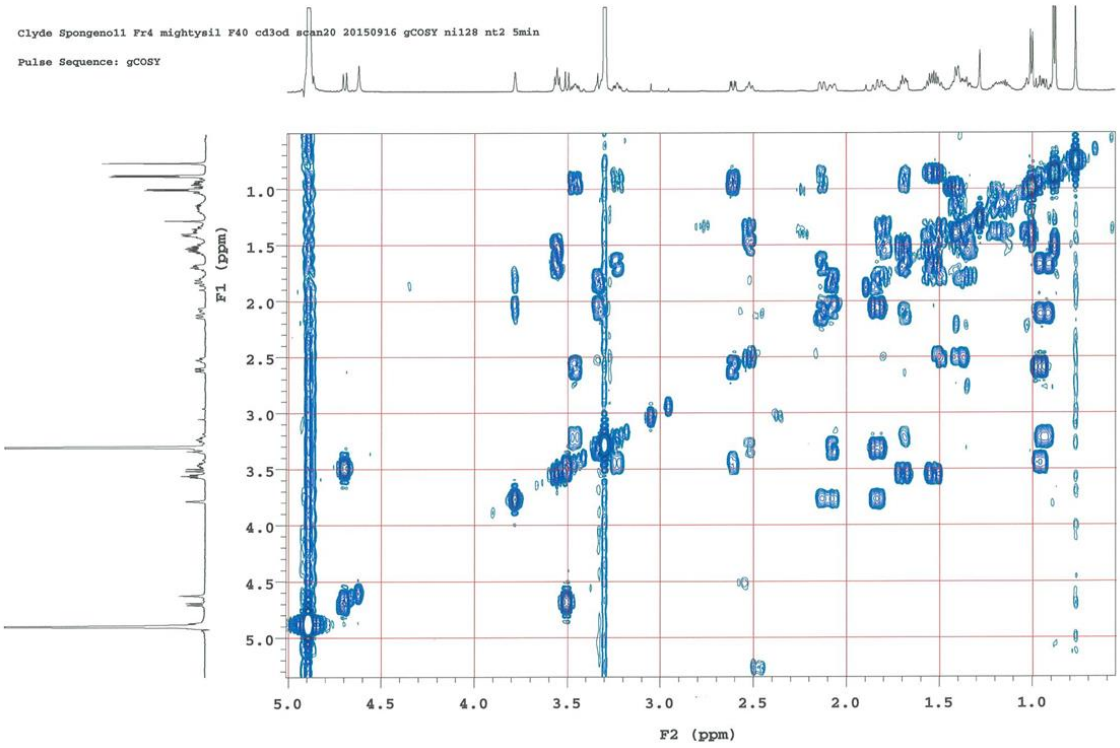

The gradient COSY spectrum (CD_3OD, 600 MHz, ni = 128) of **6**.

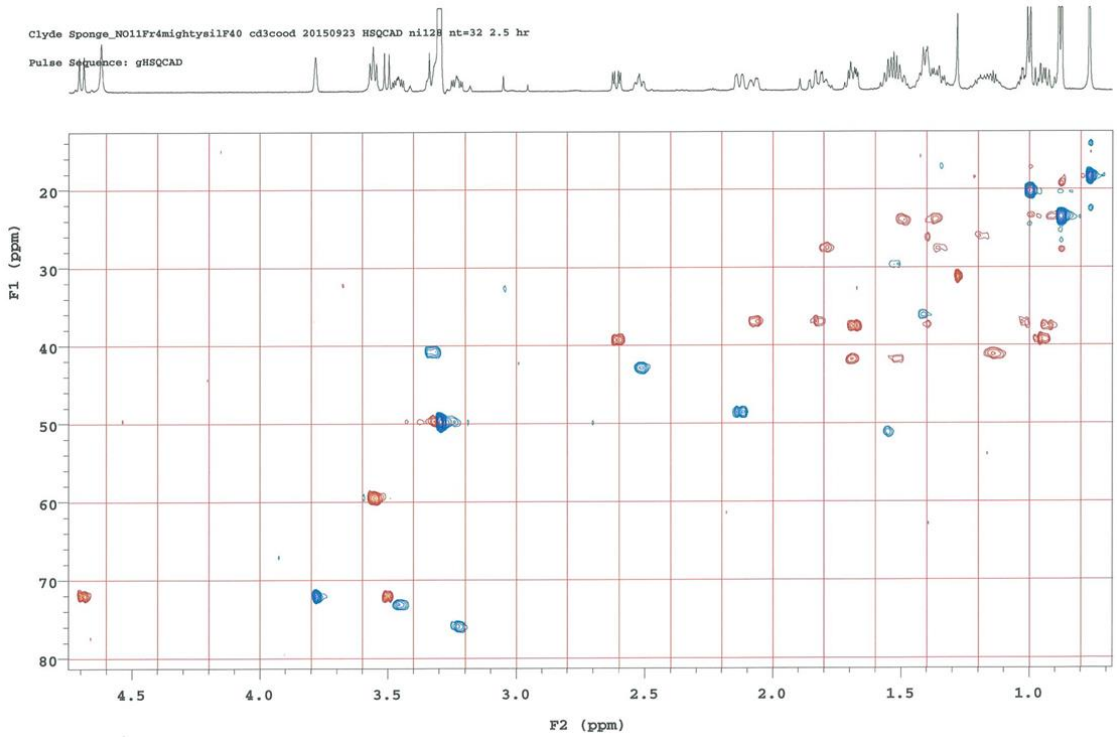

The gradient HSQC spectrum (CD_3OD, 600 MHz, ni = 128) of **6**.

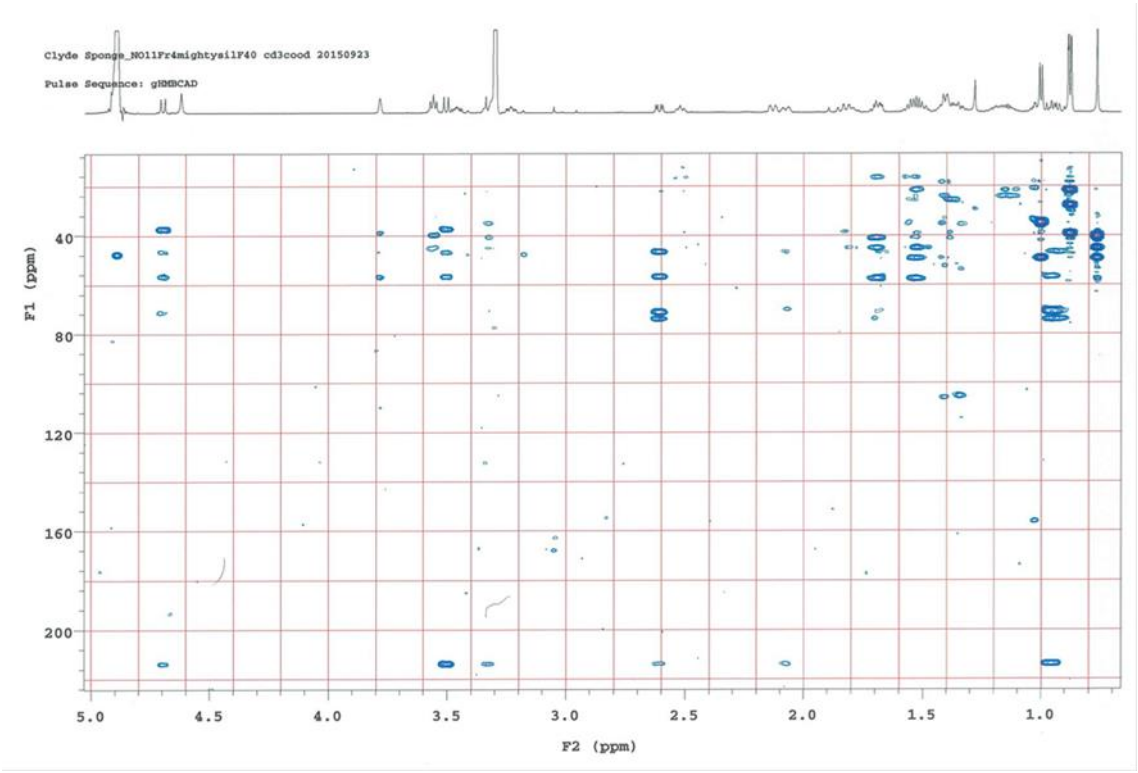

The gradient HMBC spectrum (CD_3OD, 600 MHz, ni = 128) of **6**.

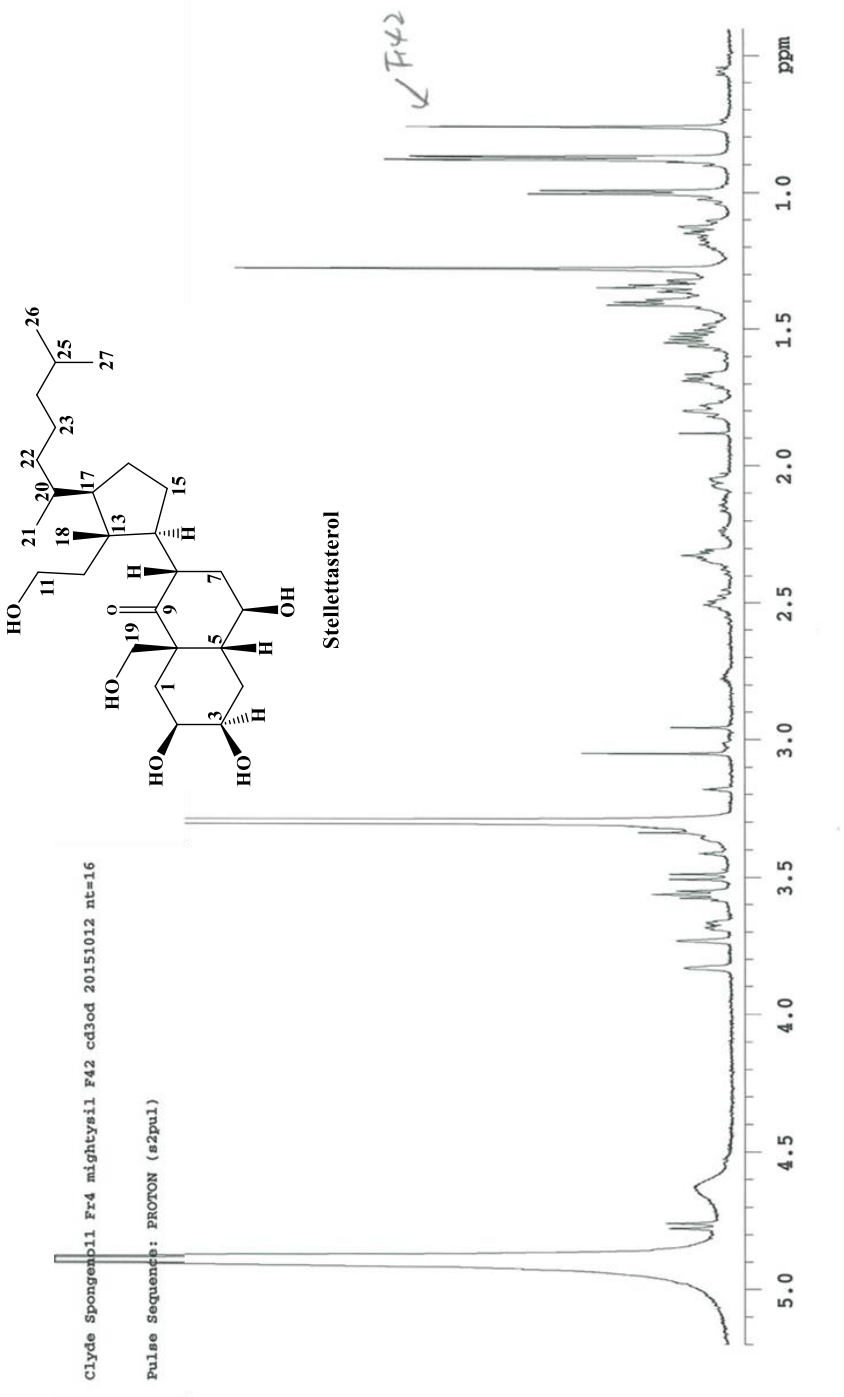

The ^{1}H NMR spectrum (CD_3OD, 600 MHz) of **7**.

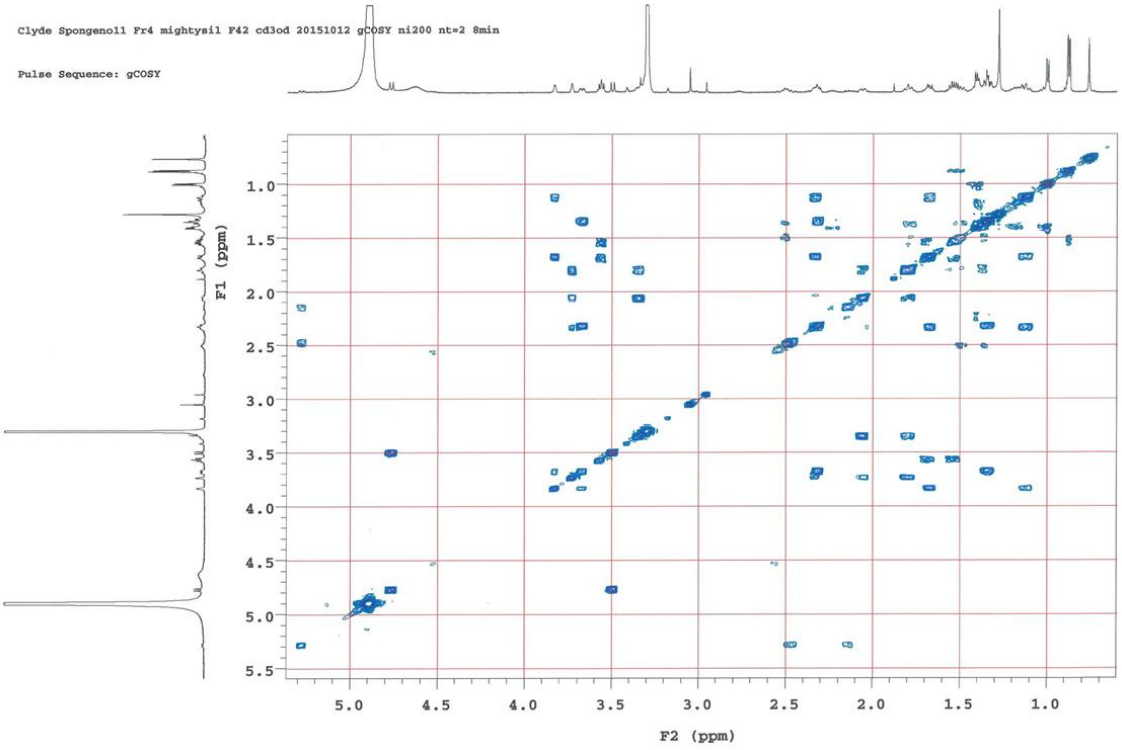

The gradient COSY spectrum (CD_3OD, 600 MHz, ni = 200) of **7**.

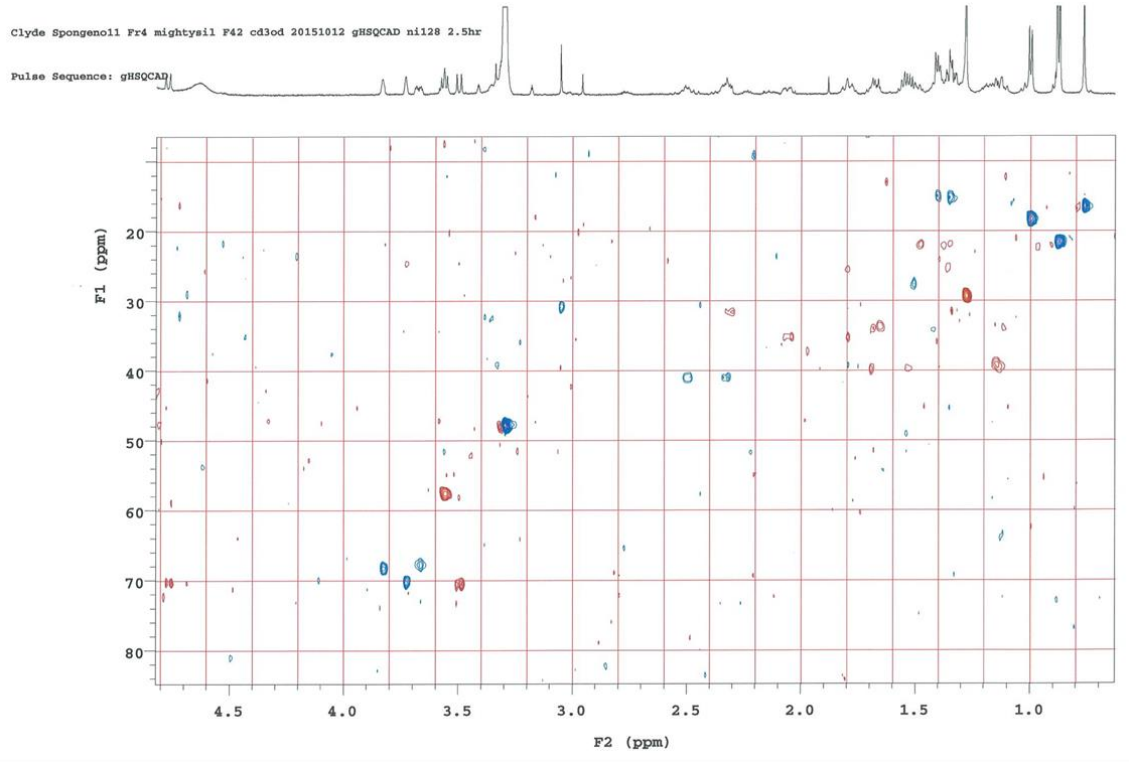

The gradient HSQC spectrum (CD_3OD, 600 MHz, ni = 128) of **7**.

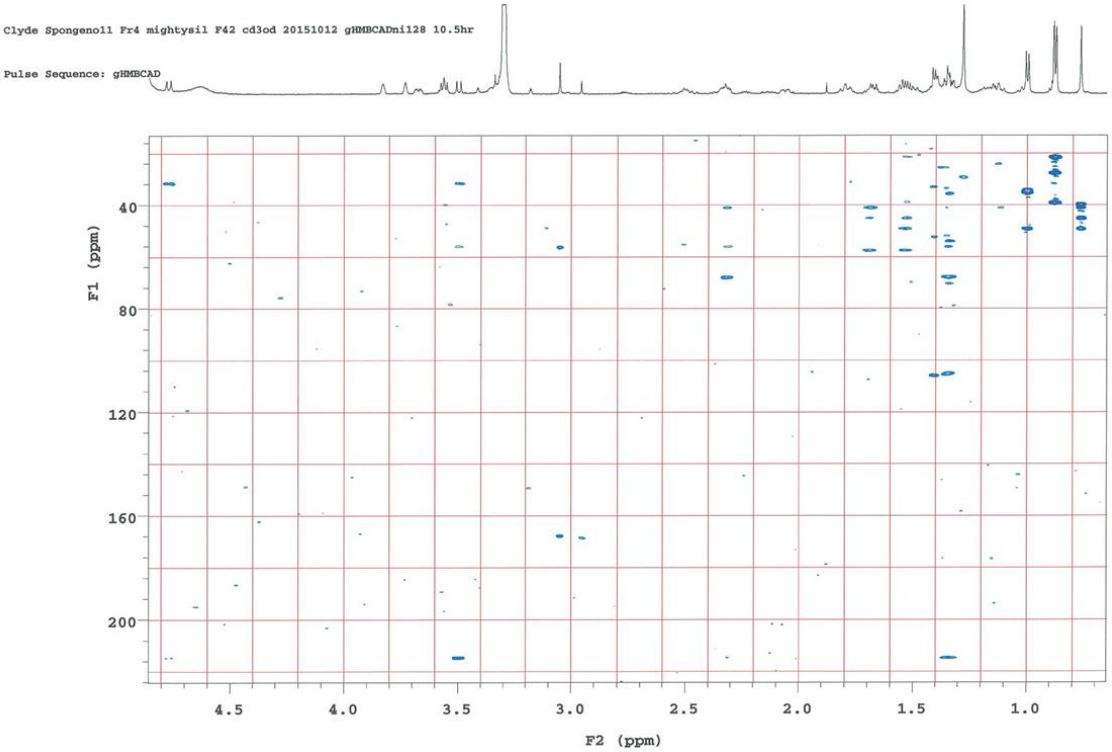

The gradient HMBC spectrum (CD_3OD, 600 MHz, ni = 128) of **7**.

References

1. Smayda, T.J. Harmful algal blooms: Their ecophysiology and general relevance to phytoplankton blooms in the sea. *Limnol*. *Oceanogr*. **1997**, *42*, 1137–1153.
2. Farstad, D.J.; Chow, T. Brief case report and review of ciguatera poisoning. *Wilderness Environ*. *Med*. **2001**, *12*, 263–269.
3. Lewis, R.J.; Sellin, M.; Poli, M.A.; Norton, R.S.; Mcloed, J.S.; Shell, M.M. Purification and characterization of ciguatoxins from moray eel *(Lycodontis javanicus, Muraenidae). Toxicon* **1991**, *29*, 1115–1127.
4. Food and Agriculture Organization of the United Nations, Rome. Food and Agriculture Organization.2004. Marine biotoxins FAO food and nutrition paper 80 Risk assessment of toxins associated with PSP, DSP, ASP in Seafood. p5-52. 2. Paralytic Shellfish Poisoning (PSP). Food and Agriculture Organization of the United Nations, Rome. Food and Agriculture Organization **2004**.
5. Murata, M.; Legrad, A.M.; Ishibashi, Y.; Yasumoto, T. Structures and configurations of ciguatoxin from the moray eel *Gymnothorax javanicus* and its likely precursor from the dinoflagellate *Gambierdiscus toxicus*. *J. Am. Chem. Soc*. **1990**, *112*, 4380–4386.
6. Yasumoto, T.; Igarashi, T.; Legrand, A.M.; Cruchet, P.; Chinain, M.; Fujita, T.; Naoki, H. Structural elucidation of ciguatoxin congeners by fast-atom bombardment tandem mass spectroscopy. *J. Am. Chem. Soc*. **2000**, *122*, 4988–4989.
7. Naoki, H.; Fujita, T.; Cruchet, P.; Legrand, A.M.; Igarashi, T.; Yasumoto, T. Structural determination of new ciguatoxin congeners by tandem mass spectrometry in Mycotoxins and Phycotoxins in Perspectives at the Turn of Millennium Proceedings of the Xth International Symposium on Mycotoxins and Phycotoxins in Brazil. **2000**, Brazil. 475–482.
8. Lewis. R.J. The changing face of ciguatera. *Toxicon* **2001**, *39*, 97–106.
9. Lewis, R.J and Holmes, M.J. Origin and transfer of toxins involved in ciguatera. *Comp. Biochem. Physiol*. **1993**, *106*, 615–628.

10. Holmes, M.J.; Lewis, R.J.; Poli, M.A.; Gillespie, N.C. Strain dependent production of ciguatoxin precursors (gambiertoxins) by *Gambierdiscus toxicus* (Dinophyceae) in culture. *Toxicon* **1991**, *29*, 761–75.

11. Vetter, I.; Touska, F.; Hess, A.; Hinsbey, R.; Sattler, S.; Lampert, A.; Sergejeva, M.; Sharov, A.; Collins, L.S.; Eberhardt, M.; Engel, M.; Cabot, P.J.; Wood, J.N.; Vlachová, V.; Reeh, P.W.; Lewis, R.J.; Zimmermann, K. Ciguatoxins activate specific cold pain pathways to elicit burning pain from cooling. *EMBO J*. **2012**, *31*, 3795–808.

12. Fleming, L.E.; Baden, D.G.; Bean, J.A.; Weisman, R.; Blythe, D.G. Seafood toxin diseases: Issues in epidemiology and community outreach. In: Reguera B, Blanco J, Fernandez MK, Wyatt T, editors. Harmful Algae. Xunta de Galicia and Intergovernmental Oceanographic Commission of UNESCO; 1998c. p. 245–248.

13. Hungerford, J.M. Scombroid poisoning: A review. *Toxicon* **2010**, 56, 231–243

14. FAO/WHO [Food and Agriculture Organization of the United Nations/World Health Organization]. **2013**. Public health risks of histamine and other biogenic amines from fish and fishery products. Meeting report.

15. Taylor, S.L. Histamine food poisoning: toxicology and clinical aspects. *Crit. Rev. Toxicol.* **1986**, *17*, 91–128.

16. Hallegraeff, G. M. Harmful algal blooms: a global overview. In Hallegraeff, G. M., Anderson, D. M. and Cembella, A. D. (Eds) Manual on Harmful Marine Microalgae. IOC Manuals and Guides no. 33, UNESCO, Paris, **1995**, p. 1–22.

17. Lindahl, O. Occurrence and Monitoring of harmful algae in the marine environment. In Miraglia, M., Van Egmond, H., Brera, C. & J. Gilbert, eds. 1998. Mycotoxins and Phycotoxins – developments in chemistry, toxicology and food safety. Proceedings of the IX International IUPAC Symposium on Mycotoxins and Phycotoxins, p. 409–423. Fort Collins, Colorado, Alaken Press, **1998**.

18. Mons, M.N., Van Egmond, H.P.; Speijers, G.J.A. Paralytic shellfish poisoning: A review. RIVM Report 388802**. 1998**.

19. Quilliam, M.A. Committee on natural toxins and food allergens. Phycotoxins. General Referee Reports. *J.AOAC. Int.* **2001**, *84*, 194–201.
20. Suehiro, M. Historical review on chemical and medical studies of globefish toxin before World War II. *Jpn. Soc. Hist. Pharm*. **1994**, *29*, 428–434.
21. Yokoo, A. Chemical studies on tetrodotoxin Rept. III. Isolation of spheroidine. *J. Chem. Soc*. **1950**, *71*, 591–592.
22. Noguchi, T.; Maruyama, J.; Ueda, Y.; Hashimoto, K.; Harada, T. Occurrence of tetrodotoxin in the Japanese ivory shell *Babylonia japonica*. *Bull. Japan. Soc. Sci. Fish*. **1981**, *47*, 901–913.
23. Sheumack, D.D.; Howden, M.E.H.; Spence, I.; Quinn, R.J. Maculotoxin: A Neurotoxin from the venom glands of the octopus *Hapalochlaena maculosa* identified as tetrodotoxin. *Science* **1978**, *199*, 188–189.
24. Maruyama, J.; Noguchi, T.; Narita, H.; Jeon, J.K.; Otsuka, M.; Hashimoto, K. Occurrence of tetrodotoxin in a starfish, *Astropecten scoparius*. *Agric. Biol. Chem*. **1985**, *49*, 3069–3070.
25. Yasumura, D.; Oshima, Y.; Yasumoto, T.; Alcala, A.C.; Alcala, L.C. Tetrodotoxin and paralytic shellfish toxins in Philippine crabs. *Agric. Biol. Chem*. **1986**, *50*, 593–598.
26. McNabb, P.; Selwood, A.I.; Munday, R.; Wood, S.A.; Taylor, D.I.; MacKenzie, A.L.; van Ginkel, R.; Rhodes, L.L.; Cornelisen, C.; Heasman, K.; Holland, P.T.; King, C. Detection of tetrodotoxin from the grey sided-gilled sea slug-*Pleurobranchaea maculata*, and associated dog neurotoxicosis on beaches adjacent to the Hauraki Gulf, Auckland, New Zealand. *Toxicon* **2010**, *56*, 466–473.
27. Vlamis, A.; Katikou, P.; Rodriguez, I.; Rey, V.; Alfonso, A.; Papazachariou, A.; Zacharaki, T.; Botana, A.M.; Botana, L.M. First Detection of tetrodotoxin in Greek shellfish by UPLC-MS/MS potentially linked to the presence of the dinoflagellate *Prorocentrum minimum*. *Toxins* **2015**, *7*, 1779–1807.
28. McNabb, P.S.; Taylor, D.I.; Ogilvie, S.C.; Wilkinson, L.; Anderson, A.; Hamon, D.; Wood, S.A.; Peake, B.M. First detection of tetrodotoxin in the bivalve *Paphies australis* by liquid chromatography coupled to triple quadrupole mass spectrometry with and without precolumn reaction. *J. AOAC Int.* **2014**, *97*, 325–333.

29. Turner, A.D.; Powell, A.; Schofield, A.; Lees, D.N.; Baker-Austin, C. Detection of the pufferfish toxin tetrodotoxin in European bivalves, England, 2013 to 2014. *Euro Surveill.* **2015**, *20*. Available online: http://www.eurosurveillance.org/ViewArticle.aspx?ArticleId=21009 (accessed on 22 August 2015).
30. Kim, Y.H.; Brown, G.H.; Mosher, H.S.; Fuhrman, F.A. Tetrodotoxin: Occurrence in Atelopid frogs of Costa Rica. *Science* **1975**, 189, 151–152.
31. Pires, O.R., Jr.; Sebben, A.; Schwartz, E.F.; Largura, S.W.R.; Bloch, C., Jr.; Morales, R.A.V.; Schwartz, C.A. Occurrence of tetrodotoxin and its analogues in the Brazilian frog *Brachycephalus ephippium* (Anura: Brachycephalidae). *Toxicon* **2002**, 40, 761–766.
32. Yotsu, M.; Iorizzi, M.; Yasumoto, T. Distribution of tetrodotoxin, 6-epitetrodotoxin, and 11-deoxytetrodotoxin in newts. *Toxicon* **1990**, 28, 238–241.
33. Mebs, D.; Yotsu-Yamashita, M. Tetrodotoxin in North-American newts. *Toxicon* **2012**, 60, 1–120.
34. Moore, J.; Anderson, N.; Narahashi, T. Tetrodoixin blocking early conductance channel on sodium. *Fed. Proc. Am. Soc. Exp. Biol*. **1966**, *25*, 569–572.
35. Kao, C.Y.; Furman, F.A. Pharmacological studies on tetrodotoxin, a potent neurotoxin. *J. Pharmacol. Exp. Ther.* **1963**, *140*, 31–40.
36. Nieto, F.R.; Cobos, E.J.; Tejada, M.A.; Sánchez-Fernández, C.; González-Cano, R.; Cendán, C.M. *Mar Drugs* **2012**, *10*, 281–305.
37. Noguchi, T.; Jeon, J.K.; Arakawa, O.; Sugita, H.; Deguchi, Y.; Shida, Y.; Hashimoto, K. Occurrence of tetrodotoxin and anhydrotetrodotoxin in *Vibrio* sp. isolated from the intestines of axantihd crab, *Atergatis floridus*. *J. Biochem.* **1986**, *99*, 311–314.
38. Yasumoto, T.; Yasumura, D.; Yotsu, M.; Michishita, T.; Endo, A.; Kotaki, Y. Bacterial production of tetrodotoxin and anhydrotetrodotoxin. *Agric. Biol. Chem*. **1986**, *50*, 793–795.
39. Hanifin, C.T. The chemical and evolutionary ecology of tetrodotoxin (TTX) toxicity in terrestrial vertebrates. *Mar. Drugs* **2010**, *8*, 577–593.

40. Ritson-Williams, R.; Yotsu-Yamashita, M.; Paul, V. Ecological functions of tetrodotoxin in a deadly polyclad flatworm. *Proc. Natl. Acad. Sci. USA* **2006**, *103*, 3176–3179.
41. Yotsu-Yamashita, M. Chemistry of puffer fish toxin. *J. Toxicol. Toxin Rev.* **2001**, *20*, 51–66.
42. Yotsu-Yamashita, M.; Abe, Y.; Kudo, Y.; Ritson-Williams, R.; Paul, V.J.; Konoki, K.; Cho, Y.; Adachi, M.; Imazu, T.; Nishikawa, T.; Isobe, M. First identification of 5,11-dideoxytetrodotoxin in marine animals, and characterization of major fragment ions of tetrodotoxin and its analogs by high resolution ESI-MS/MS. *Mar. Drugs* **2013**, *11*, 2799–2813.
43. Kudo, Y.; Yamashita, Y.; Mebs, D.; Cho, Y.; Konoki, K.; Yasumoto, T.; Yotsu-Yamashita, M. C5–C10 directly bonded tetrodotoxin analogues: possible biosynthetic precursors of tetrodotoxin from newts. *Angew. Chem. Int. Ed*. **2014**, *53*, 14546–14549.
44. Yasumoto, T.; Yotsu, M.; Murata, M.; Naoki, H. New tetrodotoxin analogue from the newt *Cynops ensicauda*. *J. Am. Chem. Soc*. **1988**, *110*, 2344–2345.
45. Jang, J.H.; Yotsu-Yamashita, M. 6,11-DideoxyTTX from the puffer fish, *Fugu pardalis. Toxicon* **2007**, *50*, 947–951.
46. Yotsu-Yamashita, M.; Yamagishi, Y.; Yasumoto, T. 5,6,11-Trideoxytetrodotoxin from the puffer fish, *Fugu poecilonotus*. *Tetrahedron Lett*. **1995**, *36*, 9329–9332.
47. Khora, S.S.; Yasumoto, T. Isolation of 11-oxotetrodotoxin from the puffer *Arothron nigropunctatus*. *Tetrahedron Lett*. **1989**, *30*, 4393–4394.
48. Wu, B.Q.; Yang, L.; Kao, C.Y.; Levinson, S.R.; Yotsu-Yamashita, M.; Yasumoto, T. 11-Oxo-tetrodotoxin and a specifically labelled 3H-tetrodotoxin. *Toxicon* **1996**, *34*, 407–416.
49. Yotsu-Yamashita, M.; Sugimoto, A.; Takai, A.; Yasumoto, T. Effects of specific modifications of several hydroxyls of tetrodotoxin on its affinity to rat brain membrane. *J. Pharmacol. Exp. Ther*. **1999**, *289*, 1688–1696.
50. Wan, C.K.; Tsui, S.H.; Tong, H.K. A case series of puffer fish poisoning, Hong Kong. *J. Emerg. Med.* **2007**, *14*, 215–220.

51. Brillantes, S.; Samosorn, W.; Faknoi, S.; Oshima, Y. Toxicity of puffers landed and marketed in Thailand. *Fish. Sci.* **2003**, *69*, 1224–1230.
52. Islam, Q.T.; Razzak, M.A.; Islam, M.A.; Bari, M.I.; Basher, A.; Chowdhury, F.R.; Sayeduzzaman, A.B.M.; Ahasan, H.A.M.N.; Faiz, M.A.; Arakawa, O.; Yotsu-Yamashita, M.; Kuch, U.; Mebs, D. Puffer fish poisoning in Bangladesh: clinical and toxicological results from large out breaks in 2008. *Trans. R. Soc. Trop. Med. Hyg.* **2011**, *105*, 74–80.
53. Noguchi, T.; Onuki, K.; Arakawa, O. Tetrodotoxin poisoning due to pufferfish and gastropods, and their intoxication mechanism. *ISRN Toxicology* **2011**, *2011*, 276939.
54. Kheifets, J.; Rozhavsky, B.; Girsh, S.Z.; Marianna, R.; Soroksky, A. Severe tetrodotoxin poisoning after consumption of *Lagocephalus sceleratus* (pufferfish, fugu) fished in Mediterranean Sea, treated with cholinesterase inhibitor. *Case Rep. Crit. Care* **2012**, *2012*, 782507.
55. Bentur, Y.; Ashkar, J.; Lurie, Y.; Levy, Y.; Azzam, Z.S.; Litmanovich, M.; Golik, M.; Gurevych, B.; Golani, D.; Eisenman, A. Lessepsian migration and tetrodotoxin poisoning due to *Lagocephalus sceleratus* in the eastern Mediterranean. *Toxicon* **2008**, *52*, 964–968.
56. Cole, J.B.; Heegaard, W.G.; Deeds, J.R.; McGrath, S.C.; Handy, S.M. Tetrodotoxin poisoning outbreak from imported dried puffer fish—Minneapolis, Minnesota, 2014. *Morb. Mort. Wkly. Rep.* **2015**, *63*, 1222–1225.
57. Cohen, N.J.; Deeds, J.R.; Wong, E.S.; Hanner, R.H.; Yancy, H.F.; White, K.D.; Thompson, T.M.; Wahl, M.; Pham, T.D.; Guichard, F.M.; Huh, In.; Austin, C.; Dizikes, G.; Gerber, S.I. Public health response to puffer fish (tetrodotoxin) poisoning from mislabeled product. *J. Food Prot.* **2009**, *72*, 810–817.
58. Loison, G. Poisonous fish of the South Pacific. Noumea, New Caledonia: South Pacific Commission. *SPC Q. Bull.* **1955**, *5*, 28–31.
59. Sato, S.; Kodama, M.; Ogata, T.; Saitanu, K.; Furuya, M.; Hirayama, K.; Kakinuma, K. Saxitoxin as a toxic principle of a freshwater puffer, *Tetraodon fangi*, in Thailand. *Toxicon* **1997**, *35*, 137–140.
60. Nakamura, M.; Oshima, Y.; Yasumoto, T. Occurrence of saxitoxin in puffer fish. *Toxicon* **1984**, *22*, 381–385.

61. Nakashima, K.; Arakawa, O.; Taniyama, S.; Nonaka, M.; Takatani, T.; Yamamori, K.; Fuchi, Y.; Noguchi, T. Occurrence of saxitoxins as a major toxin in the ovary of a marine puffer *Arothron firmamentum*. *Toxicon* **2004**, *43*, 207–212.
62. Landsberg, J.H.; Hall, S.; Johannessen, J.N.; White, K.D.; Conrad, S.M.; Abbott, J.P.; Flewelling, L.J.; Richardson, R.W.; Dickey, R.W.; Jester, E.L.; Etheridge, S.M.; Deeds, J.R.; Dolah, F.M.V.; Leighfield, T.A.; Zou, Y.; Beaudry, C.G.; Benner, R.A.; Rogers, P.L.; Scott, P.S.; Kawabata, K.; Wolny, J.L.; Steidinger, K.A. Saxitoxin puffer fish poisoning in the United States, with the first report of *Pyrodinium bahamense* as the putative toxin source. *Environ. Health Perspect*. **2006**, *114*, 1502–1507.
63. HP of Ministry of Health, Labour and Welfare of Japan. Available online: http://www.mhlw.go.jp/ topics/syokuchu/poison/animal_01.html (accessed on 22 August 2015). (In Japanese)
64. Oshima, Y. Postcolumn derivatization liquid chromatographic method for paralytic shellfish toxins. *J. AOAC Int*. **1995**, *78*, 528–532.
65. Yasumoto, T.; Michishita, T. Fluorometric determination of tetrodotoxin by high performance liquid chromatography. *Agric. Biol. Chem.* **1985**, *49*, 3077–3080.
66. Shoji, Y.; Yotsu-Yamashita, M.; Miyazawa, T.; Yasumoto, T. Electrospray ionization mass spectrometry of tetrodotoxin and its analogs: Liquid chromatography/ mass spectrometry, tandem mass spectrometry, and liquid chromatography/tandem mass spectrometry. *Anal. Biochem*. **2001**, *290*, 10–17.
67. Dawson, R.M.C.; Elliott, D.C.; Elliott, W.H and Jones, K.M. Data for Biochemical Research, 3rd ed., Oxford University Press, New York, NY, **1986**, p. 297.
68. Nakamura, M.; Yasumoto, T. Tetrodotoxin derivatives in puffer fish. *Toxicon* **1985**, *23*, 271–276.
69. Puilingi, C.G.; Kudo, Y.; Cho, Y.; Konoki, K.; Yotsu-Yamashita, M. Tetrodotoxin and its analogues in the pufferfish *Arothron hispidus* and *A. nigropunctatus* from the Solomon Islands. A comparison of their toxin profiles with the same species from Okinawa, Japan. *Toxins* **2015**, *7*, 3436–3454.

70. Yotsu-Yamashita, M.; Jang, J.H.; Cho, Y.; Konoki, K. Optimization of simultaneous analysis of tetrodotoxin, 4-epitetrodotoxin, 4,9-anhydrotetrodotoxin, and 5,6,11-trideoxytetrodotoxin by hydrophilic interaction liquid chromatography–tandem mass spectrometry. *Forensic Toxicol.* **2011**, *29*, 61–64.
71. Jang, J.; Lee, J.S.; Yotsu-Yamashita, M. LC/MS analysis of tetrodotoxin and its deoxy analogs in the marine puffer fish *Fugu niphobles* from the southern coast of Korea, and in the brackish water puffer fishes *Tetraodon nigroviridis* and *Tetraodon biocellatus* from Southeast Asia. *Mar. Drugs* **2010**, *8*, 1049–1058
72. Nakagawa, T.; Jang, J.; Yotsu-Yamashita, M. Hydrophilic interaction liquid chromatography electrospray ionization mass spectrometry of tetrodotoxin and its analogs. *Anal. Biochem*. **2006**, *352*, 142–144.
73. Teruya, N.; Oshiro, N.; Tamanaha, K. Toxicity of puffers from Okinawa. Available online: http://www.pref.okinawa.jp/site/hoken/eiken/syoho/documents/s40_93-98.pdf (accessed on 24 August 2015). (In Japanese)
74. Sato, S., Ogata, T., Borja, V., Gonzales, C., Fukuyo, Y., Kodama, M. Frequent occurrence of paralytic shellfish poisoning toxins as dominant toxins in marine puffer from tropical water. *Toxicon* **2000**, *38*, 1101–1109.
75. Campbell, S.; Harada, R.M.; DeFelice, S.V.; Bienfang, P.K.; Li, Q.X. Bacterial production of tetrodotoxin in the pufferfish *Arothron hispidus. Nat. Product Res. Part A* **2009**, *17*, 1630–1640.
76. Bragadeeswaran, S.; Therasa, D., Prabhu, K.; Kathiresan, K. Biomedical and pharmacological potential of tetrodotoxin-producing bacteria isolated from marine pufferfish *Arothron hispidus* (Muller, 1841). *J. Venom Anim. Toxins Incl. Trop. Dis*. **2010**, *16*, 421–431.
77. Yotsu-Yamashita, M.; Hayashi, Y.; Khora, S.S.; Sato, S.i.; Yasumoto, T. Isolation and structural assignment of 11-nortetrodotoxin-6(*S*)-ol from the puffer *Arothron nigropunctatus*. *Biosci. Biotechnol. Biochem*. **1992**, *56*, 370–371.

78. Vázquez, N.; Yotsu-Yamashita, M.; Sierra-Beltrán, A.P.; Yasumoto, T.; Ochoa, J.L. Toxicities and distribution of tetrodotoxin in the tissues of puffer fish found in the coast of the Baja California Peninsula, Mexico. *Toxicon* **2000**, *38*, 729–734.
79. Chulanetra, M.; Sookrung, N.; Srimanote, P.; Indrawattana, N.; Thanongsaksrikul, J.; Sakolvaree, Y.; Chongsa-Nguan, M.; Kurazono, H.; Chaicumpa, W. Toxic marine puffer fish in Thailand Seas and tetrodotoxin they contained. *Toxins* **2011**, *3*, 1249–1262.
80. Jang, J.; Yotsu-Yamashita, M. Distribution of tetrodotoxin, saxitoxin, and their analogs among tissues of the puffer fish *Fugu pardalis*. *Toxicon* **2006**, *48*, 980–987.
81. Yotsu-Yamashita, M.; Sugimoto, A.; Terakawa, T.; Shoji, Y.; Miyazawa, T.; Yasumoto, T. Purification, characterization, and cDNA cloning of a novel soluble saxitoxin and tetrodotoxin binding protein from plasma of the pufferfish, *Fugu pardalis*. *Eur. J. Biochem.* **2001**, *268*, 5937–5946.
82. Yotsu-Yamashita, M.; Okoshi, N.; Watanabe, K.; Araki, N.; Yamaki, H.; Shoji, Y.; Terakawa, T. Localization of pufferfish saxitoxin and tetrodotoxin binding protein (PSTBP) in the tissues of the pufferfish, *Takifugu pardalis*, analyzed by immunohistochemical staining. *Toxicon* **2013**, *72*, 23–28.
83. Hashiguchi, Y.; Lee, J.M.; Shiraishik, M.; Komatsu, S.; Miki, S.; Shimasaki, Y.; Mochioka, N.; Kusakabe, T.; Oshima, Y. Characterization and evolutionary analysis of tributyltin-binding protein and pufferfish saxitoxin and tetrodotoxin-binding protein genes in toxic anc nontoxic pufferfish. *J. Evol. Biol*. **2015**, *5*, 1103–1118.
84. Diener, M.; Christian, B.; Ahmed, M.; Luckas, B. Determination of tetrodotoxin and its analogs in the puffer fish Takifugu oblongus from Bangladesh by hydrophilic interaction chromatography and mass-spectrometric detection. *Anal. Bioanal. Chem*. **2007**, *389*, 1997–2002.

85. Jang, J.H.; Lee, J.S.; Yotsu-Yamashita, M. LC/MS analysis of tetrodotoxin and its deoxy analogs in the marine puffer fish *Fugu niphobles* from the southern coast of Korea, and in the brackishwater puffer fishes *Tetraodon nigroviridis* and *Tetraodon biocellatus* from Southeast Asia. *Mar. Drugs* **2010**, *8*, 1049–1058.
86. Silva, M.; Azevedo, J.; Rodriguez, P.; Alfonso, A.; Botana, L.M.; Vasconcelos, V. New gastropod vectors and tetrodotoxin potential expansion in temperate waters of the Atlantic Ocean. *Mar. Drugs* **2012**, *10*, 712–726.
87. Mebs, D.; Arakawa, O.; Yotsu-Yamashita, M. Tissue distribution of tetrodotoxin in the red-spotted newt *Notophthalmus viridescens*. *Toxicon* **2010**, *55*, 1353–1357.
88. Rodriguez, P.; Alfonso, A.; Vale, C.; Alfonso, C.; Vale, P.; Tellez, A.; Botana, L.M. First toxicity report of tetrodotoxin and 5,6,11-trideoxyTTX in the trumpet shell *Charonia lampas lampas* in Europe. *Anal. Chem.* **2008**, *80*, 5622–5629.
89. Luo, X.; Yu, R.C.; Wang, X.J.; Zhou, M.J. Toxin composition and toxicity dynamics of marine gastropod *Nassarius* spp. collected from Lianyungang, China. *Food Addit. Contam.* A **2012,** *29*, 117–127.
90. Pires, O.R.; Sebbena, A.; Schwartza, E.F.; Bloch, C.J.; Rodrigo, A.V. Morales, R.A.V.; Schwartza, C.A. The occurrence of 11-oxotetrodotoxin, a rare tetrodotoxin analogue, in the brachycephalidae frog *Brachycephalus ephippium*. *Toxicon* **2003**, *42*, 563–566.
91. Yotsu-Yamashita, M.; Mebs, D. Occurrence of 11-oxotetrodotoxin in the red-spotted newt, *Notophthalmus viridescens*, and further studies on the levels of tetrodotoxin and its analogues in the newt efts. *Toxicon* **2003**, *41*, 893–897.
92. Kudo, Y.; Finn, J.; Fukushima, K.; Sakugawa, S.; Cho, Y.; Konoki, K.; Yotsu-Yamashita, M. Isolation of 6-deoxytetrodotoxin from the pufferfish, *Takifugu pardalis*, and a comparison of the effects of the C-6 and C-11 hydroxy groups of tetrodotoxin on its activity. *J. Nat. Prod*. **2014**, *77*, 1000–1004.
93. Taniyama, S.; Isami, Y.; Matsumoto, T.; Nagashima, Y.; Takatani, T.; Arakawa, O. Toxicity and toxin profile of tetrodotoxin detected in the scavenging gastropod *Nassarius (Alectrion) glans.* "Kinshibai". *Shokuhin Eiseigaku Zasshi* **2009**, *50*, 22–28. (In Japanese).

94. Arakawa, O.; Noguchi, T.; Shida, Y.; Onoue, Y. Occurrence of 11-oxotetrodotoxin and 11-nortetrodotoxin-6(*R*)-ol in a xanthid crab *Atergatis floridus* collected at Kojima, Ishigaki Island. *Fish. Sci.* **1994**, *60*, 769–771.

95. Lee, M.J.; Jeong, D.Y.; Kim, W.S.; Kim, H.D.; Kim, C.H.; Park, W.W.; Park, Y.H.; Kim, K.S.; Kim, H.M.; Kim, D.S. A tetrodotoxin-producing *Vibrio* strain, LM-1, from the puffer fish Fugu *vermicularis radiatus. Appl. Environ. Microbiol.* **2000**, *66*, 1698–1701

96. Yang, G.; Xu, J.; Liang, S.; Ren, D.; Yan, X.; Bao, B. A novel TTX-producing *Aeromonas* isolated from the ovary of *Takifugu obscurus*. *Toxicon* **2010**, *56*, 324–329.

97. Cheng, C.A.; Hwang, D.F.; Tsai, Y.H.; Chen, H.C.; Jeng, S.S.; Noguchi, T.; Ohwada, K.; Hasimoto, K. Microflora and tetrodotoxin-producing bacteria in a gastropod, *Niotha clathrata*. *Food Chem. Toxicol.* **1995**, *33*, 929–934.

98. Codex Alimentarius, CODEX STAN 292-2008. Available online: http://www.codexalimentarius.org/input/download/standards/11109/CXS_292e.pdf (accessed on 22 August 2015).

99. EU Regulation 853/2004. Regulation (EC) no. 853/2004 of the European Parliament and of the Council of 29 April 2004. Laying down specific hygiene rules for food of animal origin. *Off. J. Eur. Commun.* **2004**, *L226*, 22–82.

100. U.S. Food and Drug Administration, National Shellfish Sanitation Program Guide for the Control of Molluscan Shellfish 2011 Revision. Available online: http://www.fda.gov/downloads/Food/GuidanceRegulation/FederalStateFoodPrograms/UCM350344.pdf (accessed on 22 August 2015).

101. Veterinary Sanitation Division Director-General. Notification No. 30 of Veterinary Sanitation Division, from the Veterinary Sanitation Division Director-General, Veterinary Sanitation Division, Environmental Health Bureau, Ministry of Health, Labour and Welfare, 1980. Available online: http://www.mhlw.go.jp/topics/syokuchu/kanren/kanshi/s58_1202-2.html (accessed on 22 August 2015). (In Japanese)

102. Newman, D.J and Cragg, G.M. Natural Products as Sources of New Drugs over the Last 25 Years. *J. Nat. Prod*. **2007**, *70*, 461–477.

103. Blunt, J.W.; Copp, B.R.; Hu, W.P.; Munro, M.H.G.; Northcote, P.T.; Prinsep, M.R. Marine natural products. *Nat. Prod. Rep*. **2008**, *25*, 35–94.
104. Faulkner, D. J.; Marine natural products. *Nat. Prod. Rep*. **2002**, 19, 1– 48.
105. Hooper, J.N.A.; Van Soest, R.W.M. Systema porifera: a guide to the classification of sponges. Dordrecht, Netherlands: Kluwer Academic/Plenum Publishers; **2002**.
106. Ebada, S.S.; Lin, W.H.; Proksch, P. Bioactive sesterterpenes and triterpenes from marine sponges: occurrence and pharmacological significance. *Mar Drugs* **2010**, *8*, 313–346.
107. Ivanchina, N.V.; Kicha, A.A.; Stonik, V.A. Steroid glycosides from marine organisms. *Steroids* **2011**, *76*, 425–454.
108. Kalinin, V.I.; Ivanchina, N.V.; Krasokhin, V.B.; Makarieva, T.N.; Stonik, V.A. Glycosides from marine sponges (porifera, demospongiae): structures, taxonomical distribution, biological activities and biological roles. *Mar Drugs* **2012**, *10*, 1671–1710.
109. Okada, Y.; Matsunaga, S.; Van Soest, R.W.M.; Fusetani, N. Sokodosides, steroid glycosides with an isopropyl chain, from the marine sponge *Erylus placenta*. *J. Org. Chem*. **2006**, *71*, 4884–4888.
110. Kitagawa, I.; Kobayashi, M.; Okamoto, Y.; Yoshikawa, M.; Hamamoto, Y. Structures of sarasinosides A1, B1, and C1; new norlanostane-triterpenoid oligoglycosides from the Palauan marine sponge *Asteropus sarasinosum*. *Chem. Pharm. Bull*. **1987**, *35*, 5036–5039.
111. Schmitz, F.J.; Ksebati, M.B.; Gunasekera, S.P.; Agarwal, S. Sarasinoside A1-a saponin containing amino sugars isolated from a sponge. *J. Org. Chem*. **1988**, *53*, 5941–5947.
112. Ksebati, M.B.; Schmitz, F.J.; Gunasekera, S.P. Pouosides A-E, novel triterpene galactosides from a marine sponge *Asteropus* sp. *J. Org. Chem.* **1988**, *53*, 3917–3921.
113. Lee, H.S.; Seo, Y.; Cho, K.W.; Rho, J.R.; Shin, J.; Paul, V.J. New triterpenoid saponins from the sponge *Melophlus isis*. *J. Nat. Prod*. **2000**, *63*, 915–919.

114. Kobayashi, M.; Okamoto, Y.; Kitagawa, I. Marine natural products. XXVIII. The structure of sarasinosides A1, A2, A3, B1, B2, B3, C1, C2, and C3, Nine new norlanostane-triterpenoidal oligoglycosides from the palauan marine sponge *Asteropus sarasinosum. Chem. Pharm. Bull*. **1991**, *39*, 2867–2877.

115. Puilingi, C.G.; Kudo, Y.; Cho, Y.; Konoki, K.; Yotsu-Yamashita, M. A new sarasinoside congener sarasinoside M_2 from a marine sponge collected in the Solomon Islands. *Biosci. Biotechnol. Biochem*. **2017**, *81*, 222–225.

116. Dai HF, Edrada RA, Ebel R, Nimtz, M.; Wray, V.; Proksch, P. Norlanostane triterpenoidal saponins from the marine sponge *Melophlus sarassinorum*. *J. Nat. Prod*. **2005**, *68*, 1231–1237.

117. Wu, S.H.; Luo, X.D.; Ma, Y.B.; Liu, J.K.; Wu, D.G.; Zhao, B.; Lu, Y.; Zheng, Q.T. Two novel secoergosterols from the fungus *Tylopilus plumbeoviolaceus. J. Nat. Prod*. **2000**, *63*, 534–536.

118. Santalova, E.A.; Denisenko, V.A.; Dmitrenok, P.S. Two new sarasinosides from the sponge *Melophlus sarasinorum. Nat. Prod. Commun.* **2006**, *1*, 265–271.

119. D'Auria, M.V.; Paloma, L.G.; Minale, L.; Riccio, R. Jereisterol A and B: Two 3β-methoxy-secosteroids from the pacific sponge *Jereicopsis graphidiophora. Tetrahedron Lett.* **1991**, *32*, 2149–2152.

120. Lee, J.H.; Jeon, J.; Lee, Y.J.; Lee, H.S.; Sim, C.J.; Oh, K.B.; Shin, J. Nortriterpene glycosides of the sarasinoside class from the sponge *Lipastrotethya* sp. *J. Nat. Prod*. **2012,** *75*, 1365–1372.

121. http://www.marinespecies.org/aphia.php?p=taxdetails&id=131834 accessed September 2015.

122. Aoki, S.; Cao, L.W.; Matsui, K.; Rachmat, R.; Akiyama, S.; Kobayashi, M. Kendarimide A, a novel peptide reversing P-glycoprotein-mediated multidrug resistance in tumor cells, from a marine sponge of *Haliclona* sp. *Tetrahedron*. **2004**, *60*, 7053–7059.

123. de Jesus, R.P and Faulkner, D.J. Chlorinated acetylenes from the San Diego sponge *Haliclona lunisimilis*. *J. Nat. Prod.* **2003**, *66*, 671–674.

124. Erickson, K.L.; Beutler, J.A.; Cardellina, J.H.; Boyd, M.R. Salicylihalamides A and B, novel cytotoxic macrolides from the marine sponge *Haliclona* sp. *J. Org. Chem*. **1997**, *62*, 8188–8192.

125. Fu, X.; Ferreira, M.L.G.; Schmitz, F.J.; Kelly, M. Tamosterone sulfates: A C-14 epimeric pair of polyhydroxylated sterols from a new Oceanapiid sponge genus. *J. Org. Chem*. **1999**, *64*, 6706–6709.
126. Sperry, S.; Samuels, G.J.; Crews, P. Vertinoid polyketides from the saltwater culture of the fungus *Trichoderma longibrachiatum* separated from a *Haliclona* marine sponge. *J. Org. Chem*. **1998**, *63*, 10011–10014.
127. Viegelmann, C.; Parker, J.; Ooi, T.; Clements, C.; Abbott, G.; Young, L.; Kennedy, J.; Dobson, A.D.W.; Edrada-Ebel, R. Isolation and identification of antitrypanosomal and antimycobacterial active steroids from the sponge *Haliclona simulans. Mar. Drugs* **2014**, *12*, 2937–2952.
128. Charan, R.D.; Garson, M.J.; Brereton, I.M.; Willis, A.C.; Hooper, J.N.A. Haliclonacyclamines A and B, cytotoxic alkaloids from the tropical marine sponge *Haliclona* sp. *Tetrahedron* **1996**, *52*, 27, 9111–9120.
129. Gabriel, A.F.; Li, Z.; Kusuda, R.; Tanaka, C.; Miyamoto, T. Six new polyacetylenic alcohols from the marine sponges *Petrosia* sp. and *Halichondria* sp. *Chem. Pharm. Bull*. **2015**, *63*, 469–475.
130. Capon, R.J and Faulkner, D.J. Herbasterol, an ichthyotoxic 9,11-secosterol from the sponge *Dysidea herbacea. J. Org. Chem*. **1985**, *50*, 4771–4773.
131. Li, H.; Matsunaga, S.; Fusetani, N. A new 9,11-secosterol, stellettasterol from a marine sponge *Stelletta* sp. *Experientia* **1994**, *50*, 771–773.